
GRINREY
Advanced
Research in
Solar Energy
Sandip A. Kale
Editor
Research Transcripts in Energy

Research Transcripts in Energy

Volume 01

Advanced Research in Solar Energy

Book Series by Grinrey Publications

- Research Transcripts in Energy
- Research Transcripts in Engineering
- Research Transcripts in Materials
- Research Transcripts in Computer, Electrical and Electronics Engineering

www.grinrey.com

Research Transcripts in Energy

Volume 01

Advanced Research in Solar Energy

Sandip A. Kale

Editor

GRINREY

Advanced Research in Solar Energy

Sandip A. Kale, editor (Technology Research and Innovation Centre, Pune, India)

Series: Research Transcripts in Energy

ISBN: 978-81-948951-7-6

Published by: Grinrey Publications

511, Ganesh Nakashtram, Dhayari, Pune, Maharashtra, India

www.grinrey.com

Email: contact@grinrey.com

Contents

Preface

Chapter 1 **Experimental Studies on Developed Direct Solar Dryer for Conversion of Grapes into Raisins with Temperature Control**
Nitin Sharma and Namrata Sengar 1

Chapter 2 **Design and Analysis of Solar Water Pumping System**
Lakhdara Amira, Bahi Tahar and Moussaoui Abdelkrim 15

Chapter 3 **Study of Thermal Comfort for office/Institute Buildings Based on Carbse Tool and Suggestive Passive Measures for Kota**
Antima Sharma, DeepmalaMeena and Namrata Sengar 25

Chapter 4 **Industrial Waste Water Treatment Using Natural Filtration and Solar Distillation Methods**
Hemant Kumar, Shivanshu Sharma and Namrata Sengar 37

Chapter 5 **Experimental Study of Electrical Outputs for Air-Blower Cleaned, Water Cleaned and Unclean Solar PV Panels**
Mahesh Kumar, Koushal Shringi and Namrata Sengar 49

Chapter 6 **Design, Development and Experimental Study of Solar PV Air Cooler**
Saiful Islam and Namrata Sengar 61

Chapter 7 **Design and Implementation of MPPT Based Boost Converter Topology for Photovoltaic System**
Kruthi Jayaram 75

Chapter 8 **A Novel PID Using a Genetic Algorithm to Track the Maximum Power Point of the PV System**
Zahira EL HARIZ, Hicham Aissaoui and Mohammed Diany 87

Chapter 9 **Photovoltaic Generation System and Grid Source Connected to Load Using qZ Source**
Henchiri Abdelhamid, Bahi Tahar and Lakhdara Amira 99

Chapter 10 **Control and Management of a Photovoltaic System** 107

Equipped with a Storage Battery
Lekhchine Salima, Bahi Tahar and Layate Zakaria

Index 128

1 Experimental Studies on Developed Direct Solar Dryer for Conversion of Grapes into Raisins with Temperature Control

Nitin Sharma[*, a] and Namrata Sengar[a]

[a]Department of Pure and Applied Physics, University of Kota, Kota, India

*Corresponding author: mr.nitinsharma001@gmail.com

ABSTRACT

This chapter presents the experimental studies of the temperature variations in developed direct solar dryer while conversion of grapes into raisins. Optimum temperature of solar drying of grapes is in the range 28^{o}C to 55^{o}C so a small DC fan and speed control device running with solar PV panel is attached to the dryer to control the temperature in the dryer. The solar dryer is a flat plate solar collector with an aperture area as 2972.65cm^{2}. Experiments were performed without and with load, and the temperature profiles are reported. During load experiments with the developed solar dryer, the weight of 1kg of grapes reduced to 0.260 kg in five days and raisins were developed. The efficiency of the system was found to be in the range 4% to 7%. The efficiency of the system can be further improved with load optimization and slight modifications to make it suitable for households and cottage industries.

Keywords: Grapes, Raisins, Solar dryer, Temperature profile

Advanced Research in Solar Energy | ISBN: 978-81-948951-7-6
Book Series: Research Transcripts in Energy | Vol: 01

1. INTRODUCTION

Drying is one of the oldest techniques for preservation of food and agricultural products. The main objective of drying is to reduce the moisture content up to the safe storage level so that the products can be stored for a longer period without any spoilage. The low moisture content prevents the growth of microorganisms such as moulds, bacteria, and yeasts in the food products.

Solar energy is the most widely used renewable energy source in the drying process. The traditional open sun drying is the largest application of solar energy as it is a cheap drying technique, but some problems are associated such as longer drying time, difficulty in controlling the drying process, losses of the natural colours and minerals, losses of products due to insect, bird, weather changes, requirement of large drying area. To reduce these problems solar dryers are developed for use in drying the agriculture products and fruits. Solar dryers utilize the principle of conversion of solar radiation into thermal energy which heats the air and food products in the dryer and aids in removal of moisture from the food [1]. There are different types of dryers such as direct solar dryer, indirect solar dryer, hybrid solar dryer, mixed solar dryer, cabinet solar dryer, greenhouse solar dryer etc. [2]. Grapes are widely popular as a fruit world over. Grapes are main part for wine production, are used for preparing the raisins, the food industry uses grapes for various purposes like making jam and juice. Drying grapes either by open sun drying, shade drying or mechanical drying produces raisins. The grapes in India are used for making wine, jams, raisin and raw eating. Maharashtra is the India's largest producer of grapes and Nasik leads the list of grape producing areas in Maharashtra [3]. Open sun drying is oldest technique for drying the grapes and produces raisins but in this method drying rate is very slow. The drying time required for natural grapes is 20 days and for pre-treated grapes is 8–10 days. In this method there is possibility of contamination of the dried grapes. The direct exposure to intense sun radiation may also result in colour deterioration. [4]. The open drying process using sun can take a period of 9–15 days depending upon the climatic conditions of the location and dryer used [5-8]. For effective drying of grapes the temperature range 28^{o}C to 55^{o}C is considered optimum [9].

Though a number of studies have been carried out for solar dryers, the present work aimed at specific study of the temperature profile of each component of the solar dryer while conversion of grapes into raisins with control of temperature. The study is important from the point of view of understanding the temperature variations inside the dryer and for controlling the temperatures for optimum drying of the grapes through a small fan and speed control device running with solar PV panel. The present work reports the experimental

observations related to the temperature variation of the dryer component with ambient air temperature and solar radiation values and estimates the efficiency of the system for drying. This work will form a basis for the development of an efficient temperature controlled solar dryer in future for households or cottage industries.

2. DESIGN DETAILS OF DEVELOPED SOLAR DRYER

The solar dryer is a flat plate solar collector with aperture area as 2972.65cm^2. The absorber plate (tray) is placed directly behind the transparent cover. Solar radiation trapped by glass heats up the air and heated air then circulates in whole system. Exhaust chimney is provided in the dryer to allow the hot air to move out from the dryer. The chimney is of length 53cm. Copper tubes are fixed at side walls of dryer so that whole system remains hot for long time, copper tubes is of 1125cm in length and having diameter 1.27 cm. The whole system is made up of GI sheet and insulated by polystyrene sheet and plywood.

Fig. 1. Complete experimental setup of solar dryer at University of Kota

The rolling wheels are attached for easy movement of the dryer. The whole dryer is painted black from inside so that more heat is absorbed by the system. The system is kept south facing to maximize the solar radiation incidence on collector. The solar dryer was initially developed as a passive solar dryer and tested for drying of ginger [10]. Some modifications were done in the dryer after the study to improve handling and convenience of operation. A fan with speed control device operated by PV panel was attached to control the temperatures inside dryer. The speed control device can increase and decrease the speed of exhaust fan. The designed dryer is tested at roof of University of Kota. The complete set up of direct type solar dryer is as shown in Fig. 1 and the schematic diagram of the solar dryer indicating the measurement positions of the thermocouple channels during load test is shown in Fig.2.

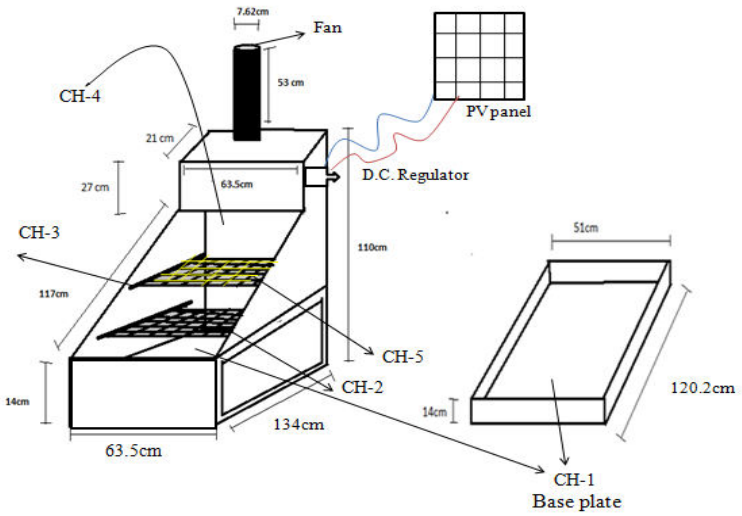

Fig. 2. Schematic diagram of developed solar dryer indicating measurement positions of thermocouple channels for load test

3. EXPERIMENTAL OBSERVATIONS

The performance tests of solar dryer presents the experiments without load and with load on the developed solar dryer and observations related to the temperature inside the dryer, drying rate and efficiency.

3.1. Experimental observations without load

The without load test was carried out to understand the trends of various operating parameters with respect to time. The positions of various thermocouple channels of the temperature data logger for the experiment without load for recording temperatures are presented in table 1.

Table 1: Details of thermocouple channels

Channel 1	Temperature of dryer base plate
Channel 2	Temperature of middle (second) tray inside dryer
Channel 3	Temperature of first tray inside dryer
Channel 4	Air temperature inside dryer
Channel 5	Ambient air temperature

The temperature profile without load at various positions inside dryer is as shown in fig. 3. It was observed that the solar radiation increased up to 1:00 PM and then decreased. Similarly, the ambient temperature increased with the day time and begins to fall in the afternoon hours. The maximum temperature was attained inside dryer at 12:55pm. Maximum base plate temperature attained inside dryer was 87°C, when the radiation was 975W/m^2 while the minimum

temperature was 43°C at 5 pm when the radiation was 323W/m^2. The maximum ambient temperature was recorded 35°C at 12:55 pm, while the minimum ambient temperature was at 10am. From fig. 3 and 4 it can be inferred that the temperature rise is the function of solar radiation and ambient temperature.

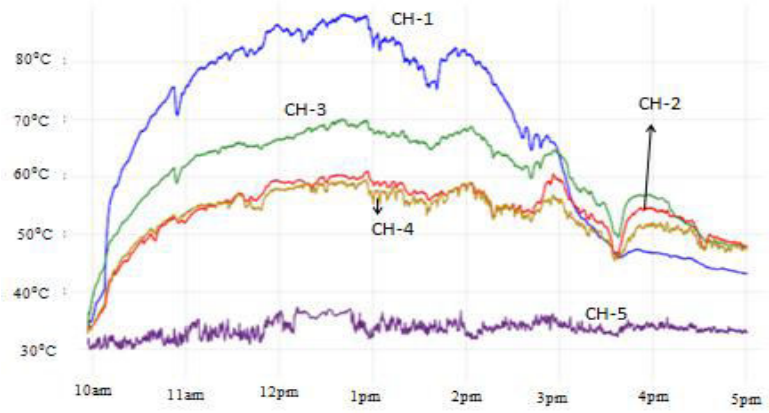

Fig. 3. Thermal performance curve for solar dryer without load test (Temperature plotted with time 27-03-2019)

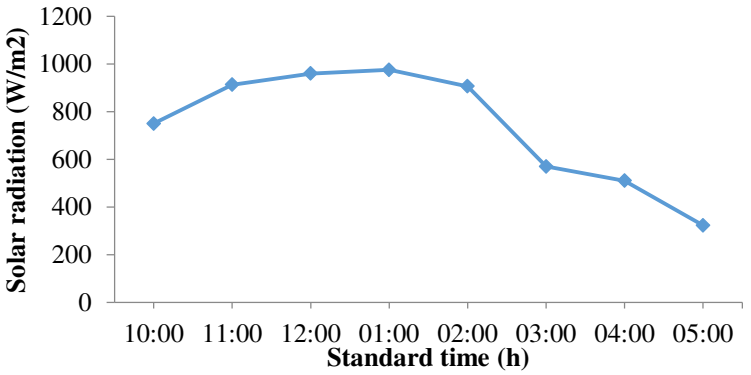

Fig. 4. Solar radiation (W/m^2) with standard time (27-03-19)

3.2. Experimental observations with load

Experiments were performed to evaluate the thermal performance and efficiency of the dryer for drying of grapes. The experiment was conducted with one kg load of grapes. The observations were recorded for the temperature profile of the various parts of the dryer, ambient temperature and variation of solar radiation with standard time. Five thermocouple channels of the temperature data logger were placed inside the dryer and one was placed outside to record ambient air temperature. The details of the channels are shown in table 2.

Table 2: Details of thermocouple channels

Channel 1	Temperature of dryer base plate
Channel 2	Temperature of middle (second) tray inside dryer
Channel 3	Temperature of first tray (upper tray) inside dryer
Channel 4	Air temperature inside dryer
Channel 5	Temperature of mesh with grapes placed on first tray
Channel 6	Ambient air temperature

3.2.1. Day 1

One kg grapes were put on upper tray (first tray) on a wire mesh inside dryer. Weight of the grapes was recorded at the starting and at the end of the day around 5 p.m. The temperature profile corresponding to the data logger channels and the solar radiation variation are shown in fig.5 and 6.

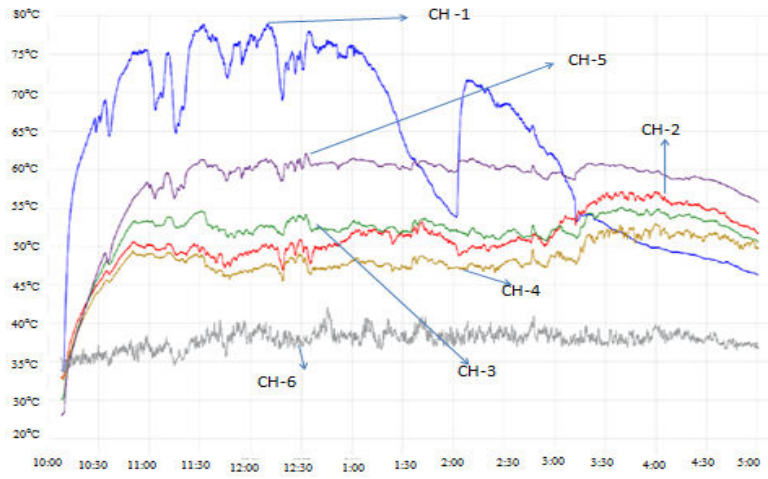

Fig. 5. Temperature profiles of various channels with standard time during load testing of solar dryer (1-04-19)

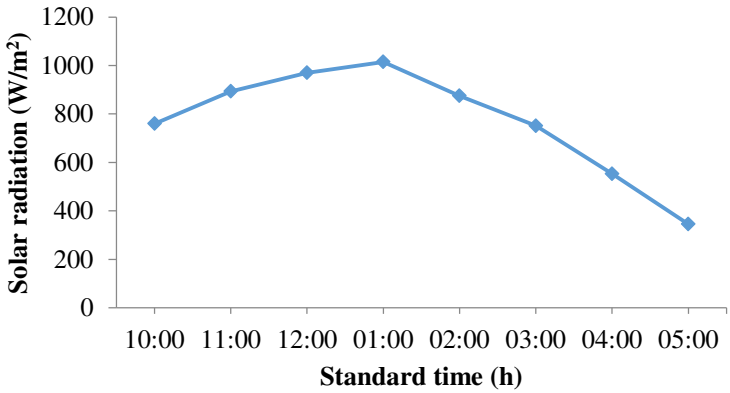

Fig. 6. Solar radiation (W/m^2) with standard time (1-04-19)

After drying process at 5 pm, the weight of grapes has been recorded as 854 grams. Thus, 146 grams of moisture was removed in 7 hours of effective drying process. With the help of exhaust fan the inside temperature of the dryer was controlled. CH-5 shows the maintained temperature of the grapes tray around 50-60℃. Humidity measured inside dryer was 23% at 10am and 10% at 5pm. For maintaining temperature inside dryer the fan was started at 11:00am with speed 1.3m/sec. CH-1 shows the decrease in the base plate temperature from 1 to 2 pm by shadow effect of dryer walls and by decrease in the solar radiation. CH-1 shows the increase of the base plate temperature at 2:00pm by tracking of dryer. Fan is put off at 3:00pm to maintain the inside temperature.

3.2.2. Day 2

Weight of the grapes was recorded at the starting of the second day and found to be 810gm at 10am. The grapes were put inside dryer for drying and at the end of the day the weight was around 709 gm at 5p.m. The temperature profile corresponding to the data logger channels and the solar radiation variation on second test day are shown in fig.7 and 8. CH-5 shows the maintained temperature of the grapes tray around 55-65℃. Humidity measured inside dryer was 21% at 10am and 10% at 5pm. For maintaining the temperature inside the dryer, the fan was started at 11:00am with speed 1.3m/sec. CH-1 shows the increase of the base plate temperature at 2:30pm by tracking of dryer. Fan was put off at 3:00pm to maintain the inside temperature. After drying process at 5 pm weight of grapes was found to be 709 grams as 101 grams of moisture was removed in 7 hours of effective drying process.

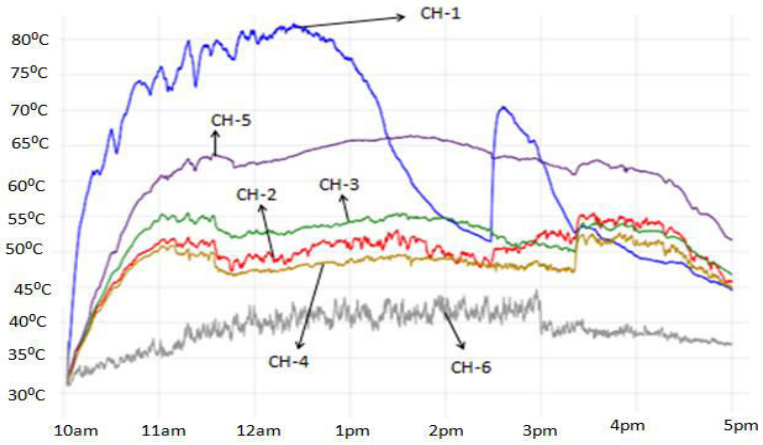

Fig. 7. Temperature profiles of various channels with standard time during load testing of solar dryer (2-04-19)

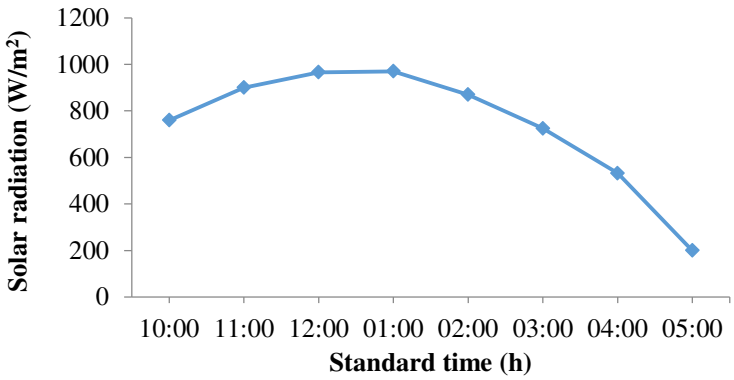

Fig. 8. Solar radiation (W/m^2) with standard time (2-04-19)

3.2.3. Day 3

On third day at 10 am 676 grams grapes were put in the dryer upper tray. CH-5 shows the maintained temperature of the grapes tray around 55-65℃. Humidity measured inside dryer was 24% at 10am and 10% at 5pm. For maintaining temperature inside dryer the fan starts at 11:00am with speed 1.3m/sec. CH-1 shows the increase of the base plate temperature at 1:35pm by tracking of dryer. Fan is put off at 3:00pm to maintain the inside temperature. After drying process at 5 pm weight of grapes was 516 grams as 160 grams of moisture was removed during the drying process.

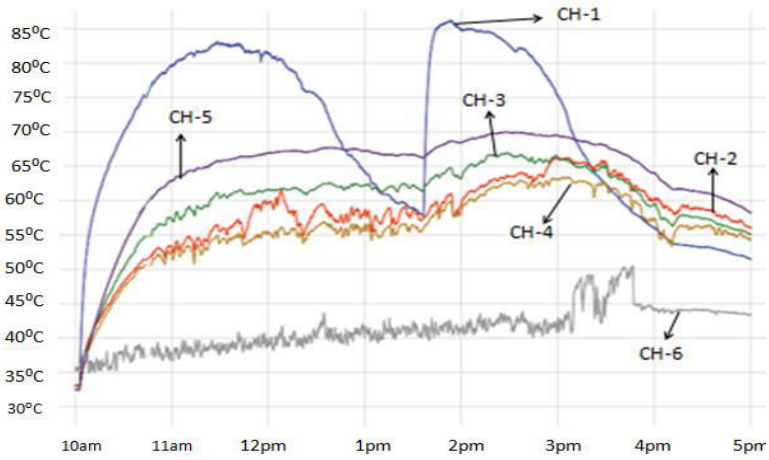

Fig. 9. Temperature profiles of various channels with standard time during load testing of solar dryer (3-04-19)

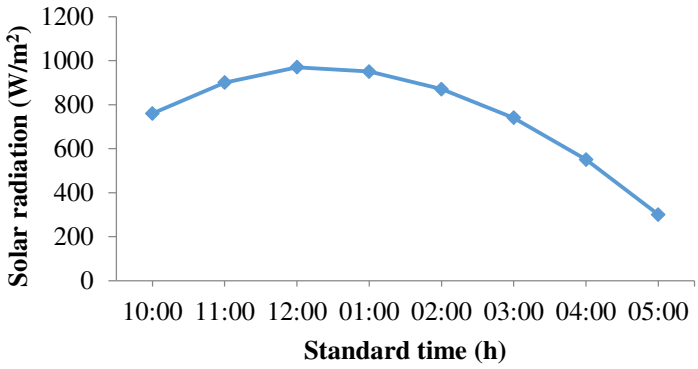

Fig. 10. Solar radiation (W/m^2) with standard time (3-04-19)

3.2.4. Day 4

On 4th day at 10 am 490 grams grapes were put in the dryer upper tray. Ch-5 shows the maintained temperature of the grapes tray around 55-65℃. Humidity measured inside dryer was 22% at 10am and 10% at 5pm. For maintaining temperature inside dryer the fan was started at 11:00am with speed 1.3m/sec. CH-1 shows the decrease in the base plate temperature after 2:10pm by shadow effect of dryer walls and by decrease in the solar radiation. Fan is put off at 2:00pm to maintain the inside temperature. After seven hours of drying process at 5 pm weight of grapes was found to be 388 grams as 102 grams of moisture was removed.

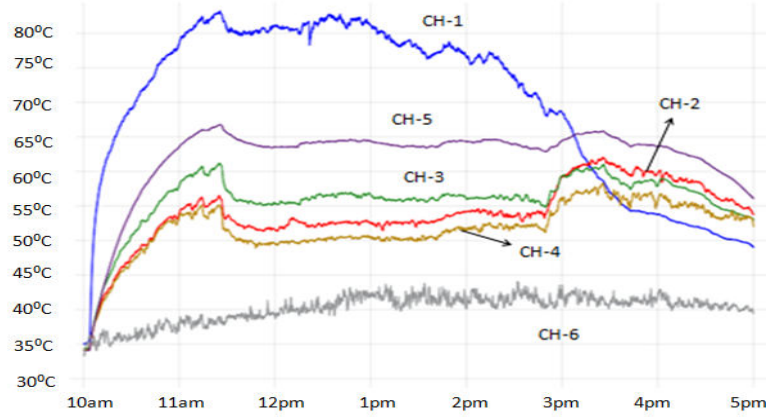

Fig. 11. Temperature profiles of various channels with standard time during load testing of solar dryer (04-04-19)

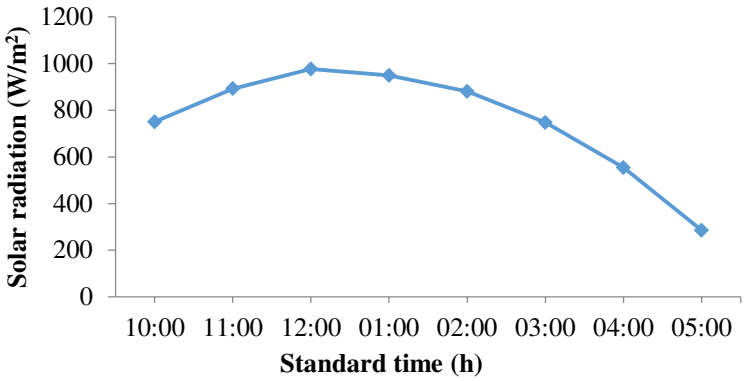

Fig. 12. Solar radiation (W/m^2) with standard time (04-04-19)

3.2.5. Day 5

On 5th day at 10 am 367 grams grapes were put in the dryer upper tray which has area of 2856 cm^2. Humidity measured inside dryer was 21% at 10am and 10% at 5pm. For maintaining temperature inside dryer the fan was started at 11:30am with speed 1.3m/sec. All channels show the temperature decrease inside dryer from 12:45pm to 1:45pm by decrease in the solar radiation. Fan is put off at 12:45pm to maintain the inside temperature. After seven hours drying duration at 5 pm the weight of grapes was recorded 260 grams as 107 grams of moisture got removed.

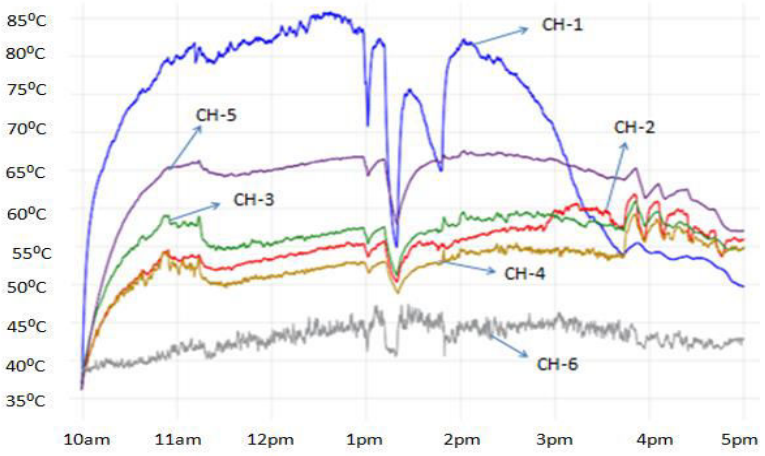

Fig. 13. Temperature profiles of various channels with standard time during load testing of solar dryer (05-04-19)

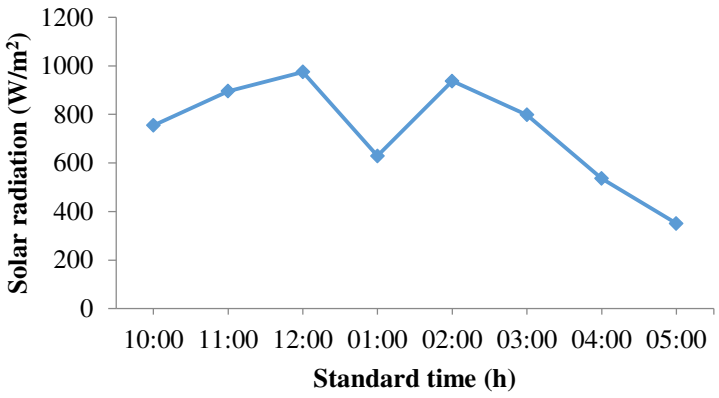

Fig. 14. Solar radiation (W/m^2) with standard time (05-04-19)

4. PERFORMANCE EVALUATION AND DISCUSSION

4.1. Moisture content

Moisture content of grapes was determined by calculating weight of grapes before drying and after drying for each day. The difference in weight is divided by initial weight and percentage is taken.

4.2. Drying rate

Drying rate is calculated by dividing the weight loss from the grapes due to moisture removal by the time period.

4.3. Efficiency

The thermal efficiency is defined as the ratio of thermal energy utilized for drying to the thermal energy available for drying [11].

$$\eta = \frac{m_v L}{I_{av} A_{in} t} x100 \qquad (1)$$

where, η = thermal efficiency, m_v is mass of moisture evaporated in total drying time, A_{in} is effective area of collector, I_{av} is the daily average solar radiation on the dryer surface area, t is the time in second and L is the latent heat of water (for moisture).

Table 3: Efficiency and drying rate of grapes in the developed solar dryer

Day	Initial weight (kg)	Final weight (kg)	Solar radiation I_{av} (W/m^2)	Moisture removal (%)	Efficiency (%)	Drying Rate (kg/hr)
1	1	0.854	0.770	14.6	5.71	0.020
2	0.810	0.709	0.740	12.46	4.07	0.014
3	0.676	0.516	0.755	23.66	6.34	0.022
4	0.490	0.388	0.754	20.81	4.03	0.014
5	0.367	0.260	0.734	29.15	4.35	0.015

From the above figures 3-14 and table 3, it can be seen that the dryer was able to achieve the required temperatures for drying of grapes. The weight of 1kg of grapes reduced to 0.260 kg in five days and raisins were developed. The daily basis reduction in moisture content has been observed as on day one it was 14.06%, on day two 12.46%, on day three 23.66%, on day four 20.81% and on day five 29.15%. The humidity levels inside dryer were generally in the range 21-24% in the morning when solar drying was started, by the evening the humidity levels observed inside dryer were around 10%. The grapes were again placed inside dryer after weighing at 5 p.m. to make use of the remaining heat inside dryer during the night. As a result slight decrease in mass is observed when the experiment was started next day.

During the experiments solar radiation remained on an average around 700 W/m^2 with clear sky except for cloud cover on 5^{th} April for short duration at 1:00 p.m. It can be seen from fig. 13 and 14 that due to cloud cover the temperature corresponding to different channels fell down, major change in temperature was for base plate temperature (25-30^oC). The temperature of other components reduced just by around 5-7^oC. It is interesting to observe that there is a time lag of around 15 minutes between decrease in solar radiation and the observed decrease in temperatures of the various channels. This short term cloud cover did not have any major impact on overall performance, 29% of moisture reduction was observed with 4.35% efficiency on this day. Drying rate and the efficiency are observed to be highest on the third day. The efficiency of system lies within 4% to 7% for the conducted experiments. The reason for low efficiency is that the load is not optimized. Further works will be taken up to optimize the load for this developed system.

This developed solar drying system is a compact system which can be easily manually tracked and air speed can be controlled. This solar drying system holds promise to become a useful device for domestic drying applications and to be beneficial for cottage industries.

5. CONCLUSIONS

The grapes were converted in raisins within five days with the help of direct type solar dryer. Temperature variations in various system components were observed along with ambient air temperature, air temperature inside the dryer and global solar radiation on daily basis. Temperature control appropriate for grape drying was maintained between 55-60^oC with a small DC fan coupled with solar PV panel. The efficiency of system was found to be in the range 4% to 7% for drying of one kg grapes. There is scope of future studies to optimize the load and improve the efficiency of the system with slight modifications.

This system can be a useful aid in domestic drying applications and can be promising for use in cottage scale industries.

ACKNOWLEDGEMENT

Authors gratefully acknowledge the support of Royal Academy of Engineering, UK through Newton-Bhabha Higher Education Partnership Project.

REFERENCES

1. A.G.M.B. Mustayen, S.Mekhilef, R.Saidur, Performance study of different solar dryers: A review, *Renewable and Sustainable Energy Reviews*, 34, 2014, 463–470.
2. Pushpendra Singha, Vipin Shrivastava, Anil Kumar, Recent developments in greenhouse solar drying: A review, *Renewable and Sustainable Energy Reviews* 82 , 2018, 3250–3262.
3. http://www.walkthroughindia.com/offbeat/top-10-largest-grapes-producing-states-of-india/.
4. Pangavhane, D.R., Sawhney, R.L., Review of research and development work on solar dryers for grape drying. *Energy Conversion and Management* 43, 2002, 45–61.
5. Karathanos, V.T., Belessiotis, V.G., Sun and artificial air drying kinetics of some agricultural products. *Journal of Food Engineering* 31, 1997, 35–46.
6. Mahmutoglu, Teslime, Ferhunde, Emir, Birol Saygi, Y., Sun/solar drying of differently treated grapes and storage stability of dried grapes. *Journal of Food Engineering* 29 (3–4), 1996, 289–300.
7. Togrul, Inci Turk, Dursun, Pehlivan, Modelling of thin layer drying kinetics of some fruits under open-air sun drying process. *Journal of Food Engineering* 65, 2004, 413–425.
8. Fadhel, A., Kooli, S., Farhat, A., Bellghith, A., Study of the solar drying of grapes by three different processes. *Desalination* 185, 2005, 535–541.
9. Ilhem Hamdi, Sami Kooli, Aymen Elkhadraoui, Zaineb Azaizia, Fadhel Abdelhamid, Amenallah Guizani, Experimental study and numerical modeling for drying grapes under solar greenhouse, *Renewable Energy* 127 , 2018, 936-946.
10. M. Khan, N. Sengar, S. Mahavar, Fabrication and testing of a low cost passive solar dryer In S. Riffat, N. Ismail, Y. Su, & M. Idayu Ahmad (Eds.), Proceedings of the 18th International Conference on Sustainable

Energy Technologies (SET 2019), 20-22 August 2019, Kuala Lumpur, Malaysia, Vol.3, paper no. 259, pp.21.

11. A. Saleh, I. Badran, Modeling and experimental studies on a domestic solar dryer, *Renewable Energy* 34, 2009, 2239-2245.

Cite this article

Nitin Sharma and Namrata Sengar, Experimental Studies on Developed Direct Solar Dryer for Conversion of Grapes into Raisins with Temperature Control, In: Sandip A. Kale editor, Advanced Research in Solar Energy, Pune, Grinrey Publications, 2021, pp. 1-14

2 Design and Analysis of Solar Water Pumping System

Lakhdara Amira[a,*], Bahi Tahar[b] and Moussaoui Abdelkrim[a]

[a]Departmentof Electrical and automatic Engineering_LGEG, 8 may 1945 Guelma University, Guelma, Algeria
[b]Department of Electrical, LASA laboratory, Badji Mokhtar Mokhtar University, Annaba, Algeria

*Corresponding author: lakhdara.amira1985@gmail.com

ABSTRACT

According to the current state of the art, stand-alone photovoltaic installations are increasingly intended for water pumping, and have become a very competitive solution for remote areas. Indeed, photovoltaic pumping systems can offer the advantage of the lowest maintenance and the opportunity to save energy. Therefore, the simplest solar water pumping systems are the ones that operate directly when the sun is shining, but the performance of these systems depends on climatic conditions including solar irradiation and ambient temperature. However, in a remote area these installations do not require electrical storage systems despite the various climatic conditions. This work concerns the design, modeling and functional analysis of a photovoltaic water pumping system operating under the sun, with a view to its installation in an isolated area so that the water stored in a tank is consumed in real time or in case of need even if the pumping operation is not operational. The simulation is carried out using Matlab/Simulink environment, to evaluate the pumping installation performances. The simulation results show that the pumping system works as desired.

Keywords: Pumping system, photovoltaic, climatic conditions, solar energy

Advanced Research in Solar Energy | ISBN: 978-81-948951-7-6
Book Series: Research Transcripts in Energy | Vol: 01

1. INTRODUCTION

In recent years, governments around the world have insisted that part of the energy be produced from renewable sources [1,2]. Since Algeria is considered the biggest country on the African continent by its surface of 2.381741 km^2, of which 4/5 are occupied by the Sahara where the weather is generally sunny, it's around 3650 hours of sunshine / year. The photovoltaic energy is strongly applied for pumping water mainly in sunny areas, taking advantage of the free fuel source which is sunlight. The presence of a solar pumping system is a cost-effective and safe solution for supplying water using clean energy, by taking advantage of the vast Algerian Sahara, which is characterizedby its distance from the electrical distribution network, the installation of electricity production systems is a remarkable solution to meet the needs of the population[3]. This environment is therefore suitable for the installation of photovoltaic pumping systems.

The photovoltaic pump system converts solar energy into electrical energy to drive a pump from an electric motor. Despite the initial investment in this system is expensive, systems can be installed as small as possible, but run as often as possible. In this case the solar pumping system cannot supply a large amount of water quickly but will be relatively inexpensive to use for many continuous hours[4]. Therefore, water storage will often be an essential element for solar pumping.

The aim of this work is the functioning of the photovoltaic pump system over the sun and to perform an indirect storage in the form of a water tank in the reason of the elimination of batteries. There are two parts: the first part is devoted to the modeling of the system (PV, Permanent Magnetic DC Motor (PMDC), Pump) and the simulation, the analysis and interpretation of simulation results are presented in the second part to validate the performance of this system under various climatic conditions.

2. MODELING OF THE SYSTEM

The performances of solar pumping depends on the characteristics of the chosen site (Irradiation, Temperature,...) and the characteristics of the chain equipment (PV, Electronics Inverters, PMDC, Pump and the Storage system) [5,6].

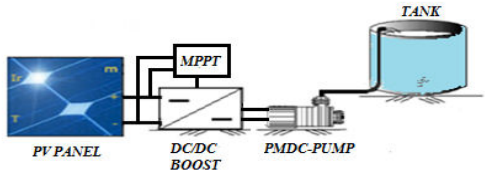

Fig. 1. Schematic bloc diagram of PV system

2.1. Photovoltaic Panel

The photovoltaic cell is also represented by the "standard" model with a diode[7].

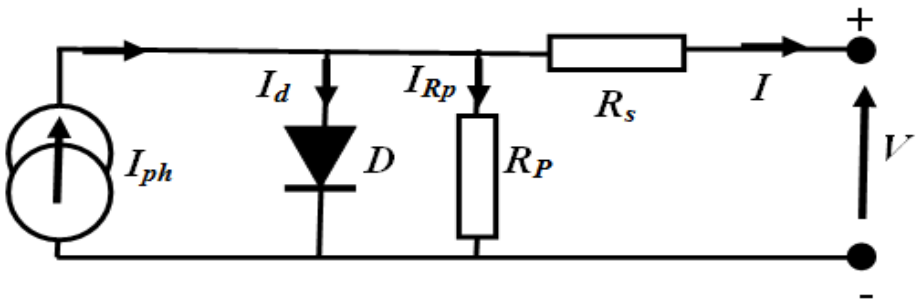

Fig. 2. Electric model equivalent to a diode of the photovoltaic cell

Where,$R_p(\Omega)$: parallel resistance which characterizes the currents of the junction; $R_s(\Omega)$: serial resistance which characterizes the various resistances of the contacts and connection; $I_{cc}(A)$: Short-circuit current (Photovoltaic) which depends on the sunshine and the temperature; $I_d\ (A)$: Current through the diode; $I_{Rp}(A)$: Current through the parallel resistor.
From Figure.2, we can deduce:

$$I = I_{ph} - I_d - I_{R_p} \tag{1}$$

With,

$$I_{Rp} = \frac{V + R_s \times I}{R_p} \tag{2}$$

And,

$$I_d = I_0 \times e^{\frac{V+R_s I}{V_t}} - 1 \tag{3}$$

So,

$$I_{ph} = (I_0 \times e^{\frac{V+R_s \times I}{V_t}} - 1) - (\frac{V + R_s \times I}{R_p}) \tag{4}$$

To show the influence of irradiation and temperature on behavior, characteristics $I=f(V)$ and $P=f(V)$ obtained by simulation are shown in the

Figure.3. Furthermore, the short circuit current and the open circuit voltage can be determined from those characteristics.

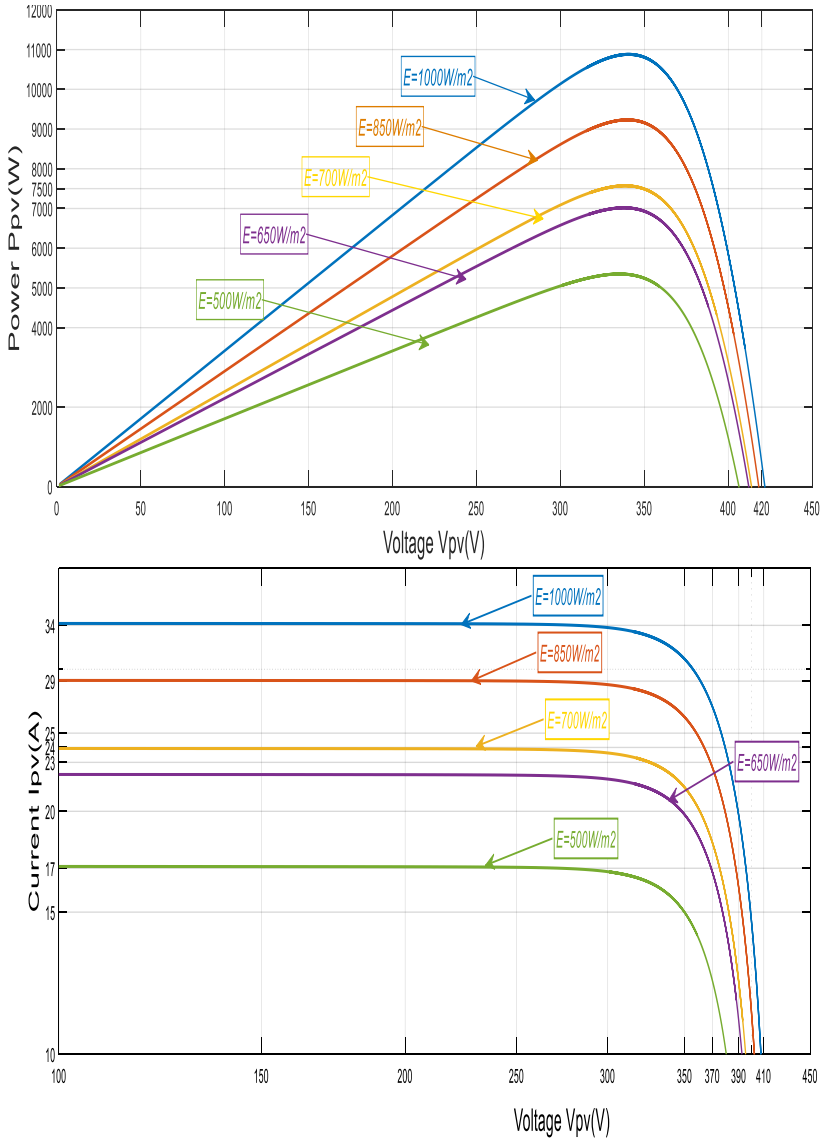

Fig. 3. Characteristics I=f(v), P=f(v) variation of E

2.2. DC-DC Boost converter

Power systems use Boost converter to increase the output voltage at the input of the inverter, its block diagram is that of Figure.4.

We notice that the semiconductor *(S)* requires a command *(D)*. However, the closing (T_f) (blocked: non-passing) and opening (T_o) (passing) periods for a period of the control cycle (T_c) defines the duty cycle *(D)*.

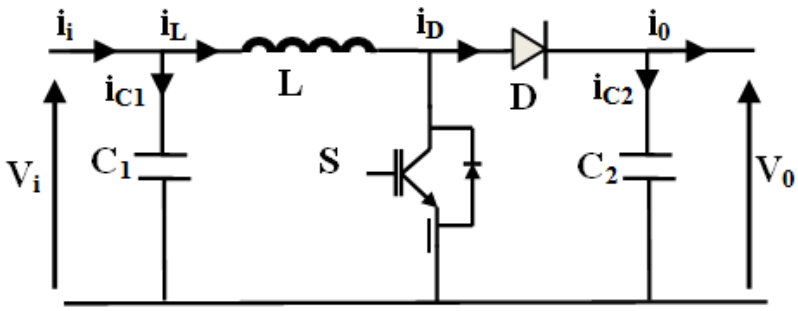

Fig. 4. Schematic diagram of a Boost converter

$$D = \frac{T_o}{T_c} = 1 - \frac{V_i}{V_o} \tag{5}$$

Where, V_i: input voltage and V_o: output voltage. The inductance and the capacitance are calculated respectively as below [8]:

$$L = \frac{D.V_i}{\delta.I_i.f)} \tag{6}$$

$$C = \frac{D.I_o}{\delta.V_o.f)} \tag{7}$$

Where, f: switching frequency, I_i: input current, I_o: output current and the ripple limit ($\delta = 1\%$).

Thus after sizing the Boost chopper, the figure.5 shows that for an input voltage of 100 V, the output has stages corresponding to the three values of the duty cycle *(D)*.

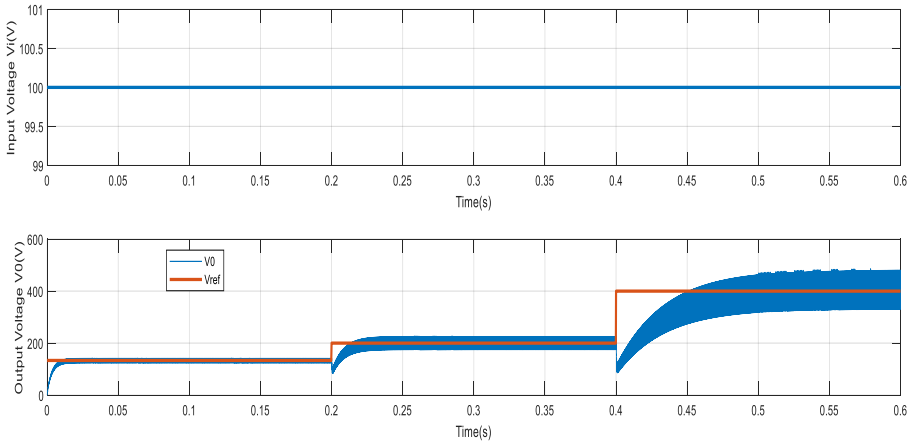

Fig. 5. Input voltage (Vi) and output voltage (Vo) of a Boost chopper with changes of (D)

2.3. Permanent Magnetic Motor

The DC motor of a photovoltaic pump converts electrical energy into mechanical energy. The PMDC motor does not need external excitation because its field winding is permanent magnetic. This type of the motor is defined by the following relationships [9,10]:
The voltage is defined by:

$$U = R_a.I_a + L_a.\frac{dI_a}{dt} + K_m.\omega_m \tag{8}$$

Where, U: DC source voltage *(V)*, I_a: armature current *(A)*, R_a: armature resistance *(Ω)*, L_a: armature inductance *(H)*, K_m: torque constant (V.s/rad) and ω_m: motor speed (rpm).

The electrical torque T_{em} *(N.m)*,

$$T_{em} = K_m.I_a \tag{9}$$

The dynamic equation is:

$$J\frac{d\omega_r}{dt} = T_{em} - T_l - B\times\omega_m \tag{10}$$

Where, J: inertia constant *(kg.m²)* and B: constant *(N.m.s)*.
So, the PMDC equivalent circuit is shown by the Figure 6.

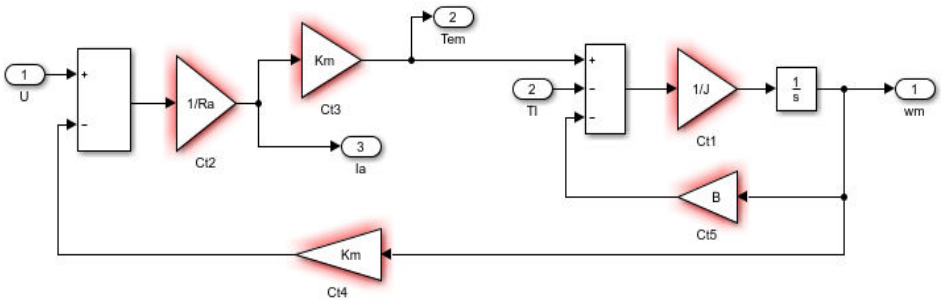

Fig. 6. Permanent magnetic DC motor model

2.4. Pump modeling

The pump is a machine that converts mechanical power into liquid power, it is directly coupled to the motor and characterized by the torque, the speed and the flow [11,12].

$$T = 4{,}8.10^{-6}.\omega^2 + 0{,}00019.\omega + 0{,}092 \tag{11}$$

$$Q = \frac{\eta . P}{\rho . g . H} \tag{12}$$

$$H = 4{,}923.10^{-3}.\omega^2 - 1{,}5826.10^{-5}.\omega.Q + 18144.Q^2 \tag{13}$$

Where, *(P)*: input power required *(ω)*, *(ρ)*: fluid density *(kg/m^3)*, *(H)*: energy head added to the flow *(m)*, *(g)*: standard acceleration of gravity *(9.81 m/s^2)*, *(Q)*: flow rate *(m^3/s)* and *(η)*: efficiency of the pump plant.

3. SIMULATION RESULTS

The operation of the system considered is analyzed taking into account a variable irradiation profile and at a temperature equal to its standard value 25°C, as shown in Figure 7.Starting with a constant irradiation level between 0s and 0.2s, the corresponding voltage as well as the other quantities represented by the same figure remain invariable.The PMDC supply voltage increases when the irradiation goes from 200W/m^2 to 1000W/m^2. This increase causes the speed of the PMDC to increase, consequently the increase in mechanical power, which results in a flow rate of the centrifugal pump proportional to the irradiation.At 0.8s there is a decrease in the irradiation from 1000W/m^2 to 600W/m^2 which causes a decrease in the speed of the PMDC which in turn causes the decrease in the pump flow.

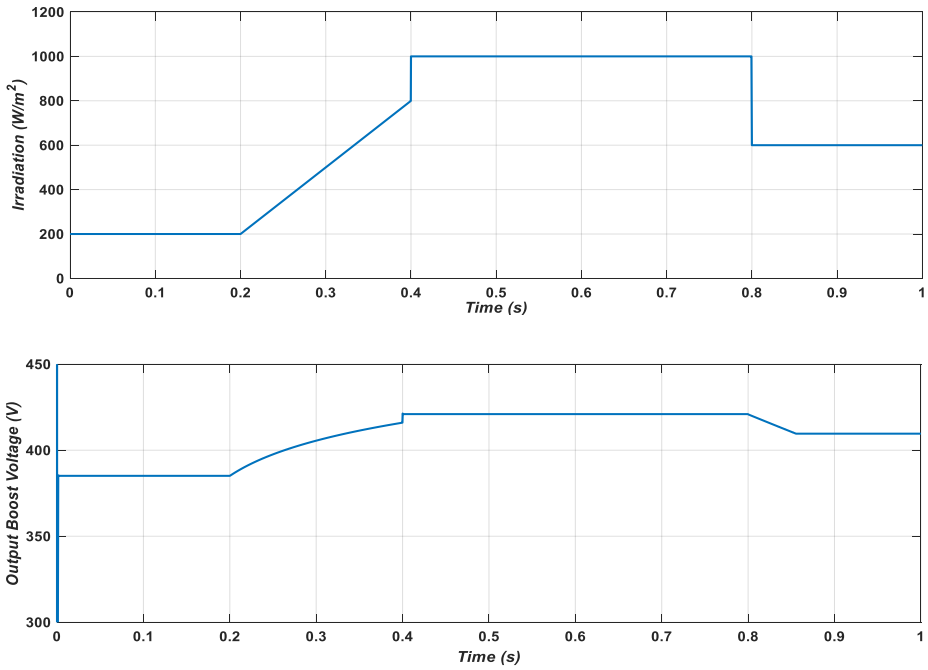

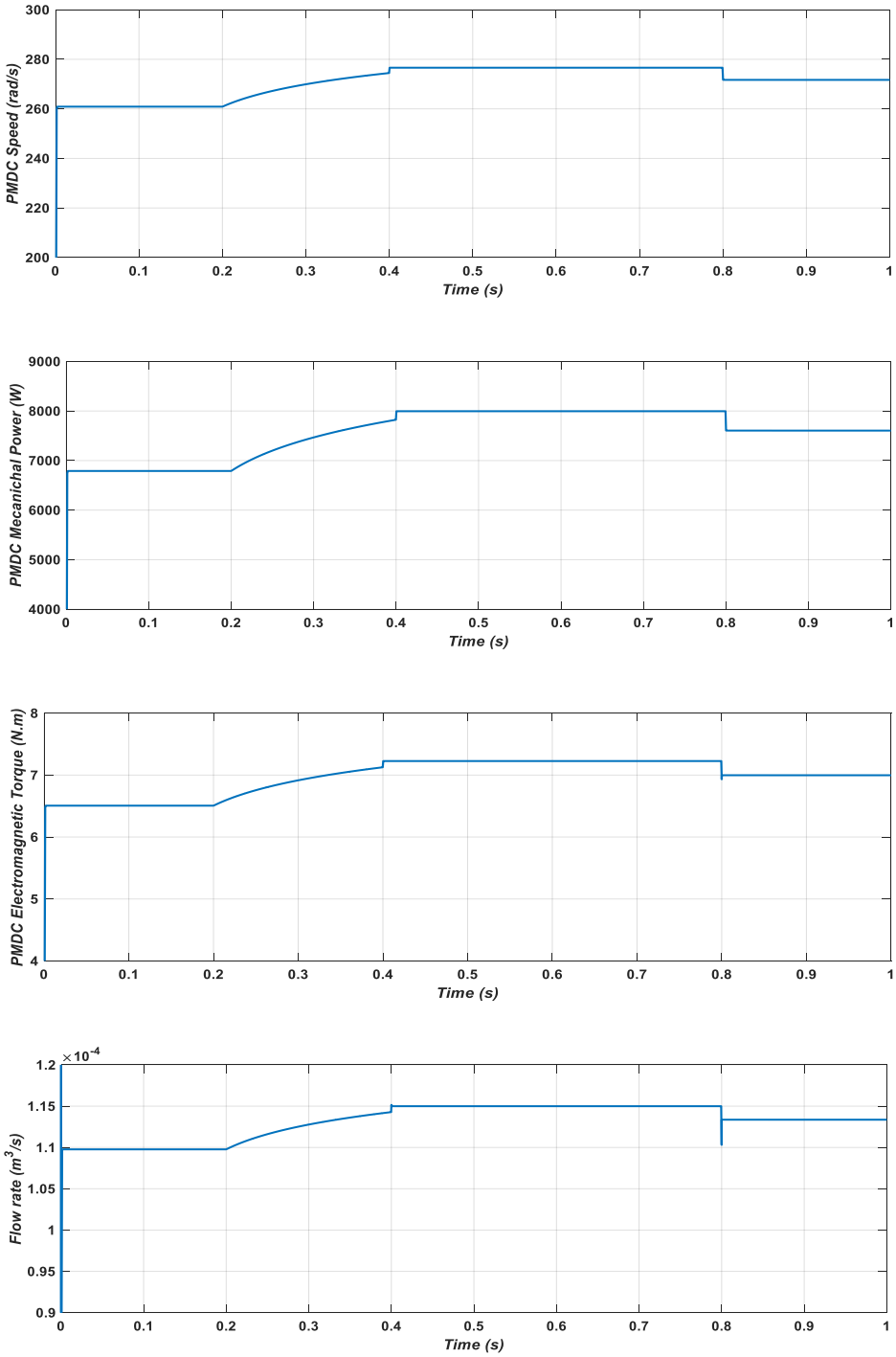

Fig. 7. Characteristics of solar water pumping system

4. CONCLUSION

This work consists of the study and operation analysis of a pumping system intended to be installed in an isolated site. Our intention waste analysis of this operation over the sun under a variable irradiation. Thus, the generalization and encouragement of such facilities for the population living in the vast Algerian Saharian areas is a promising solution to satisfy their water needs, by a simple disposal in a tank without resorting to the use of storage by battery or other alternatives , this system is less expensive and reduces the aggressiveness of the saharian climate.

NOMENCLATURE

F	:	Switching frequency (Hz)
I_a	:	Armature current (A)
I_{cc}	:	Short-circuit current (A)
I_d	:	Current through the diode (A)
I_i	:	Input current (A)
I_o	:	Output current (A)
K_m	:	Torque constant (V.s/rad)
L_a	:	Armature inductance (H)
R_a	:	Armature resistance (Ω)
R_p	:	Parallel resistance (Ω)
R_s	:	Serial resistance (Ω)
T_{em}		Electrical torque (N.m)
U	:	DC source voltage (V)
V_i	:	Input voltage (V)
V_o	:	Output voltage (V)
ω_m	:	Motor speed (rpm)

REFERENCES

1. C.K. Panigrahi, Pradosh Ranjan Parida, M. Das, J. Pati, Design and Modeling of Photovoltaic Water Pumping System, *IJLTEMAS*, Volume III, Issue XII, December 2014.
2. Hamad Raad Salih, Ali Abdulwahhab Abdulrazzaq, Basarab Dan Guzun, Dynamic Modeling of Pump Drive System utilizing Simulink/MATLAB, *Program International Research Journal of Engineering and Technology*, Volume: 03 Issue: 01 , Jan-2016.
3. M.R.Yaiche, A.Bouhanik, S.M.A.Bekkouche, A.Malek, T.Benouaz, Revised solar maps of Algeria based on sunshine duration, *Energy Conversion and Management*, Volume 82, June 2014, Pages 114-123.

4. Shinde, Wandre Sarika, Solar photovoltaic water pumping system for irrigation: A review, *African Journal of Agricultural ResearchER*,Volume 10, DO- 0.5897/AJAR2015.9879 .
5. M. Benghanem, K.O. Daffallah, A. Almohammedi, Estimation of daily flow rate of photovoltaic water pumping systems using solar radiation data, Results in Physics 8 (2018) 949–954.
6. Dhafer Mezghani, Abdelkader Mami, Input-Output Linearizing Control Of Pumping Photovoltaic System: Tests And Measurements By Micro-Controller Stm32, *International Journal of Advances in Engineering & Technology, Sept 2012*, Vol. 4, Issue 2, pp. 25-37.
7. Z. Layate, T. Bahi, S. Lekhchine, Control of a photovoltaic pumping system, Conférence Internationale en automatique et traitement de signal (ATS-2018), Proceeding of Engineering and Technology, Vol.36 pp.29-34.
8. Muamer M. Shebani,Tariq Iqbal, Dynamic Modeling, Control, and Analysis of a Solar Water Pumping System for Libya, *Hindawi Journal of Renewable Energy*,Volume 2017, Article ID 8504283, 13 pages.
9. Mohan Kashyap, Saurabh Chanana, Jai Singh Arya, Solar Powered Pmdc Motor Drive, *Atlantis PressConference on Advances in Communication and Control Systems 2013 (CAC2S 2013)*, pp 18-22.
10. M. O. Charles, D. E. Oku, F. O. Faithpraise, E. P. Obot, Simulation and Control of PMDC Motor Current and Torque, *International Journal of Advanced Scientific and Technical Research*, 7 (5) 2015, pp 367-375.
11. Sumit K. Gupta, M. Rizwan Khan, Kaushar Jahan, Modeling, Analysis and Control of Solar Water Pumping System, *Impending Power Demand and Innovative Energy Paths*, ISBN: 978-93-83083-84-8, pp 356-363.
12. Hamad Raad Salih, Ali Abdulwahhab Abdulrazzaq, Basarab Dan Guzun, Dynamic Modeling of Pump Drive System utilizing Simulink/MATLAB Program, *International Research Journal of Engineering and Technology*, Vol 03 Issue: 01, Jan-2016, pp 21-24.

Cite this article

Lakhdara Amira, Bahi Tahar and Moussaoui Abdelkrim, Design and Analysis of Solar Water Pumping System, In: Sandip A. Kale editor, Advanced Research in Solar Energy, Pune, Grinrey Publications, 2021, pp. 15-24

3 Study of Thermal Comfort for Office / Institute Buildings Based on CARBSE Tool and Suggestive Passive Measures for Kota

Antima Sharma[a], Deepmala Meena[b,*], Namrata Sengar[b]

[a]Department of Physics, Carrier Point University, Kota, India
[b]Department of Pure and Applied Physics, University of Kota, Kota, India

*Corresponding author: deepmala.gcb@gmail.com

ABSTRACT

The chapter presents a study of thermal comfort conditions and suggestions for passive measures for naturally ventilated daytime operated buildings which serve as offices and institutes. The study is reported for Kota, Rajasthan, India. For the study, weather and comfort analysis tool developed by Centre for Advanced Research in Building Science and Energy (CARBSE) has been used to estimate the distribution of operating hours in terms of too hot, warm, comfortable, cold and too cold hours. Temperature and humidity distribution with the operating hours are presented. The estimated requirement for operation modes of the buildings in form of natural ventilation, heating, mild cooling, cooling, cooling-dehumidification and dehumidification is reported and on basis of their analysis suggestive passive measures suitable for Kota region are discussed to enhance thermal comfort and reduce energy consumption. Major requirements in Kota are for natural ventilation (28%), mild cooling (27%) and cooling (22%). Thus, the passive measures such as light paint, shading, roof gardens, high reflective coating, low emissivity coating on windows, improving ventilation etc. would be suitable for Kota.

Keywords: Buildings, Offices, Operation modes, Passive measures, Thermal comfort

Advanced Research in Solar Energy | ISBN: 978-81-948951-7-6
Book Series: Research Transcripts in Energy | Vol: 01

1. INTRODUCTION

The aim of buildings is to protect the occupants from the climatic vagaries and provide a comfortable environment to carry out productive work. Buildings consume energy in all phases starting from construction, operation and demolition, and are also responsible for carbon emissions [1]. In order to provide thermal comfort, energy consumption in the building sector during the operation phase has increased manifold due to heating/cooling demands. The energy and electricity demands for building sector in India have been projected to increase by more than twelve times in 2047 from the value in 2012 [2]. Therefore, the need of the hour is to focus on improved energy efficiency in buildings. The building envelopes should be designed in a more responsible manner and passive measures should be adopted to reduce the energy consumption and carbon foot print of the buildings [3,4]. The user needs of thermal comfort should be properly addressed with careful study of climatic parameters of the location and building operation modes.

Few studies have been reported related to buildings and passive measures in Rajasthan [5–8], and for the Kota region even less studies are there [9]. It is important to understand the climatic parameters, building envelope designs, heating/cooling loads and energy consumption in order to improve the thermal comfort and energy efficacy. Study of climatic parameters and building operation modes is important in deciding the appropriate active or passive measures for buildings.

There are two approaches for comfort zones: (i) Fixed Temperature Approach- The comfort zone is specified with temperature 23±1°C and 50±5% relative humidity. (ii) Adaptive Comfort Approach- It assumes that people can adapt in many ways to improve their thermal comfort and therefore a single fixed temperature is not necessary for thermal comfort. This approach is also known as a variable temperature approach. There are two types of thermal comfort models - heat balance model and adaptive comfort model based on above approaches [10-11]. Heat balance models are developed based on experiments in climatic chambers whereas adaptive comfort models are developed on basis of survey and data collection through field studies [12].

Centre for Advanced Research in Building Science and Energy (CARBSE) at CEPT University has developed a ‘Comfort and Weather Analysis’ tool. This tool is supported by the Ministry of New and Renewable Energy of Government of India and Shakti Sustainable Energy Foundation, New Delhi. It is an online tool which can be accessed freely over internet [13]. CARBSE tool is based on adaptive models and uses Indian Model for Adaptive Comfort (IMAC) to develop a relation for neutral temperature for Indian conditions. The tool has

been designed to help the user generate thermal comfort and outdoor weather analysis for Indian cities. IMAC is based on the field surveys conducted in 16 buildings during three seasons. These buildings are in five different cities, which represent five Indian climate zones [14].

Here in present study CARBSE tool has been used for the study of climatic parameters and building operation modes for daytime spaces used as offices/institutes in Kota. This tool not only gives the knowledge of climatic parameters, but also introduces thermal comfort ranges corresponding to relative humidity and temperature for each month over the year. The tool also provides information about the required process for comfort in each month. With the help of this tool climatic parameters, thermal comfort ranges and process requirements for different months has been estimated in Kota region, and on the basis of the analysis of the results, suitable passive measures have been suggested in the present work.

2. METHODOLOGY

Kota is situated in the high solar potential region of Rajasthan, India (25.18°N and 75.83°E). According to climatic data of Kota, May is generally the hottest month of the year, with temperatures soaring as high as 48^0C. January is generally the coldest month of the year. The minimum temperature in winter may range from 9^0C to 28^0C [9]. Comfort and weather analysis tool developed by Centre for Advanced Research in Building Science and Energy is used for analyzing thermal comfort and proposed operation modes of daytime spaces in Kota.

The tool has been used to generate the following information for naturally ventilated daytime spaces in Kota region,

- ASHRAE 55 comfort zone distribution on a daytime basis for Kota.
- The number of operating hours related to temperature distribution that belong to comfort zone.
- The number of operating hours related to humidity distribution
- Suggested operation modes with respect to operating hours
- Percentage distribution of suggested operation modes

3. RESULTS

The results obtained by the use of CARBSE weather and comfort analysis tool for naturally ventilated daytime spaces in the Kota region are shown in Figure 1-5.

3.1. Operating hours (%) for naturally ventilated day time spaces

Figure 1 shows the percentage of operating hours of each month in different zone for daytime naturally ventilated spaces for example offices in Kota. In January, it can be seen that 135 hours (44%) remain too cold, 35 hours (11%) remain cold, 132 hours (43%) remain comfortable, and 6 hours (2%) remain too hot. In February 93 hours (33%) remain too cold, 27 hours (10%) remain cold, 105 hours (38%) remain comfortable, 19 hours (7%) remain warm, 36 hours (13%) remain too hot. In March 12 hours (4%) remain too cold, 11 hours (4%) remain cold, 107 hours (35%) remain comfortable, 33 hours (11%) remain warm, 147 hours (47%) remain too hot. It can be observed that number of too hot hours increase and number of too cold hours decrease with months.

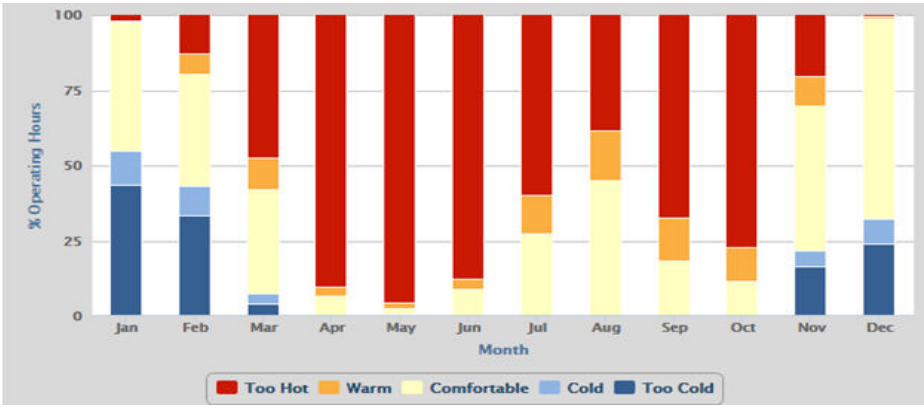

Fig. 1. Operating hours (%) distribution for daytime naturally ventilated spaces in Kota

In the month of April 20 hours (7%) remain comfortable, 9 hours (3%) remain warm, 271 hours (90%) remain too hot. There are no cold and too cold in this month. In May 2 hours (1%) remain cold, 6 hours (2%) remain comfortable, 5 hours (2%) remain warm and 297 hours (96%) remain too hot which is the maximum number of hours than any other month. There is no too cold zone in this month. In June 26 hours (9%) remain comfortable, 11 hours (4%) remain warm and 263 hours (88%) remain too hot. There are no cold and too cold in this month.

Generally monsoon arrives in late June in Kota and July-August experience rains. In July 84 hours (27%) remain comfortable, 40 hours (13%) remain warm and 186 hours (60%) remain too hot. It can be observed that too hot hours decrease with month. Coming to August, 139 hours (45%) remain comfortable, 52 hours (17%) remain warm and 119 hours (38%) remain too hot. In September 54 hours (18%) remain comfortable, 43 hours (14%) remain warm

and 202 hours (67%) hours remain too hot. In October 34 hours (11%) remain comfortable, 36 hours (12%) remain warm and 239 hours (77%) remain too hot. No coldness and no too coldness in this month. There are no cold and too cold zones in July to October.

In November 49 hours (16%) remain too cold, 16 hours (5%) remain cold, 144 hours (48%) remain comfortable, 29 hours (10%) remain warm and 62 hours (21%) remain too hot. In December 74 hours (24%) remain too cold, 26 hours (8%) remain cold, 206 hours (66%) remain comfortable, 2 hours (1%) remain warm and 2 hours (1%) remain too hot. It can be observed that comfortable hours are maximum in this month.

3.2. Temperature distribution of daytime spaces

Figure 2 shows the temperature distribution for the naturally ventilated day time spaces. From the figure it can be seen that 3 hours remain at 12^0C temperature. 240 hours remain below 20^0C temperatures, 1592 hours come between 20^0C to 30^0C temperature and 1818 hours remain above 30^0C temperature, 4 hours remain at 46^0C temperature. It can be seen that 96 hours remain at 21^0C out of which only 7 hours come in comfort zone. 21^0C is lowest limit of comfort zone below this temperature comfort zone is not considered. 116 hours remain at 22 ^{0}C temperature out of which 86 hours come in comfort zone. 133 hours remain at 23^0C temperature out of which 113 hours come in comfort zone.

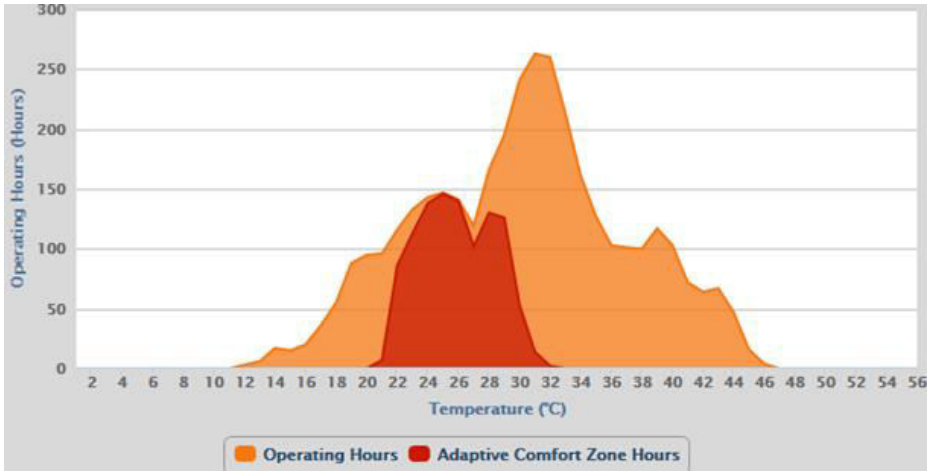

Fig. 2. Temperature distribution for daytime spaces in Kota

260 hours remain at 32^0C temperature, but only 2 hours come in comfort zone. 32^0C is the highest limit of comfort zone, above this limit temperature does not come in comfort zone. From observation it can be seen that 25^0C is the most comfortable temperature for day time spaces because maximum operating hours

(146 hours) at these temperature remain in comfort zone. Outdoor temperature ranges from 12 ^{0}C to 46 ^{0}C. Comfort zone ranges from 21^{0}C to 32^{0}C. Maximum hours (263 hours) are found at 31^{0}C. Total operating hours in day time over year is 3650 hours in which only 1057 hours come in comfort zone.

3.3. Humidity distribution of daytime spaces

Figure 3 shows the humidity distribution for day time spaces like offices over a year. It can be seen from the figure that 9% relative humidity is found for 1 hour, 674 hours lie between 10% to 25% relative humidity, 1707 hours range from 25% to 50% relative humidity, 958 hours ranges from 50% to 75%, 310 hours ranges from 75% to 99%, 99% is the maximum relative humidity which occurs for 9 hours. 38% relative humidity is found for 84 hours which is maximum number of hours,

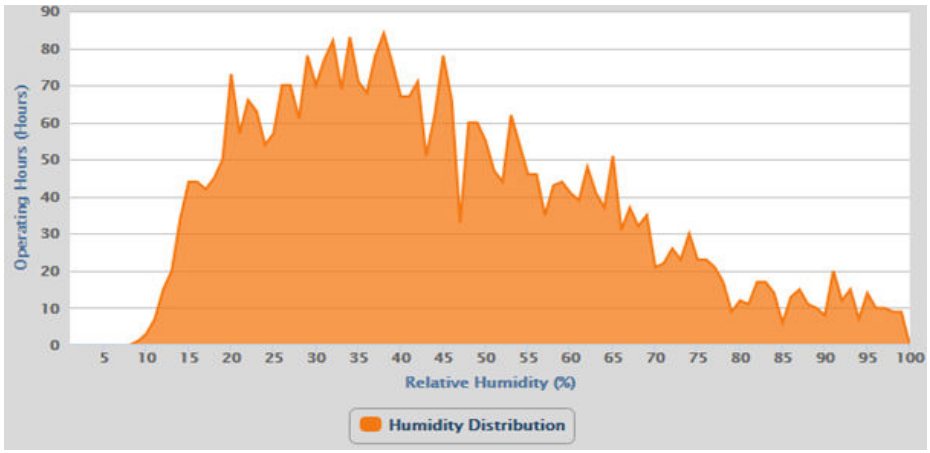

Fig. 3. Humidity distribution for daytime spaces in Kota

3.4. Suggested operation mode for day time spaces-monthly

Figure 4 shows monthly estimated operation modes for day time spaces like offices in Kota. Taking a look at January, it can be seen that heating requirement is 8%, which is more than any other month because it is the coldest month of the year. Natural ventilation is proposed for 85% and dehumidification is suggested for 7% of the total operating hours in this month. There is no need of cooling and mild cooling in this month. February is coming in winter month, but it is less cold than January so heating is decreased and it is 5% only. Natural ventilation is 84%, mild cooling is 10% and dehumidification is 1% only. No cooling is required in this month.

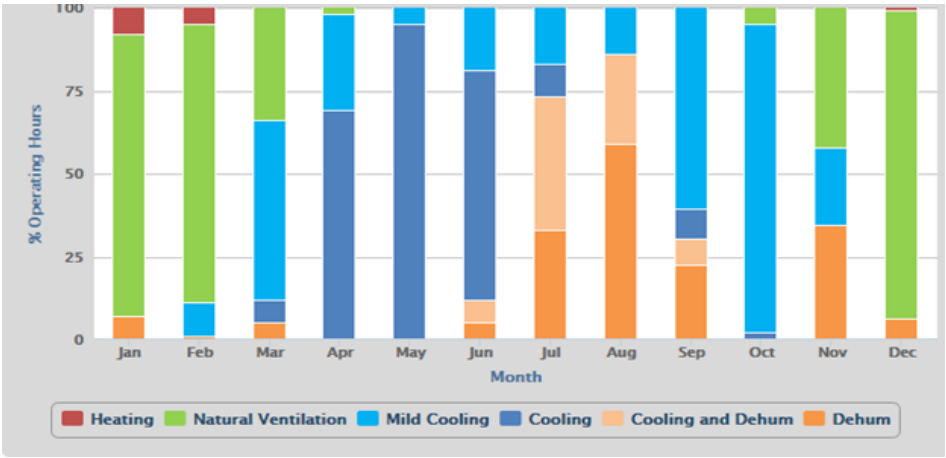

Fig. 4. Suggested operation modes for daytime spaces in Kota on monthly basis

In March, temperatures increase so mild cooling and cooling need increase, which are 54% and 7% respectively, dehumidification is 5% and natural ventilation requirement is 34% of the operating hours in this month. No heating is required in this month. In April temperature increases more, and cooling need is further increased accordingly which is 69%, mild cooling is 29%, natural ventilation is only 2% of the operating hours. No need of dehumidification and heating in this month.

May is the hottest month of the year, so cooling is maximum required in this month and it is 95% which is more than any other month of the year. Mild cooling is 5%. Ventilation is not advised as of hot air from outside will bring in heat and in this month there is no need for dehumidification. No heating is required in this month. In June temperature is slightly lower than May so cooling is also decreased and it is 69%, mild cooling is 19%, cooling and dehumidification is 7% and dehumidification is only 5% of the operating hours. No heating and natural ventilation is suggested in this month.

In July humidity increases so dehumidification is also increased and it is 33%. July is also a little hotter month so cooling and dehumidification is also required and it is 40%, cooling is 10% and mild cooling is 17% in this month. In August humidity level are high, so dehumidification is mostly required in this month and it is 59% which is more than any other month. Cooling and dehumidification is 27% and mild cooling is 14%. In September mild cooling is

estimated for 61%, cooling is 9%, cooling and dehumidification is 8% and only dehumidification is 22%. In October mild cooling is 93%, which is maximum than any other months. Cooling is 2% and natural ventilation is 5%. No dehumidification and no heating in this month.

In November natural ventilation is 42%, mild cooling is 23% and dehumidification is 34%. In November temperature is mostly in the comfortable range, so there is no heating and cooling needs in this month. In December temperature become low as it comes in winter month, so heating is required, but it is only 1%. The natural ventilation requirement is 93%, which is more than any other month and dehumidification is estimated about 6% of the operating hours. Due to cold, no cooling and mild cooling are required in this month.

3.5. Percent distribution of estimated operation modes for daytime spaces

Figure 5 shows the percentage requirement of different estimated modes for comfort for day time spaces such as offices/institutes over the year in Kota. It can be seen that heating required is only 1% which is minimum, cooling and dehumidification is required for 7% of the time, dehumidification required is 15%, cooling is 22%, mild cooling required is 27% and natural ventilation requirement is 28% of the duration.

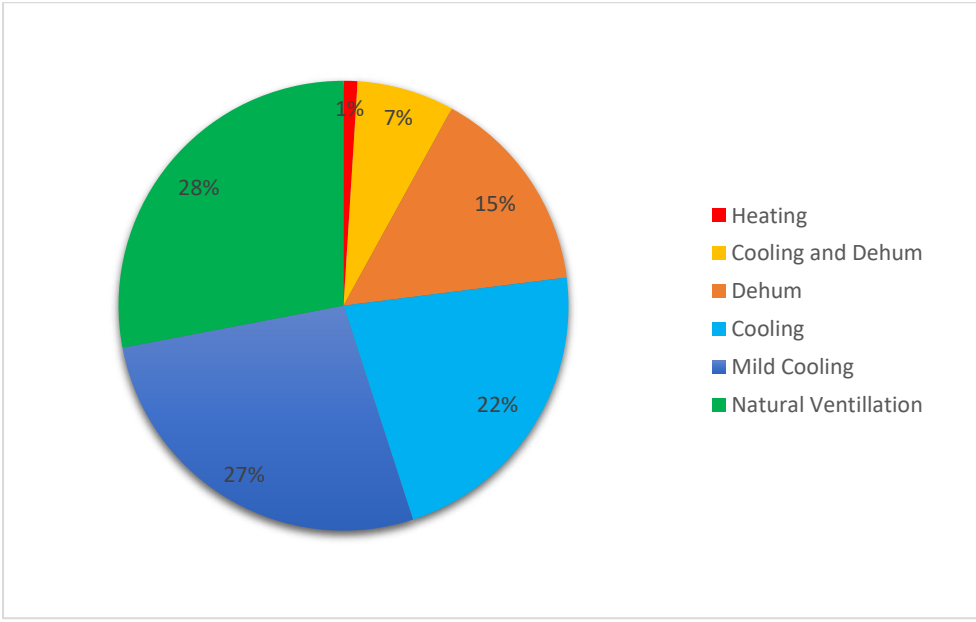

Fig. 5. Percentage distribution of estimated operation modes for daytime spaces in Kota

4. DISCUSSIONS AND SUGGESTIONS

From the results shown in figure 1-5, it is clear that for daytime spaces in Kota region the buildings need to be operated in modes such as for heating, ventilation, cooling and dehumidification to achieve thermal comfort. The need for heating is very less, only 1% of the time duration, so some passive arrangements may be made such as keeping doors and windows closed in winters so that cool air cannot enter from outside to inside. Windows should be provided in the south direction to take advantage of solar heat. Solar radiation should be allowed to enter the building and glass windows should be used to trap solar heat inside. Insulation on walls and roof may also be used, but may add to cost and may trap heat in summers [15].

As heating requirement is less for the Kota region so it is not feasible to put expenses in costly measures and retrofitting for heating of the building, instead it is advisable that people wear warm clothes and low cost passive measures are adopted.

There are many ways to cool house actively and passively, both air conditioners and evaporative coolers are common methods which are generally used for active cooling. Cooler is only effective where humidity is not much but in humid climate conditions air conditioners are better option. There are many ways for passive cooling of buildings which include insulation, using the high reflectivity coating on walls and roof. Major heat gain in buildings is from the roof and walls, so appropriate passive measures should be selected to reduce heat inflow from roof and walls [16].

Using paint of light color is helpful to some extent as light color absorbs less radiation. Garden on the roof is also a useful method of cooling. Using earthen pot inversely on roof is other method of cooling. Using shading with overhang, awnings, curtain and trees to block the sun is beneficial too. Other passive methods are solar chimney, heat exchanger, evaporative cooling, etc., but these methods are not much feasible for existing buildings. Earth sir tunnel and heat exchanger technique may not be suitable in Kota region because Kota has rocky land where installation of heat exchanger is difficult.

The courtyard is also an important building design element, which supply fresh air and day light. Low emissivity coating or application of some reflective/absorptive films on window glazing is another method to reduce solar gain or glare. In hot and dry climate window, size should be less or it should be externally shaded to avoid entry of solar radiation. These passive cooling strategies may only provide mild cooling and reduce cooling load to some extent, but if more cooling is, required then active measures need to be adopted

such as air conditioners and evaporative coolers. Use of passive measures with active measures will improve thermal comfort with less energy consumption, so for cooling needs (22% of operating hours) both measures should be utilized.

From the results, it can be seen that for daytime spaces in the Kota region natural ventilation requirement is maximum. Arrangements should be made for natural ventilation like cross ventilation so that hot air can easily go out and cool air can come in, courtyard and operable windows may be provided [16]. Operable openings and windows have advantage that these allow control on ventilation and entry of solar radiation into the buildings. In the summer when there is need to keep them open, they may be kept open and in winters when there is requirement to pack houses, they may be closed.

The dehumidification combined with cooling, and dehumidification requirements are 7% and 15% respectively in Kota region as per figure 5. However, these requirements are not high but are still needed for enhanced thermal comfort. There are some passive methods to dehumidify the building such as by improving ventilation, by absorbing moisture through the container of desiccant, covering exposed soil in the indoor plants or putting them outside the rooms, in humid conditions.

5. CONCLUSIONS

From the study, it can be concluded that for daytime spaces such as for offices and institutes in Kota region there is a need for improving thermal comfort as out of total daytime operating hours (3650 hours) over the year, only 1057 hours lie in the comfort zone. Major operation requirements for enhanced thermal comfort in office buildings are for natural ventilation (28%), mild cooling (27%) and cooling (22%). For cooling, passive measures may be used which are low cost and can be applied in existing buildings such as light paint, shading, gardening, high reflective coating, low emissivity coating windows, ventilation etc. to reduce the energy consumption and to enhance thermal comfort.

REFERENCES

1. Luisa F.Cabeza, Lídia Rincón, Virginia Vilariño, Gabriel Pérez, AlbertCastell, Life cycle assessment (LCA) and life cycle energy analysis (LCEA) of buildings and the building sector: A review, *Renewable and Sustainable Energy Reviews* 29, 2014, 394–416.
2. Energizing India, A joint project report of NITI Aayog, India and Institute of energy economics, Japan, 2017.

3. H.M. Taleb, Using passive cooling strategies to improve thermal performance and reduce energy consumption of residential buildings in U.A.E. buildings, *Front Arch Res.,* 3, 2014, 154–65p.
4. N.B. Geetha, R. Velraj, Passive cooling methods for energy efficient buildings with and without thermal energy storage – A review, *Energy Education Science and Technology Part A: Energy Science and Research*, 29(2), 2012, 913–946.
5. N.M. Nahar, P. Sharma, M.M. Purohit. Performance of different passive techniques for cooling of buildings in arid regions, *Build Environ*, 38, 2003, 109–116p.
6. D. Jain. Modeling of solar passive techniques for roof cooling in arid regions, *Build Environ*, 41, 2006; 277–87p.
7. O.P. Jakhar, A.N. Mathur. Solar Passive Cooling/heating of Building at Bikaner in Rajasthan, India, Development in renewable energy technology (ICDRET). 2009 1st International conference on 17-19 Dec 2009, INSPEC, accession number: 11262452, publisher: IEEE, Dhaka, Bangladesh, IEEE xplore 26 April 2010.
8. Chedwal R., Dhaka S., Mathur J. ,Energy saving potential through energy conservation bulding code and advance energy efficiency measures in hotel buildings of Jaipur city, India, *Energy & Buildings*, Vol. 92 , 2015, 282-295
9. Antima Sharma, Namrata Sengar, Study of Climatic Parameters and Residential Housing Structures in Kota Region, *International Journal of Housing and Human Settlement Planning*, Vol. 3: Issue 2.
10. Ricardo Forgiarini Rupp, Natalia Giraldo Vásquez, Roberto Lamberts, A review of human thermal comfort in the built environment, *Energy and Buildings* 105, 2015, 178–205.
11. Noel Djongyang, Rene´ Tchinda, Donatien Njomo, Thermal comfort: A review paper, *Renewable and Sustainable Energy Reviews,* 14, 2010, 2626–2640.
12. Diana Enescu, A review of thermal comfort models and indicators for indoor environments, *Renewable and Sustainable Energy Reviews*, 79, 2017, 1353–1379.
13. Comfort and weather analysis tool http://carbse.org/research-tools/
14. Sanyogita Manu, Yash Shukla, Rajan Rawal, Leena E. Thomas, Richard de Dear, Field studies of thermal comfort across multiple climate zones for the subcontinent: India Model for Adaptive Comfort (IMAC), *Building and Environment*, 98, 2016, 55-70.
15. A. Sharma, N. Sengar, Comparative theoretical heat transfer study of different insulating material in multilayer wall for enhancing building thermal, *International Journal of Applied and Advanced Scientific Research*, 2017, 2 (2), 2456 – 3080,.

16. A. Sharma, N. Sengar, Heat gain study of a residential building in hot-dry climatic zone on basis of three cooling load methods, *European Journal of Engineering Research and Science,* 4 (9), 2019, 186–194.

Cite this article

Antima Sharma, Deepmala Meena, Namrata Sengar, Study of Thermal Comfort for Office / Institute Buildings Based on CARBSE Tool and Suggestive Passive Measures for Kota, In: Sandip A. Kale editor, Advanced Research in Solar Energy, Pune, Grinrey Publications, 2021, pp. 25-36

4 Industrial Waste Water Treatment Using Natural Filtration and Solar Distillation Methods

Hemant Kumar[a], Shivanshu Sharma[*,a] and Namrata Sengar[b]

[a]Department of Pure and Applied Physics, University of Kota, Kota, India

*Corresponding author: shivanshugecj@gmail.com

ABSTRACT

The need of fresh water is vital for human survival and fulfillment of demand has become serious concern in countries having limited water resources. Large amount of water from industries is wasted daily all over the world, which can be reused by proper water treatment. This present work discusses the methods of waste water treatment using filtration and solar distillation methodology. The samples of industrial waste water were collected from chemical and fertilizer industry in Kota, Rajasthan. The pH, TDS and dissolved oxygen values of waste water samples and water after treatment was tested and results of different waste water samples are reported. Ammonia, cement and carbide waste water samples having TDS 310,510 and 268 PPM were treated using filtration and solar distillation methods. The treated water after filtration had TDS 274,460 and 208 PPM respectively. The treated water after solar distillation had TDS 107, 288 and 98 PPM. The obtained values of TDS, pH, and dissolved oxygen after combined treatment of filtration and distillation are close to standard values required for potable water.

Keywords: Filtration, solar distillation, total dissolved solids, waste water, water treatment

Advanced Research in Solar Energy | ISBN: 978-81-948951-7-6
Book Series: Research Transcripts in Energy | Vol: 01

1. INTRODUCTION

About seventy percent of the earth is covered with water but only one percent of it is potable water. This one percent water resource is renewed by rainfall and other methods. Demand of fresh water per capita is increasing day to day and available resources are limited and this will create big crises in future for the world. Due to rapid enhancement in population exploitation of natural resources and degradation in environment is happening all over the world. To fulfill of needs of large population industrial development is scaled up by all countries that is creating a large amount of industrial waste water daily. This industrial waste water should be treated and reused in different needs to reduce load on natural water resources [1]. The most available natural resources of water are ground water, surface water and rain water [2]. Salinity of surface water is increasing due to intrusion of seawater near coastal areas. It leads to higher amount of nitrate and pesticide in surface water supply chain [3]. Industrial waste water basically includes chemical waste, sewage water and other wastes from various manufacturing processes [4]. The major contaminants in waste water are suspended solids, nutrients, organic and inorganic compounds and heavy and toxic metals. This waste water mixed with natural resources not only affects human life but also has adverse effects on aquatic ecosystem. Due to long term direct or indirect contact of such wastes may cause health issues and it may lead towards serious diseases [5].

Waste water treatment method depends on various factors like kind of pollutant presence in waste water, characterization of waste water and selection of treatment technology [6]. The conventional method includes chemical process treatment and which may lead to further chemical waste. General methods are coagulation, filtration, incineration, ozonation, chlorination, chemical oxidation, flocculation, adsorption, reverse osmosis, ion exchange, distillation, electrolysis, etc. [7]. After waste water treatment, product water can be used in industries in various activities like heating, cooling, as solvent, as carrier of raw material and for manufacturing goods. The quality of water after water treatment should be close to the freshwater quality as possible. According to American Public Health Association, water quality must be expressed in terms of use as well with the sensory, physical, biological and chemical parameters[8].

Any kind of biological, physical or chemical substance present in water leads to reduced water quality. After treatment waste water should be tested in laboratory for quality check. Water having some contaminates and not appropriate for drinking purpose can be used in washing, bathing or irrigation purpose. Diseases like diarrhea, cholera, organ damage, mal-nutrition are spreading in under developed countries due to poor supply of fresh water [9-11].

Aravind M. A. and Rahna L. stated on their result that coir pith is effective in removing of the BOD, COD and helps to brings down the conductivity of waste water [12]. Shivang Sharma et. al. claimed in their study that rice husk is a low cost material which can be used in efficient bacterial deactivation process [13]. R. Priyanka and Sri M. Vagish collected water samples from Mandakki Bhatti, Davangere, Karnataka area and used natural filteration process using coconut shell, activated carbon, rice husk, sand and pebbles on a simple glass made filter design. In the filtered output water sample testing results they got 5.7 mg/L dissolved oxygen (D.O.), 7.1 pH value and 382 PPM total dissolved solids (TDS) values which are near to standard values required for potable water [14]. Sadon, F. N. et al explained in their work that rice husk has ability to filter heavy metals like Fe, Mn, Zn, Cu, Cd, and Pb with 90 to 100% efficiency. It can also be used to absorb different kind of dyeing agent during filteration process [15]. A. Carmalin Sophia et. al. experimental results explained that rice husk carbon is highly efficient compared to others in removal of E.coli with around 99% efficiency [16]. V. Kiruba Devi et. al. used solar distillation for waste water treatment and by testing of output samples they concluded that the values of D.O., pH, TDS are near for reuse the water in industrial or other purpose [17]. R. Asadi et. al. used industrial and sanitary waste water samples with solar distillation for waste water treatment process. They stated in their results that solar still is helpful technology to removing organic and inorganic contaminants from waste water with low cost. It can also remove bacteria from waste water [18].

Present work is an attempt to investigate the effectiveness of natural filtration and solar distillation in a combined manner for industrial waste water treatment. This work is different from the previous works as it includes both the methods for waste water treatment. It uses natural form of rice and coconut husk fiber for filteration process and more efficient design of solar distillation still with pyramid shape. Here details of the experiments and the results obtained related to pH, TDS and dissolved oxygen are reported and compared.

2. WASTE WATER TREATMENT EXPERIMENTAL SETUPS

The present work focused on study of industrial wastewater treatment by natural filters and solar distillation. Three different samples were taken from industrial units and were treated with help of natural filters and solar distillation stills. Various parameters such as pH, dissolved oxygen and total dissolved solids were determined at different steps. For natural filters the materials used were rice husk, activated carbon and coconut fibres. For solar distillation, pyramid shaped solar distillation still has been used as yield of pyramid solar still is

better than double slope solar still. The experiments have been conducted on the waste water taken to first observe the effect of filtration and then as a second step solar distillation of the filtered water was done.

2.1. Filtration

It is a process of removing contamination from waste water using physical, chemical and biological process. The filtered water can be used as drinking water, irrigation purpose, swimming and ponds water and other general domestic and commercial work as per quality requirement. The major filters we generally use are activated carbon filter, reverse osmosis, alkaline/water ionizer, UV filter and infrared filter.

Fig. 1. Activated carbon, rice husk fibre and coconut fibre respectively

In this experiment setup activated carbon, rice husk fibers and coconut husk fibers are used for filtration. Granular activated carbon (GAC) is generally used for removal of residual disinfectants and organic contaminant from water supply. This helps to improves tastes and reduce health hazards. Due to multifunctional nature of this technique it is widely used. Natural fibers like rice husk and coconut husk are generally used in polymer industries[19].

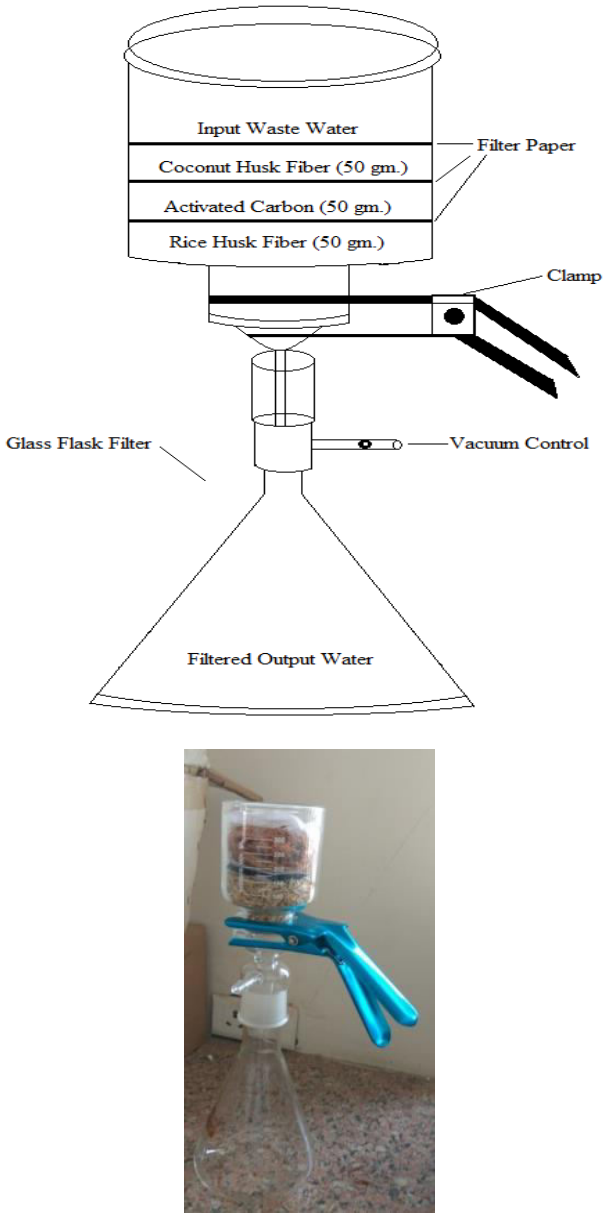

Fig. 2. Schematic and actual image of waste water filtration using activated carbon, rice and coconut husk fiber

The waste water samples of ammonia, cement and carbide from chemical and fertilizer industry at Kota, Rajasthan are used for the experimental work. 100 ml sample of water is taken for testing. 50gm. of each activated carbon, rice husk and coconut husk fiber is used as natural filter. The results of the values before and after filtration are shown in table 1.

Table 1. Experiment observation of filtration water treatment

Sr. No.	Waste Water Sample	Before Filtration Reading			After Filtration Reading		
		TDS (PPM)	pH	D.O. (mg/L)	TDS (PPM)	pH	D.O. (mg/L)
1	Ammonia (NH_3)	310	8.70	1.3	274	8.30	2.5
2	Cement	510	10.40	2.5	460	10.10	5.4
3	Carbide	268	10.62	3.6	208	10.30	5.9

2.2. Solar Distillation

Solar distillation helps to get purified water from waste water. This is one of the best choices of water purification in remote areas where other option availability is rare. This distilled water with adequate level of qualities can also be used in batteries and hospitals. In the solar distillation process water is evaporated by absorbing solar radiation and separated from dissolved solids. Further, it is condensed and collected as potable water.

In general dissolved solids, water hardness (calcium, magnesium and other mineral compounds), molybdenum and selenium, nitrates and chlorides, arsenic, fluorides and heavy metals etc. can be removed efficiently using solar distillation approach [20]. The removal efficiency of bacteria and viruses using solar distillation is up to 99.9%. It should be considered that volatile organic compounds like petrol and alcoholic compounds cannot be removed as efficiently as others. In such case activated carbon filter process is recommended [21].

The same waste water samples of ammonia, cement and carboid from chemical industry in Kota, Rajasthan are used for this experimental work. The output distilled water is collected in separate bottles and then samples of each experiment are tested to get TDS, pH, D.O. (dissolved oxygen) values. Solar radiation and temperature is measured using pyranometer and digital thermometer. The experimental observations related to solar distillation are presented in table 3.

Table 2. Design parameters of solar distillation still

Sr. No	Parameter	Pyramid type Solar water distillation
1.	Base area of inner box	50 cm × 50 cm
2.	Aperture area of inner box	46 cm × 46 cm
3.	Base area of outer box	50.2 cm × 50.2 cm
4.	Aperture area of outer box	3025 cm^2
5.	Height of inner box	15 cm
6.	Height of inner box with absorber plate	15 cm
7.	Height of outer box	15.2 cm
8.	Height of glass center from absorber surface	30 cm
9.	Glass inclination angle	30^o

Fig. 3. Schematic of distillation still and distillation of waste water after filtration

Table 3. Experimental observations for distillation of waste water after filtration

Sr. No.	Temp. (°C)	Waste Water Sample	Waste Water Sample Reading			After Distillation Reading		
			TDS (PPM)	pH	D.O. (mg/L)	TDS (PPM)	pH	D.O. (mg/L)
1	30.2	Ammonia	310	8.70	1.3	107.00	7.70	2.80
2	30.3	Cement	510	10.40	2.5	288.00	8.50	7.90
3	30.5	Carbide	268	10.62	3.6	98.00	7.90	9.90

3. RESULTS AND DISCUSSION

Results obtained from both experimental set-ups for the ammonia, cement and carbide waste water samples are presented below in fig. 4, 5 and 6. From Fig.4, 5 and 6 it can be seen that the the TDS and pH value is reduced and D.O. value is increased after water treatment by filtration and distillation.

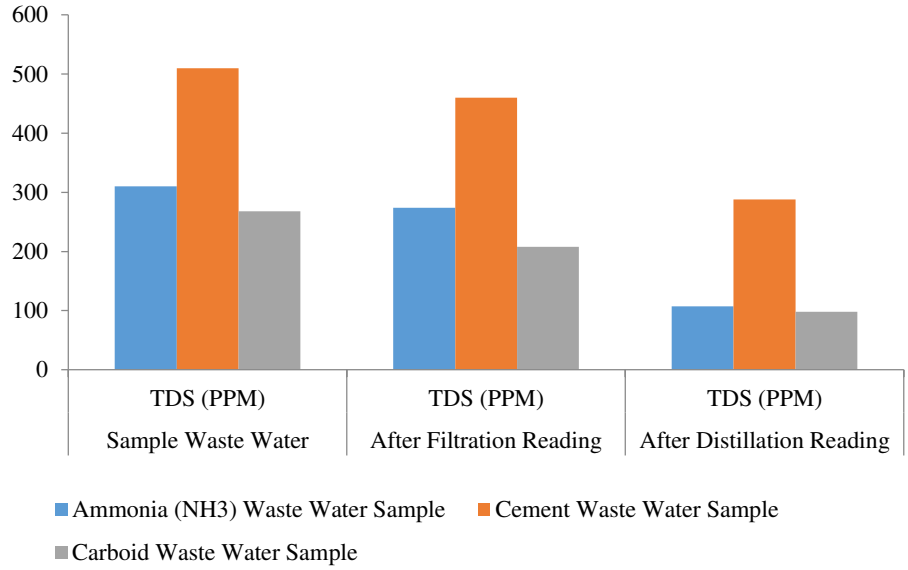

Fig. 4. Comparative TDS value before and after water treatment

It can be seen that for ammonia waste water sample the initial value of TDS was 310 ppm, pHwas 8.7 pH and D.O. was 1.30 Mg/l.After natural filtration the value was 274 ppm, 8.30 pH and 2.50Mg/L and after solar still distillation the value became 107 ppm, 7.70 pH and 2.80 Mg/L. Overall the Total Dissolved Solid value reduced to 34.50 %. For cement waste water sample TDS was 510 ppm, pH was 10.40 pH and D.O. was 2.50 Mg/L. After natural filtration the value was 460 ppm, 10.10 pH and 5.40 Mg/L after solar still distillation the value became 288 ppm, 8.50 pH, 7.90 Mg/L. Overall the Total Dissolved Solid

value reduced to 56.5 %. For carbide waste water sample initially TDS was 268 ppm, pH was 10.62 pH and D.O. was 3.60 Mg/L. After natural filtration the value was 208 ppm,10.30 pH and 5.90 Mg/L and after solar still distillation the value became 98 ppm,7.90 pH and 9.90 Mg/L. Overall the Total Dissolved Solid value reduced to 36.56 % .

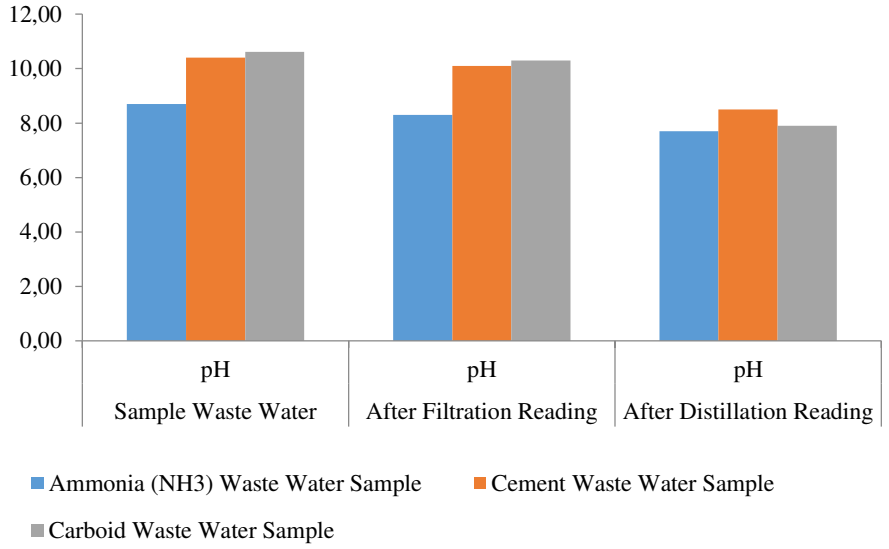

Fig. 5. Comparative pH value before and after water treatment

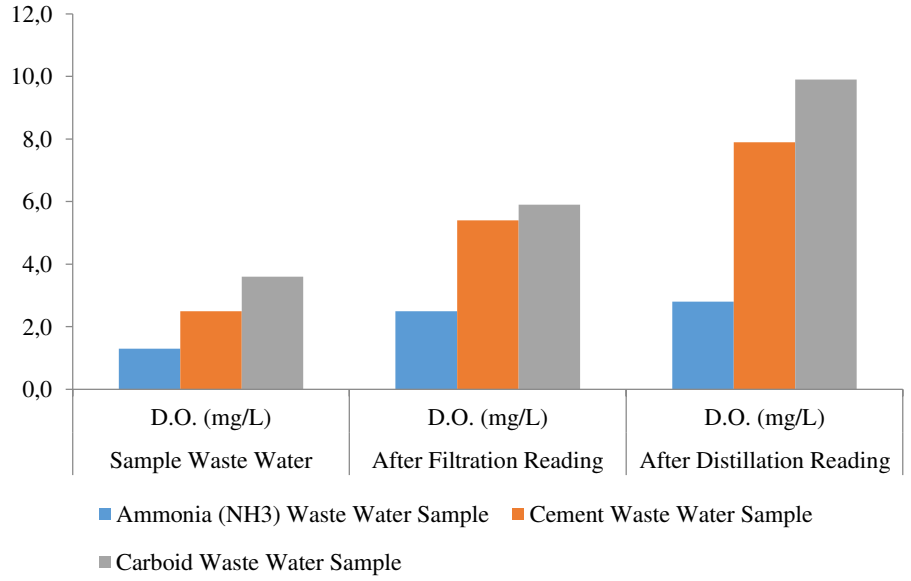

Fig. 6. Comparative D.O. value before and after water treatment

4. CONCLUSIONS

The results of the experiment show that natural filtration and solar distillation is helpful in waste water treatment. The Total Dissolved Solid (TDS) value reduced by 34.50 % for ammonia plant waste water, Total Dissolved Solid value reduced by 56.5 % for cement waste water, and Total Dissolved Solid value reduced by 36.56 % for carbide plant waste water. The obtained values of TDS, pH, and dissolved oxygen after combined treatment of filtration and distillation are quite close to standard values required for potable water. The results indicate that the combined use of natural filtration and solar distillation can prove to be a promising option for waste water treatment. This research will help to lay down the foundation of future work in the field of waste water treatment; further work is required for estimation of yield and time duration for up scaling of the system.

ACKNOWLEDGEMENT

Authors gratefully acknowledge the support of Royal Academy of Engineering, UK through Newton-Bhabha Higher Education Partnership Project.

REFERENCES

1. Meikap B. C., Roy G. K., Recent advances in biochemical reactors for treatment of wastewater, *IJEP*, 1995,15 (1), 44-49.
2. Food and Agriculture Organization Of The United Nations, Review of World Water Resources by Country, *Water Report*, 2013.
3. United Nations Environment Program, Clearing the Waters: A focus on water quality solutions, *UNEP*, 2016.
4. Garg S. K., *Water Supply Engineering*, 31, New Delhi, Khanna Publishers, 1977.
5. Ghose T. K., edition of Water Supply Engineering: Environmental Engineering, *Indian Chemical Engineering,* 2001, 43 (2), 118-122.
6. Garg S. K., *Sewage Disposal and Air Pollution Engineering*, 24, New Delhi, *Khanna Publishers*, 1979, Disposal of Municipal and Industrial Solid Waste.
7. Vinod A. V., Reddy G. V., G. V. Reddy, Dynamic behaviour of a fluidised bed bioreactor treating waste water, *Indian Chemical Engineering-Sec A*, 2003, 45 (1), 20-27.
8. Food and Agriculture Organization of The United Nations, *Review of World Water Resources by Country*, *Water Report*, 2003.

9. Burch J., Thomas K. E., *An overview of water disinfection in developing countries and the potential for solar thermal water pasteurization*, National Renewable Energy Laboratory (U.S.), 1998.
10. *Centers for Disease Control and Prevention, Atlanta*, Waterborne Diseases, 2012.
11. *Centers for Disease Control and Prevention, Atlanta,* Global Water, Sanitation, & Hygiene (WASH), 2015.
12. Aravind M. A., Rahna L., Treatment of Industrial Effluent with Coir pith and Charcoal Infused Soil Media, *International Journal of Engineering and Advanced Technology*, 2018, 8(4), 11-15.
13. Sharma S., Datta A., Kotwal A., Singh S. A Case Study on Efficient Filter Media Adding Rice Husk, *International Journal of Scientific and Technical Advancements*, 2019,5(1), 29-32.
14. Priyanka R., Vagish M., Water Quality Maintenance by Developing a Biofilter Model Using Coconut Shell Activated Carbon and Rice Husk as Absorbents, *International Research Journal of Engineering and Technology*, 2018,5(8), 41-48.
15. Sadon F. N., Ibrahem A. S., Ismail K. N., An overview of rice husk applications and modification techniques in wastewater treatment, *Journal of Purity, Utility Reaction and Environment*, 2012,1(6), 308-334.
16. Sophia A. C., Catherine D., Bhalambaal V. M., Utilization of Rice-husk and Coconut Shell Carbons for Water Disinfection, *J Environ. Science & Engg.*, 2013,55(1), 9-16.
17. Devi V. K., Priya S. S. N., Shivasankari M., Murugaiyan A., Saarathy H., Kirubakaran V., Industrial Wastewater Treatment Using Solar Still for Achieving Zero Liquid Discharge, *Waste Water Recycling and Management,* 2019, 233-238.
18. Asadi R. Z., Suja F., Ruslan M. H., Jalil N. A., The application of a solar still in domestic and industrial wastewater treatment, *Solar Energy,* 2013,93, 63-71.
19. Pisani P. L., Lahnsteiner J. G., Direct Reclamation of potable water at Windhoek's Goreangab reclamation plant, *Desalination, Water Science & Technology, Namibia,* 2017, 55, 441-448.
20. Foster R. and Eby-Martin S., Solar distillation providing potable water for border colonias, American Solar Energy Society Reno, Nevada, 2002.

21. Hanson A., Zachritz W., Stevens K., Mimbela L., Polka R., and Cisneros L., Distillate water quality of a single-basin solar still: laboratory and field studies, *Solar Energy,* 2004, 76, 635–645.

Cite this article

Hemant Kumar, Shivanshu Sharma and Namrata Sengar, Industrial Waste Water Treatment Using Natural Filtration and Solar Distillation Methods, In: Sandip A. Kale editor, Advanced Research in Solar Energy, Pune, Grinrey Publications, 2021, pp. 37-48

5 Experimental Study of Electrical Outputs for Air-Blower Cleaned, Water Cleaned and Unclean Solar PV Panels

Mahesh Kumar[a], Koushal Shringi[*,a] and Namrata Sengar[a]

[a]Department of Pure and Applied Physics, University of Kota, Kota, India

*Corresponding author: koushalshringi12@gmail.com

ABSTRACT

This article reports the experimental study of the electrical output of the solar PV panels in the form of current and voltage values with and without cleaning of the panels. Experiments were performed with three identical 40 watt solar PV panels placed on the rooftop for on-field observations. One panel was not cleaned, second was cleaned with an air blower and third was cleaned with water. Current, voltage and temperatures of the panels were recorded along with the ambient air temperature and global solar radiation. Results show that the current and voltage values are higher for the water cleaned panel, followed by the air cleaned panel. The temperatures are generally higher for the unclean panel, followed by blower cleaned and then the water cleaned panel. There is a difference of about 2W power output between the water cleaned and unclean panel, with water cleaned panel on the higher side. This accounts for about 5% of the power capacity of the panels.

Keywords: Cleaning, Current, Power, Solar PV Panel, Solar Radiation, Voltage

Advanced Research in Solar Energy | ISBN: 978-81-948951-7-6
Book Series: Research Transcripts in Energy | Vol: 01

1. INTRODUCTION

Electricity production from solar PV power plants is gaining momentum worldwide on account of being pollution free option. The performance of the PV module depends on the magnitude of solar radiation as well as environmental impacts such as humidity, rainfall wind etc. Another major limitation is decrease in output yield due to dust deposition. When dust particles are deposited on photovoltaic modules, they interfere by scattering light and reducing optical transmittance. J.Z. Casanova et. al. [1] carried out a study at the University of Malaga to identify the energy losses due to the gathering of dust on the surface of the solar PV modules. The study reports that around 4.4% of average daily energy reduction over a year may occur due to deposition of dust on the surface of the PV modules. The average daily energy losses can increase upto 20% if there are no rains for long periods. Z. A. Darwishet. al. [2] presented a review on impact of dust on the solar PV system performance.

A. Sayyahet. al. [3] presented a review covering studies on dust on solar systems as early as from 1942 to 2013. A. Rao et.al. [4] investigated the loss in performance in PV system due to deposition of dust through an outdoor and indoor experimental test bed. The experiment consisted of dynamic study of the I–V characteristics of the PV panels with change in soiling state. The results indicated that short circuit current was more impacted than the open circuit voltage of PV systems, the effect was pronounced in indoor setup in the range of 30-40%, whereas it was 4-5% in the outdoor set up. M. R. Maghami et.al. [5] reviewed the performance effects and the power loss in solar panels due to dust deposition. B.

Aissaet. al. [6] reported a study on the structural and physical properties of the desert-dust particles in the State of Qatar. J. Tanesabet. al. [7] checked the seasonal effect of dust on performance of PV module with case study on Perth, Australia and NTT, Indonesia. A. Hussain et. al. [8] conducted a study on dust samples collected from different sources and the SEM image analysis was carried out for seven types of dust samples. C. Fountoukiset. al. [9] investigated the effect of deposition of atmospheric dust onto photovoltaic modules using both field measurements and modeling for arid region in Qatar.

J. Tanesabet. al. [10] studied degradation of PV modules consisting of polycrystalline silicon (pc-Si), mono-crystalline silicon (mc-Si), and amorphous silicon (a-Si).with dust of different morphologies at Babuin, Indonesia and Perth, Australia.There are different ways and studies going on for identifying efficient cleaning mechanism for solar PV. D. Deb and N. L. Brahmbhatt [11] reviewed the various methods to mitigate soiling and studied a variety of cleaning solutions. On the basis of this study, the appropriate cleaning

mechanism can be selected for the solar PV panels depending on the location and the surrounding environment of the installations.

Work has been done at IIT Mumbai [12, 13] by collecting and investigating the soil samples from six different geographic locations of India. It was found that the energy loss due to soiling on a silicon solar cell with Mumbai dust (17.1%) was about twice that of Jodhpur dust (9.8%). Highest spectral loss was observed for the dust collected from Mumbai, followed by Pondicherry, Agra, Hanle, Jodhpur, and Gurgaon. On comparison it was observed that for same type of dust the amorphous silicon (17.7%) was worst affected, followed by cadmium telluride (15.7%), crystalline silicon (15.4%), and CIGS (14.5%) module technology. A novel method has been suggested for cleaning Solar PV panel using ambient moisture [13].

During literature review, it is noticed that for India few works have been reported regarding the issue of impact of dust on solar PV outputs. Therefore, the present work has been undertaken to study the impact of simple cleaning mechanisms on electrical outputs of solar PV panels. The study reports the experimental results for current and voltage of the unclean and cleaned solar panels with solar radiation and temperatures.

2. EXPERIMENTATION

Three solar panels of power 40 watt were taken and were placed on stands. The experiments were performed at the rooftop of University of Kota. The experimental arrangement was as follows: One panel was not cleaned during the experiment, second solar panel was cleaned with blower air and the third solar panel was cleaned with water. Cleaning with water was done using drip system which used very less amount of water. The cleaning was done initially at 10 a.m. and then at around 1 to 2 p.m.

Fig. 1. On-field experimental set up at rooftop with three solar panels each of 40W placed on stands

The various instruments used during the experimental observations were pyranometer, weather monitoring system, digital multimeter, anemometer, digital thermometer and thermocouples. During the experiments, the values of current, voltage, temperatures of the three solar panels were recorded along with the ambient air temperature and global solar radiation. Kipp and Zonen CMP10 pyranometerhas been used to record the global solar radiation during the experiments. The observations were taken with the Indian standard time and are reported here in form of graphs.

3. RESULTS AND DISCUSSION

The observations have been taken for the three solar panels placed at the rooftop of the University of Kota for several days; here some representative observations are presented. The observations for current, voltage and temperature profiles with solar radiation are shown in fig. 2-4 for 19th April.

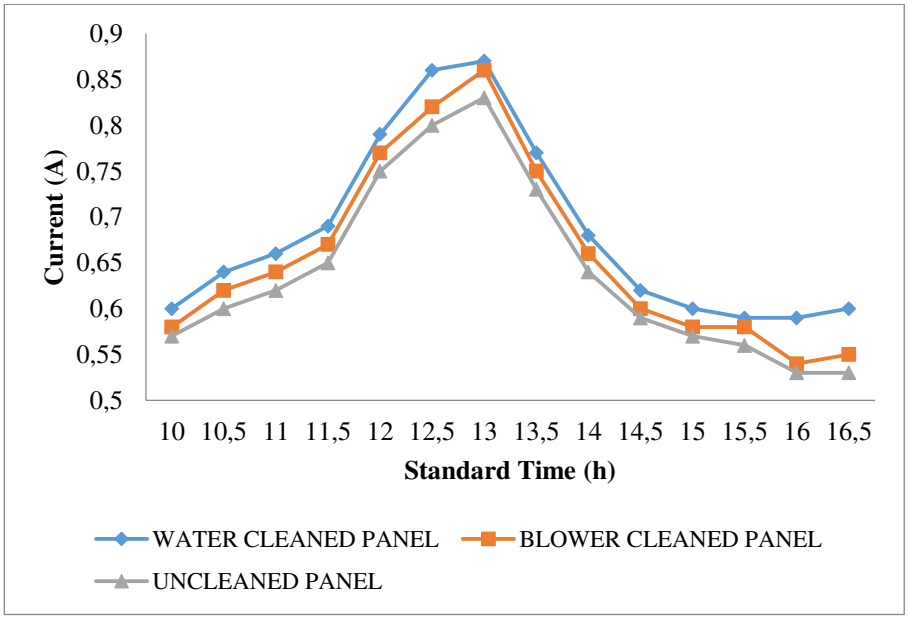

Fig. 2. Current of PV panels with standard time (19th April)

From the figures 2 and 3 it can be seen that the current and voltage values for the water cleaned panel are highest, the corresponding values are lowest for unclean panel whereas the values for the air blower cleaned panel lies in between. The panel temperatures are highest for the unclean panel, and lowest for the water cleaned panel as can be seen from figure 4. The point to notice is that the temperatures of all the three panels are greater than the ambient temperature during the experiment duration.

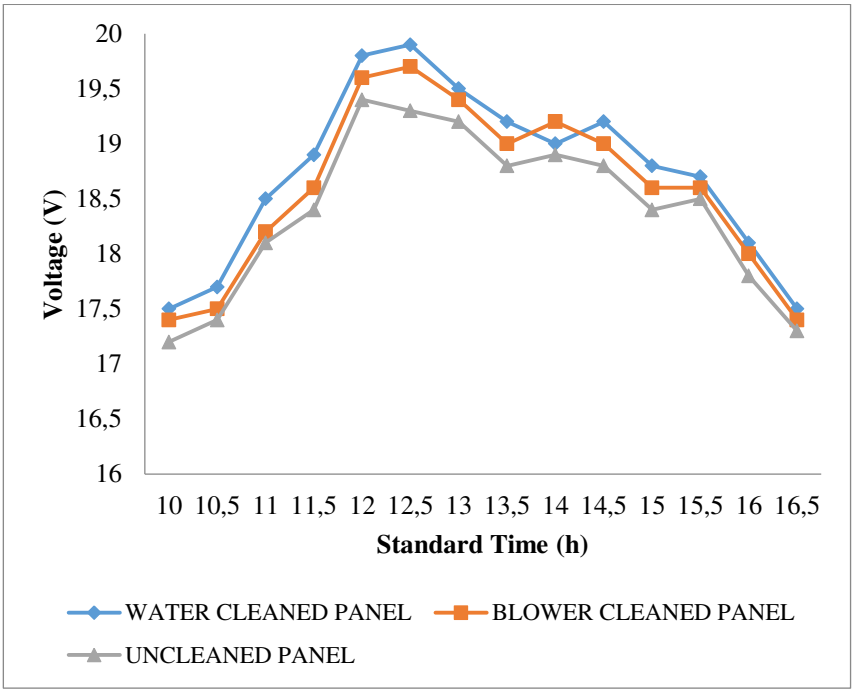

Fig. 3. Voltage of PV panels with standard time (19th April)

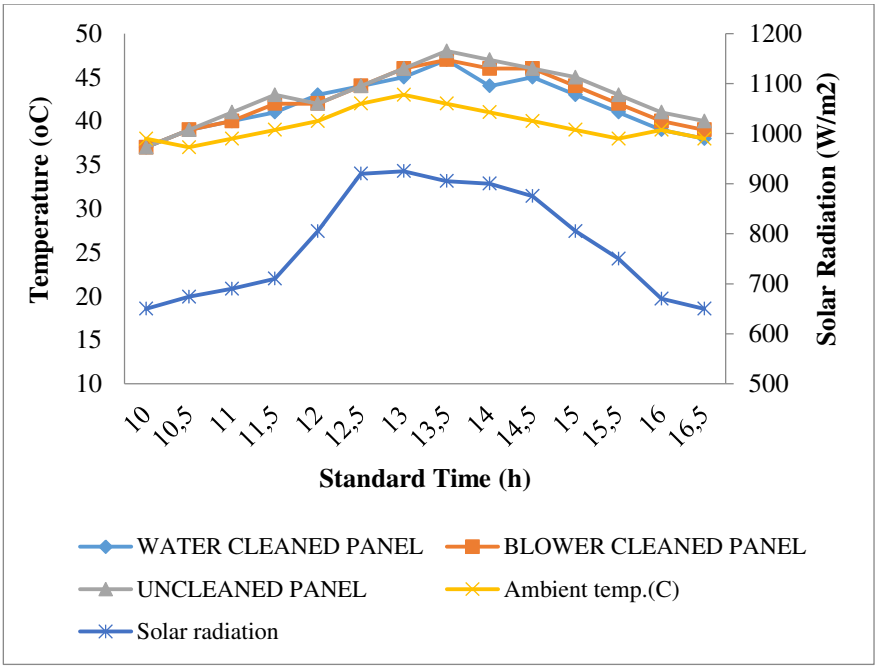

Fig. 4. Temperature of PV panels and solar radiation with standard time (19th April)

The experiment was again repeated after a day. The observations for current, voltage and temperature profiles with solar radiation are shown in Fig. 5-7 for 21st April. Here from this figure also it can be seen that the current and voltage values are higher for the water cleaned panel and the temperatures are lower in comparison to the air blower cleaned and unclean panels.

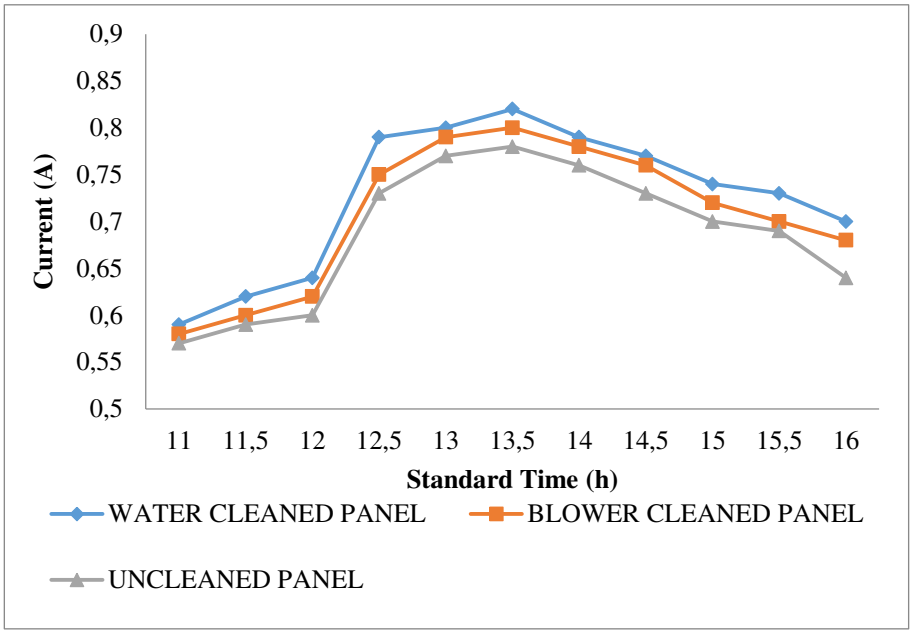

Fig. 5. Current of PV panels with standard time (21st April)

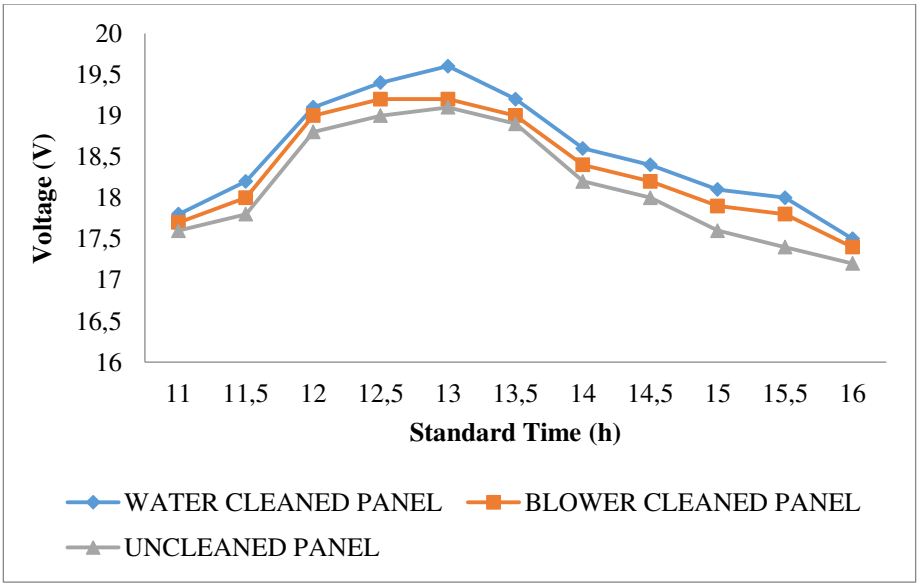

Fig. 6. Voltage of PV panels with standard time (21st April)

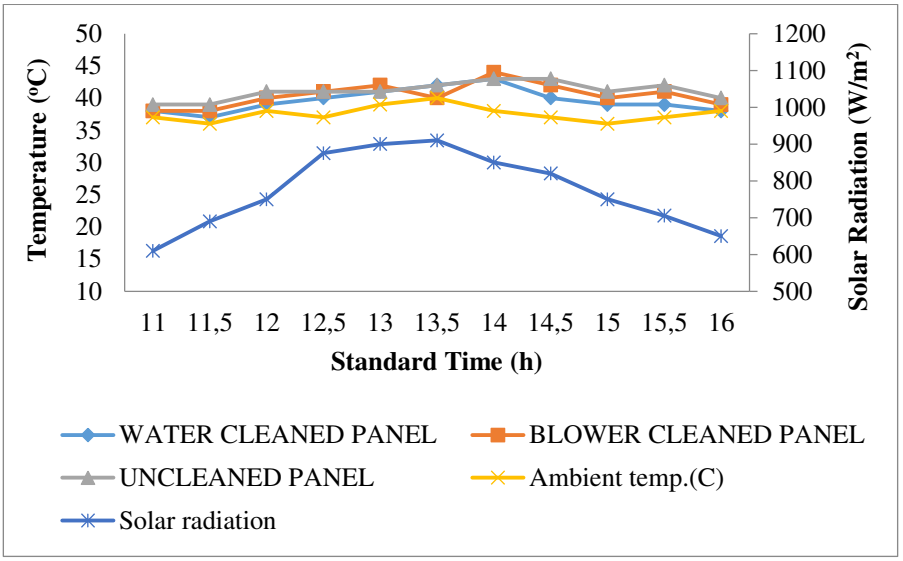

Fig. 7. Temperature of PV panels and solar radiation with standard time (21st April)

Further, the observations for current, voltage and temperature profiles of the solar PV panels with solar radiation are shown in Fig. 8-10 for 23rd April and in Fig. 11-13 for 25th April. Comparing the figures for 23rd and 25th April, it can be seen that solar radiation is higher on 25th April and therefore clear difference in the values of current, voltage and temperatures for the three solar panels is evident. Figures 11-13 clearly indicate that current and voltage outputs are more for the water cleaned panel. Current is higher by around 0.05 A and voltage by around 0.7 V.

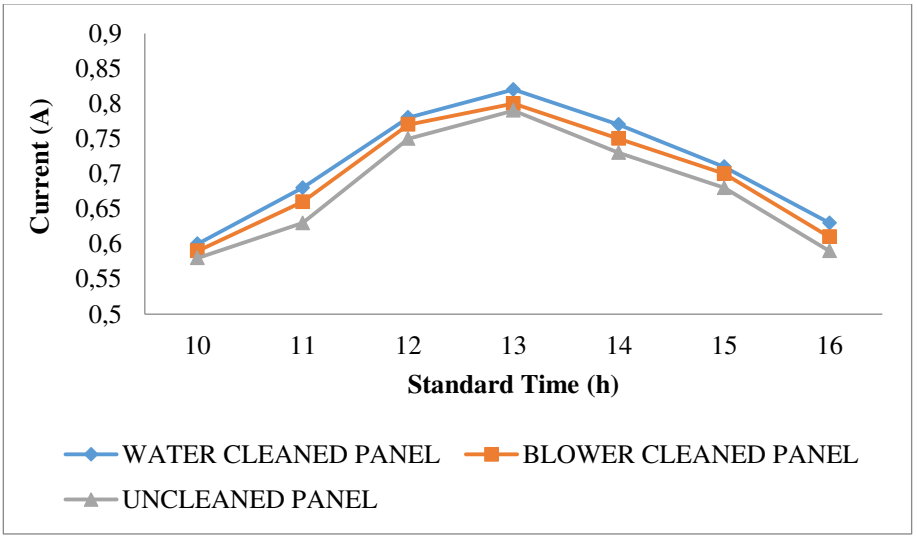

Fig. 8. Current of PV panels with standard time (23rd April)

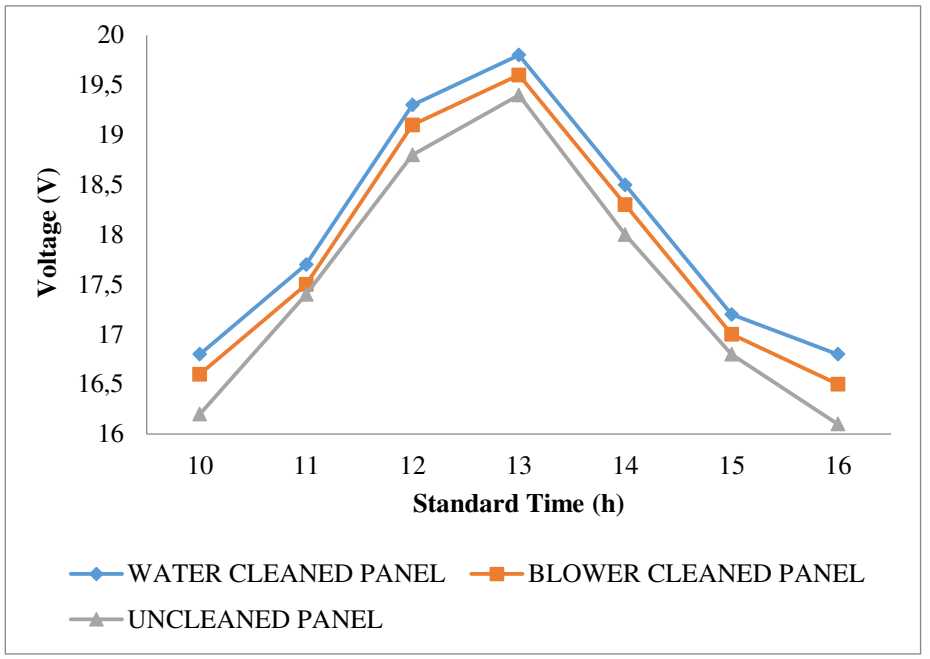

Fig. 9. Voltage of PV panels with standard time (23rd April)

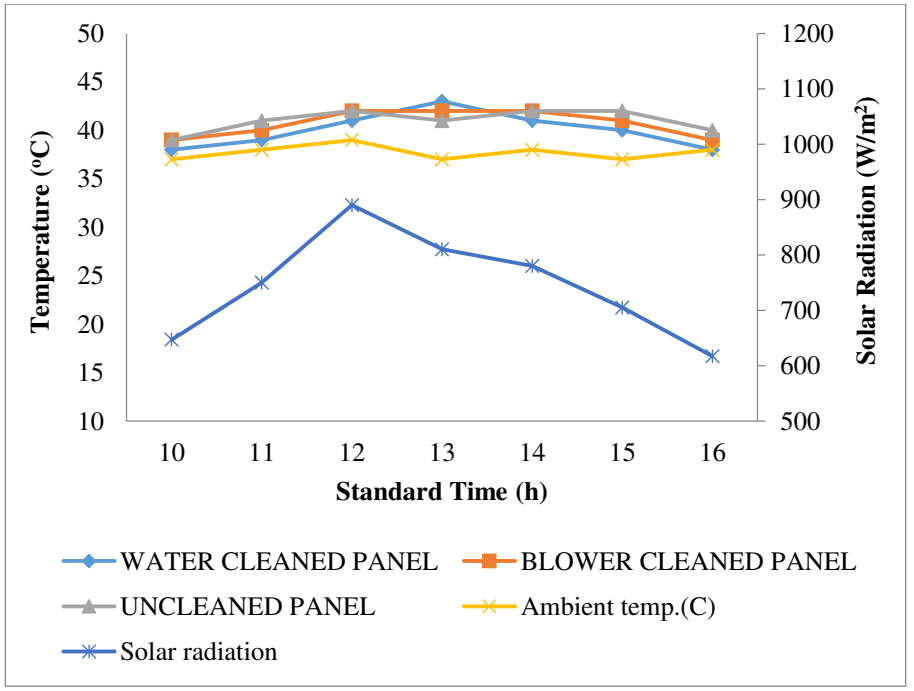

Fig. 10. Temperature of PV panels and solar radiation with standard time (23rd April)

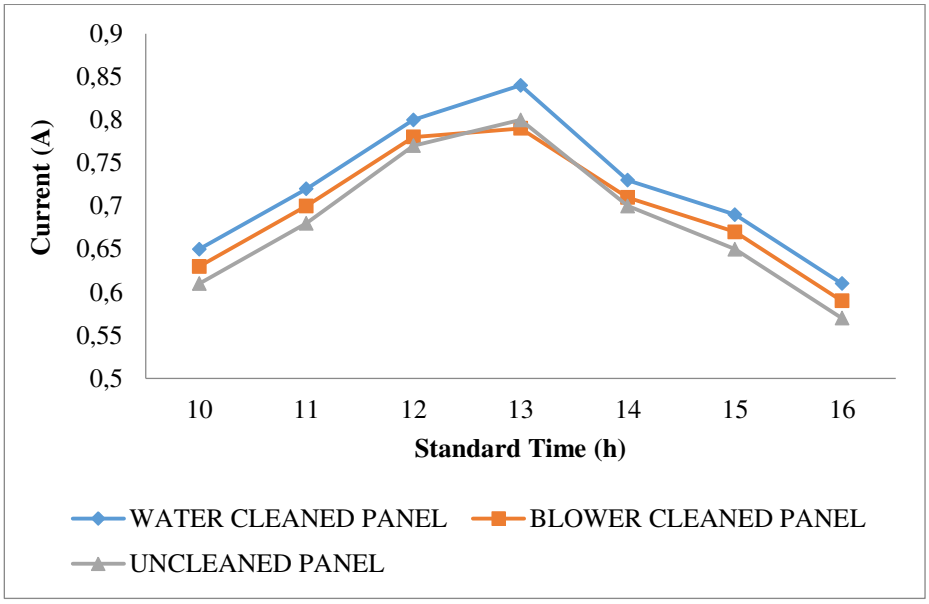

Fig. 11. Current of PV panels with standard time (25th April)

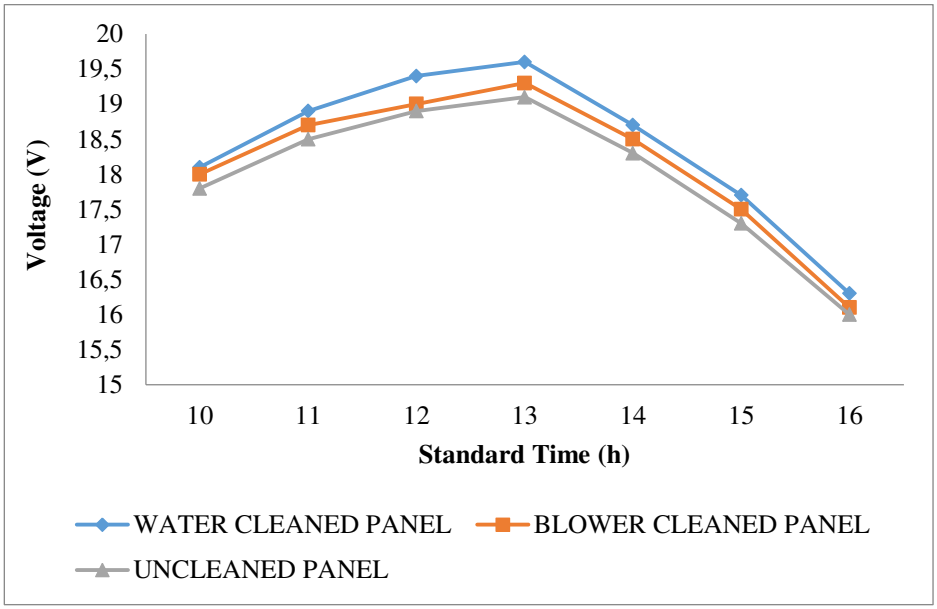

Fig. 12. Voltage of PV panels with standard time (25th April)

From the figures 2-13, it is clear that the current and voltage values are higher for the water cleaned panel as compared to the blower cleaned and the unclean panel, whereas temperatures are higher for the unclean panel. Due to cleaning around 2 W of power output maybe increased for the water cleaned panel as compared to the unclean panel, which is about 5% of the power capacity of the panels (40W). Here, it is important to note that there is effect of both cleaning

and cooling involved which results in more power output as while cleaning with water, the temperatures of the solar panel decrease slightly which results in slightly increased voltage as compared to unclean panel.

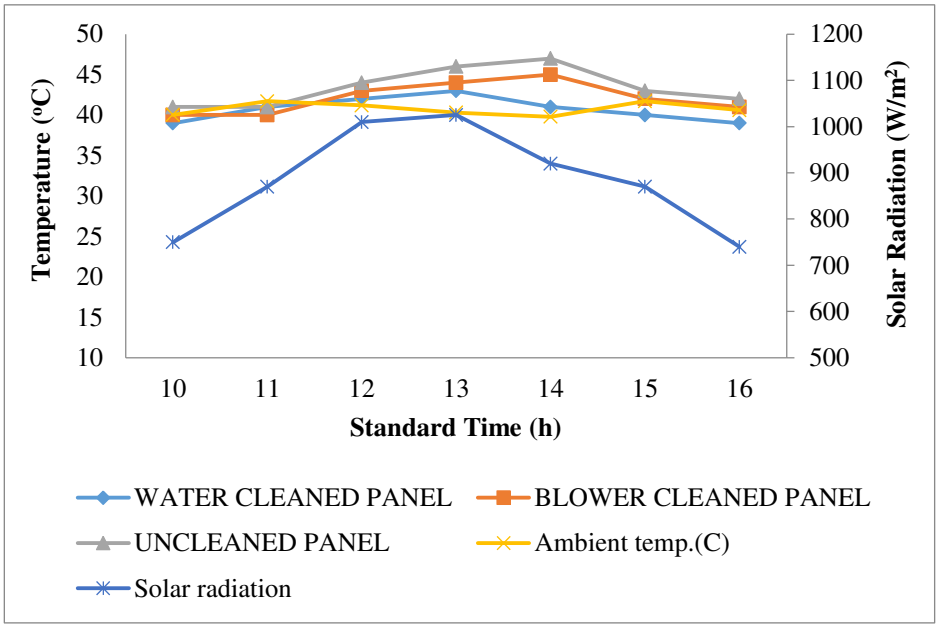

Fig. 13. Temperature of PV panels and solar radiation with standard time (25thApril)

From the present study, it is clear that around 5% of power output may be increased with appropriate solar PV panel dust cleaning method. These values of power will become significant when MW capacity solar power plants are considered. There are various methods for cleaning solar PV panels such as manual, robotics, superhydrophobic and superhydrophillic coatings. Further detailed studies are required to estimate the power loss and financial loss due to dust deposition. Identification of cost effective dust cleaning mechanism for solar power plants installations in different locations in India and world is needed. Future work will address these issues.

4. CONCLUSION

Experimental study was carried out to compare the electrical outputs in the form of current, voltage and power for air-blower cleaned, water cleaned and unclean solar PV panels. Through the experiments, it is concluded that current and voltage values are higher for water cleaned panel for all experiment duration. A difference of about 2W in output power between water cleaned and unclean panel was observed, which is about 5% of the power capacity of the panels (40W). The increased power output for water cleaned panel is on account of

both cleaning and cooling, which is also reflected from the temperature profiles of the panels. The temperature of water cleaned panels is usually lower than the air blower cleaned and unclean panel. There is scope for further work to extensively study the cleaning and cooling effect of water cleaning of solar PV panels on power outputs and develop suitable correlations and models for Rajasthan, which has highest solar power potential in India. Studies on identification of appropriate cost effective dust cleaning mechanisms for different locations of the world are also required.

ACKNOWLEDGEMENT

Authors gratefully acknowledge the support of Royal Academy of Engineering, UK through Newton-Bhabha Higher Education Partnership Project. Koushal Shringi acknowledges the support of CSIR, New Delhi for providing junior research fellowship.

REFERENCES

1. J. Zorrilla-Casanova, M. Piliougine, J. Carretero, P. Bernaola, P. Carpena, L. Mora-López, M. Sidrach-de-Cardona, Analysis of dust losses in photovoltaic modules, PV Technology, *World Renewable Energy Congress*, Sweden, 8-13 May 2011, Linkoping, Sweden, 2985-2992.
2. Zeki Ahmed Darwish, Hussein A Kazem, K. Sopian, M.A.Alghoul and Miqdam T Chaichan, Impact of Some Environmental Variables with Dust on Solar Photovoltaic (PV) Performance: Review and Research Status, *International Journal of Energy and Environment*, 4(7), 2013, 152-159.
3. Arash Sayyah, Mark N. Horenstein, Malay K. Mazumder, Energy yield loss caused by dust deposition on photovoltaic panels, *Solar Energy* 107, 2014, 576–604.
4. Abhishek Rao, Rohit Pillai, Monto Mani, Praveen Ramamurthy, Influence of dust deposition on photovoltaic panel performance, *Energy Procedia* 54 (2014) 690 – 700, 4th International Conference on Advances in Energy Research 2013, ICAER 2013, 690-700.
5. Mohammad Reza Maghami, HashimHizam, Chandima Gomes, Mohd Amran Radzi, Mohammad Ismael Rezadad, Shahrooz Hajighorbani, Power loss due to soiling on solar panel: A review, *Renewable and Sustainable Energy Reviews,*59, 2016, 1307–1316.

6. BrahimAïssa, Rima J. Isaifan, Vinod E. Madhavan and Amir A. Abdallah, Structural and physical properties of the dust particles in Qatar and their influence on the PV panel performance, *Scientific Reports*, 2016, 6:31467, DOI: 10.1038/srep31467.
7. Julius Tanesab, David Parlevliet, Jonathan Whale, Tania Urmee, Seasonal effect of dust on the degradation of PV modules performance deployed in different climate areas, *Renewable Energy* 111, 2017, 105-115.
8. Athar Hussain, Ankit Batra and Rupendra Pachauri, An experimental study on effect of dust on power loss in solar photovoltaic module, *Renewables: Wind, Water and Solar*, 4:9, 2017, 1-13.
9. Christos Fountoukis, Benjamin Figgis, Luis Ackermann, Mohammed A. Ayoub, Effects of atmospheric dust deposition on solar PV energy production in a desert environment, *Solar Energy* 164, 2018,94–100.
10. Julius Tanesab, David Parlevliet, Jonathan Whale, Tania Urmee, The effect of dust with different morphologies on the performance degradation of photovoltaic modules, *Sustainable Energy Technologies and Assessments* 31, 2019, 347–354.
11. Dipankar Deb, Nisarg L. Brahmbhatt, Review of yield increase of solar panels through soiling prevention, and a proposed water-free automated cleaning solution, *Renewable and Sustainable Energy Reviews* 82, 2018,3306–3313.
12. Jim Joseph John, SonaliWarade, GovindasamyTamizhmani, Anil Kottantharayil, Study of Soiling Loss on Photovoltaic Modules With Artificially Deposited Dust of Different Gravimetric Densities and Compositions Collected From Different Locations in India, *IEEE Journal of Photovoltaics*, 6, 2016, 236-243.
13. Jim Joseph John, PhD. Thesis, Characterization of Soiling Loss on Photovoltaic Modules, and Development of a Novel Cleaning System, Department of Electrical Engineering, IIT Mumbai, 2016.

Cite this article

Mahesh Kumar, Koushal Shringi and Namrata Sengar, Experimental Study of Electrical Outputs for Air-Blower Cleaned, Water Cleaned and Unclean Solar PV Panels, In: Sandip A. Kale editor, Advanced Research in Solar Energy, Pune, Grinrey Publications, 2021, pp. 49-60

6 Design, Development and Experimental Study of Solar PV Air Cooler

Saiful Islam[*,a] and Namrata Sengar[b]

[a]Department of Pure and Applied Physics, University of Kota, Kota, India

*Corresponding author: saifulislamsolar@gmail.com

ABSTRACT

The article describes the design-development and experimental studies of a solar PV based evaporative air cooler. The solar air cooler has been designed with a DC pump (36 W) and DC motor (36 W). Experiments have been conducted with different wattage solar panels (75W, 100W and 115W) connected to air cooler. Solar charge controller and battery are added to the system for reliable operation. Several experiments were conducted on the developed solar air cooler to assess its performance with different solar panels, with and without battery and with and without tracking. The combination of 40 W and 75 W panel (115 W) with manual tracking without battery backup worked well for the developed solar cooler for 7-8 hours during clear summer days. The solar cooler worked from 10 a.m. in the morning to 5:00 p.m. in the evening. Experiments indicate that a solar panel of power higher than 115 W would work well for the solar air cooler. The cooler can run for around 7-8 hours without battery and battery can provide back up for around 3-4 hours.

Keywords: DC cooler, Evaporative air cooler, Solar air cooler, Solar PV panels, tracking

Advanced Research in Solar Energy | ISBN: 978-81-948951-7-6
Book Series: Research Transcripts in Energy | Vol: 01

1. INTRODUCTION

In hot climatic conditions the need to feel relaxed and comfortable has become one of few needs. Presently most of the cooling systems available are not suitable for villages and remote areas due to longer power cut durations, unavailability of electricity and high cost of products. To improve the quality of life and promote sustainable development it has become essential to meet the increasing power demands in environmentally clean and affordable manner. Solar energy is a favorable option as it can be used for various applications, even as standalone system in remote areas.

Evaporative air coolers work well in hot-dry climatic zones with minimum energy expenditure. A solar based evaporative air cooler can be helpful in improving thermal comfort conditions in hot-dry areas where grid electricity supply is not present or not regular. A study has been reported by S. Elmetenani et.al. on solar based evaporative air cooler in Algerian climate. The results showed that the maximum depression of the dry bulb temperature reached is about 18.86°C [1]. Design and performance analysis of a small solar evaporative cooler with minimum energy consumption of 10 W has been discussed by H. Lotfizadeh and M. Layeghi [2]. A solar air conditioner consisting of a liquid evaporation unit, a heat exchange unit, and a solar power generation unit was patented by H. S. Emam [3]. Solar air conditioning system directly driven by stand-alone solar PV has been studied by Bin-Juine Huang et.al. [4].

Six solar air conditioners with different sizes of PV panel and air conditioners were built and tested outdoors to experimentally investigate the running probabilities of air conditioning at various solar irradiations. G. F. Abdullah studied techno-economic optimization of the size of the components comprising an solar PV system powering evaporative air cooler and heat pump water heater to meet the demand of a typical Australian house model for two different climates [5]. Experimental studies of a direct evaporative cooler with two different cooling pads based on actual weather data in India has been reported by D. Bishoyi and K. Sudhakar [6]. R. Opoku et.al. studied the performance of a hybrid solar PV-grid powered air conditioner for daytime office cooling in hot humid climates with a case study in Kumasi city, Ghana [7].

There have been very few scientific works reported on low cost solar cooling options for remote households/shops. Therefore, present work aimed at systematic scientific study of design-development of a solar air cooler and its on-field testing for performance. The design of the system is described and performance observations have been reported for several days for different panels, with and without battery and with manual tracking.

2. DESIGN DETAILS OF DEVELOPED SOLAR AIR COOLER

The developed solar air cooler consists of a DC motor and a DC pump assembled inside cooler body. Solar panel, charge controller and battery form the rest of the system's part. The specifications for the developed cooler are presented in Table 1. The specifications of the components used with the cooler are presented in Table 2 and Table 3 and the schematic diagram of cooler is shown in Fig.1.

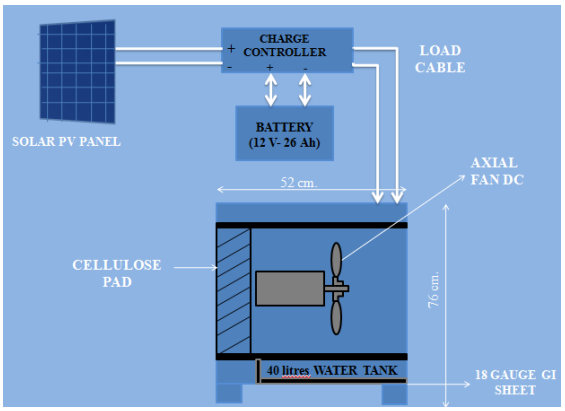

Fig. 1. Schematic figure of the developed solar PV air cooler

Table 1. Developed solar air cooler specifications

Operating Voltage	:	12 V
Operating current	:	6 Amp
Power	:	72 Watt
Load	:	DC
Required Solar Panel	:	~120 Watt
Battery	:	26 A, 12 volt
Charge Controller	:	10 Amp, 12 Volt
Wiring	:	Copper wire SWG 40/48
Control Type	:	Switch
Switch	:	Two way 10 Amp
Air Flow	:	5.20 m/s
RPM	:	1600
Speed	:	Variable
Noise	:	< 80db
Cover Area	:	~ 6 sq.m.
Auto Swing	:	Manually
Fan Type	:	Axial
Body Weight	:	4.5 kg
Water Tank	:	40 Liter
Pad	:	Cellulose
Dimension	:	52 × 52 × 76 cm
Cooler body	:	GI sheet 18 guage

Table 2. Specifications of DC motor, DC pump and charge controller

DC Fan Motor	• Operating Voltage	:	12 V
	• Operating current	:	3 Amp
	• RPM	:	~ 1200 to ~ 1600
	• Weight	:	490g
	• Dimensions	:	13 × 13 × 13 cm
DC Pump	• Operating Voltage	:	12 V
	• Operating current	:	3 Amp
	• Weight	:	Plastic, 450g
	• Water Lifting Capacity	:	1.2 m
	• Dimension	:	12.5 × 11× 9 cm
	• Water Output	:	500 LPH
Charge Controller	• Operating Voltage	:	12 V
	• Operating current	:	10 Amp (max)
	• Port	:	3
	• Weight	:	150g

A DC pump has been used in the developed system for the circulating water in cooler for evaporative cooling purpose. The specifications of the DC pump are reported in Table 3. A Pulse Width Modulation (PWM) charge controller was used for the protection of the battery from deep discharge and overcharging. The specifications are presented in Table 4 and it has been shown in figure 5. In solar air cooler a secondary type battery has been used, which is shown in figure 6. This battery has specifications of current rating 26 Ah and the voltage rating 12 Volt, total power of the battery is 312 Watt. The basic purpose behind using the battery is to provide smooth operation to the solar air cooler because PV panel does not provide fixed range of current and voltage due to variation in solar radiation. In solar air cooler project a two core 40/48 gauge copper wire is used, this wire was coated with insulating material Polyvinyl Chloride (PVC). The length of wire taken was 12 meter as solar PV panel was placed on the roof of the Kota University academic block. In the developed solar air cooler a cellulose pad is used. The cooling efficiency of this pad is more as compared to the traditional (grass type) pad, and the maintenance of this pad is also less as it needs replacement after 2 or 3 years.

For the experiments different range of PV modules are used with developed DC air cooler, which are 40 Watt, 75 Watt and 100 Watt. The modules used are polycrystalline silicon modules. The detailed specifications of these modules are presented in Table 3.

Table 3. Specifications of panels

Parameter	Rating		
Rated maximum power (P_{max})	100 Watt	75 Watt	40 Watt
Serial No. (SM- Solar $_{Maxx}$)	SM10002171342	SM07502171797	SM04001170847
Open circuit voltage (V_{oc})	21.97 V	21.72 V	21.37 V
Short circuit current (I_{sc})	6.07 A	4.6 A	2.5 A
Temperature of panel	25 °C	25 °C	25 °C
Rated voltage (V_{mpp})	17.46 V	17.33 V	17.18 V
Rated current (I_{mpp})	5.73 A	4.33 A	2.1. A

3. ON-FIELD EXPERIMENTS

The experimental studies to analyse the performance of the developed system have been conducted at Kota, Rajasthan, India (25.18°N and 75.83°E). The climate of Kota is hot and dry. The summers here are long, hot and dry, starting from late March till the end of the September month. The average temperatures during day go above 40°C in May and June and frequently exceed 45 °C, with temperatures as high as 48.4 °C have also been recorded.

The experimental setup for testing solar air cooler was at the academic block Nagarjun Bhawan of University of Kota. The various instruments used during the experimental observations were pyranometer, weather monitoring system, digital multimeter, anemometer, tachometer, digital thermometer, thermocouples and sound level meter. Kipp and Zonen CMP10 pyranometer has been used to record the solar radiation during experiments. The cooler was tested with 75 W, 100 W and 115 (40+75) W panels. The results of the observations have been reported in Tables 4-10. The experiments were performed on several days; here some representative observations have been presented.

4. RESULTS AND DISCUSSION

Experimental observations related to experiment performed on 3rd April with 75 watt, charge controller and battery connected with the DC air cooler are presented in Table 4. The solar panel was placed in south direction with the angle of inclination of 45^{o}. At 2:30 PM battery started to show low indication so cooler was stopped. The experiment was repeated with the panel of 75 W but this time instead of keeping orientation of the panel fixed, it was manually tracked three times. Initially the module was in South-East direction, at 12 PM it

rotated manually in South direction, after three hours at 3 PM it was rotated to South-West direction. The observations are presented in Table 5.

Table 4. Observation Table for 75W Module 3rd April (With battery)

Time (h)	S (W/m^2)	V_p (V)	I_p (A)	T_a (°C)	T_{sc} (°C)	v_{sca} (m/s)	u_{sca} (m/s)	N (rpm)
11:30 AM	934	20.0	4.31	38.1	34.1	3.73	1.06	1400
12:30 PM	977	19.97	4.57	39.6	33.3	3.74	1.22	1504
1:30 PM	936	19.60	4.51	39.3	31.1	3.87	1.22	1508
2:30 PM	825	19.55	4.06	39.3	30.2	2.99	1.11	1400
Low battery indication, cooler was stopped.								

Table 5. Observations of 75W Module 5th April with manual tracking (With battery)

Time (h)	S (W/m^2)	V_p (V)	I_p (A)	T_a (°C)	T_{sc} (°C)	v_{sca} (m/s)	u_{sca} (m/s)	N (rpm)
11: 00 AM	944	20.0	4.31	36.0	34.1	4.25	2.20	1504
12:00 PM	1010	20.2	4.67	38.6	33.0	4.20	2.11	1600
1:00 PM	1025	19.90	4.60	39.6	32.2	4.02	1.57	1600
2:00 PM	980	20.2	4.20	39.3	32.1	3.80	1.04	1504
3:00 PM	800	20.2	4.57	38.0	32.0	2.02	0.88	1442
4:00 PM	636	20.0	4.30	35.9	32.2	2.02	0.70	1400
Low battery indication, cooler was stopped due to low battery.								

Table 6. Observation Table of 100 W Module 10th April (With battery)

Time (h)	S (W/m^2)	V_p (V)	I_p (A)	T_a (°C)	T_{sc} (°C)	v_{sca} (m/s)	u_{sca} (m/s)	N (rpm)
11: 00 AM	950	19.70	5.52	35.70	31.7	4.25	2.22	1508
12:00 PM	1008	19.63	6.11	36.2	31.3	4.55	2.31	1600
1:00 PM	1017	19.56	6.13	37.70	31.2	4.55	2.10	1600
2:00 PM	946	19.75	5.95	38.3	30.7	3.80	1.80	1504
3:00 PM	805	19.80	4.99	36.7	30.9	2.99	1.23	1504
4:00 PM	786	19.75	3.92	36.1	31.4	2.50	0.70	1400
Low battery indication, cooler have been stopped due to low battery.								

This observation was taken with the 100 watt module. The module was placed at 23° inclination angle, the weather was clear and the module was getting proper radiation. The module was tracked, the panel was in south-east at 11 am, in south at 12 pm and in south-west direction at 2 pm, but after 2 pm it was not rotated, so the cooler stopped to run at 4 pm, due to low battery.

Table 7. Observation Table of 100W Module 13th April (without battery)

Time (h)	S (W/m^2)	V_p (V)	I_p (A)	T_a (°C)	T_{sc} (°C)	v_{sca} (m/s)	u_{sca} (m/s)	N (rpm)
11: 00 AM	969	20.7	5.97	36.2	31.4	4.11	2.22	1504
12:00 PM	1006	20.0	6.03	40.1	34.4	4.32	2.11	1600
1:00 PM	1002	20.2	5.78	40.6	35.0	4.12	2.10	1508
2:00 PM	860	20.1	4.99	40.4	34.4	3.62	1.81	1504
3:00 PM	680	20.2	5.44	40.3	32.5	2.99	1.13	1504
4:00 PM	446	20.4	4.46	37.2	32.9	2.62	0.60	1400
Solar air cooler stopped, due to cloudy weather, module output current decreased suddenly.								

This observation was done with 100W panel and the angle was 45°, but the important thing about this experiment was that the solar air cooler ran without battery till 4 pm, no battery backup was used. Another important thing to be noted is tracking, because at 11 am the module face was in south direction, at 3 pm module was tracked completely to the west direction. Due to sudden change in weather at 4 pm the output current decreased, and the solar cooler was stopped.

Table 8. (40W+75W parallel connection) Module on 20th April (without battery)

Time (h)	S (W/m^2)	V_p (V)	I_p (A)	T_a (°C)	T_{sc} (°C)	v_{sca} (m/s)	u_{sca} (m/s)	N (rpm)
10:30 AM	877	20.4	5.81	36.2	33.3	4.11	2.22	1504
11:30 AM	936	20.3	6.40	38.0	34.1	4.32	2.11	1600
12:30 PM	967	20.0	6.57	40.0	33.4	4.12	2.10	1508
1:30 PM	957	20.2	6.47	41.0	33.2	3.62	1.81	1504
2:30 PM	801	19.9	5.29	39.37	33.0	2.99	1.13	1504
3:30 PM	650	20.4	5.23	38.0	33.1	2.62	0.60	1400
4:30 PM	434	20.4	4.70	36.2	33.3	2.62	0.70	1400

In this experiment, two modules one of 75 W and other of 40 W were used. 40W and 75W modules were put in east-south and south west direction and cooler was running continuously. The tilt angle was kept at 23°. At 3 pm manual tracking was done of 40 watt panel in west direction because output current decreased at 4.92 ampere so the pump stopped to push water in air cooler, after tracking of 40 watt panel the current increased to 5.24 ampere and cooler ran again. But at 3:30 pm same problem occurred, the current decreased to 4.82 ampere and pump again stopped to throw water, so 75 watt panel was also rotated in west direction. But simple moving of panels to south direction was not enough as the increase in current was small (4.82 to 5.02). Therefore, a change in tilt angle was done which was from 23° to 30°, suddenly the current increased to 5.24 ampere and the cooler again started to run and ran till 4:30 pm.

Fig. 2. Parallel Connection of 40W+75W Modules in East-South and South-West direction

Fig. 3. 40W+75W Module at 3 pm in West Direction with 45° Angle at 21st April

Table 9. (40W+75W parallel connection) Module on 21st April (without battery)

Time (h)	S (W/m^2)	V_p (V)	I_p (A)	T_a (°C)	T_{sc} (°C)	v_{sca} (m/s)	u_{sca} (m/s)	N (rpm)
10:30 AM	881	21.4	5.91	37.8	33.3	4.84	2.22	1600
11:30 AM	959	21.0	6.44	39.2	34.1	4.67	2.11	1508
12:30 PM	979	20.6	6.66	40.8	34.6	4.90	2.42	1600
1:30 PM	943	20.7	6.45	42.5	35.3	3.84	1.81	1504
2:30 PM	819	20.7	5.77	40.3	35.7	2.99	1.13	1504
3:30 PM	604	20.6	5.88	39.2	33.7	2.75	1.11	1400
4:30 PM	455	20.8	4.82	38.0	33.7	2.62	0.70	1400

This experiment was repetition of previous experiment for finding best setup of direction and angle, without battery backup and charge controller. At 3:30 pm modules were rotated in west direction with 23° angle, but the output current was increased just at 5.02 A from 4.84 A, so we changed the tilt angle from 23° to 45°. The change in tilt angle resulted in increase in output current from 5.02 ampere to 5.88 ampere as shown in observation Table. Tracking of module in west direction with 45° at 3 pm is the best way of increasing the output current in clear weather condition.

Table 10. Parallel connected modules (40W+75W) without battery 24th April

Time (h)	S (W/m^2)	V_p (V)	I_p (A)	T_a (°C)	T_{sc} (°C)	v_{sca} (m/s)	u_{sca} (m/s)	N (rpm)
10:00 AM	760	20.4	5.60	36.8	33.3	4.77	2.22	1600
11:00 AM	902	21.0	6.42	38.2	34.2	4.62	2.11	1508
12:00 PM	989	20.4	6.55	39.8	34.4	4.87	2.09	1600
1:00 PM	943	20.7	6.52	41.5	35.1	3.84	1.81	1504
2:00 PM	820	20.7	5.77	39.3	34.9	2.99	1.10	1504
3:00 PM	604	20.4	5.88	38.2	33.8	2.65	1.09	1400
4:00 PM	455	20.4	4.75	36.4	33.5	2.62	0.70	1400
5:00 PM	402	20.2	4.64	34.7	31.4	1.99	0.60	1400

This experiment was repetition of observations as on 21st April. The observations confirmed that under clear sky conditions the cooler can run from 10 am in the morning without battery continuously till 5 pm in the evening with slight manual tracking two to three times.

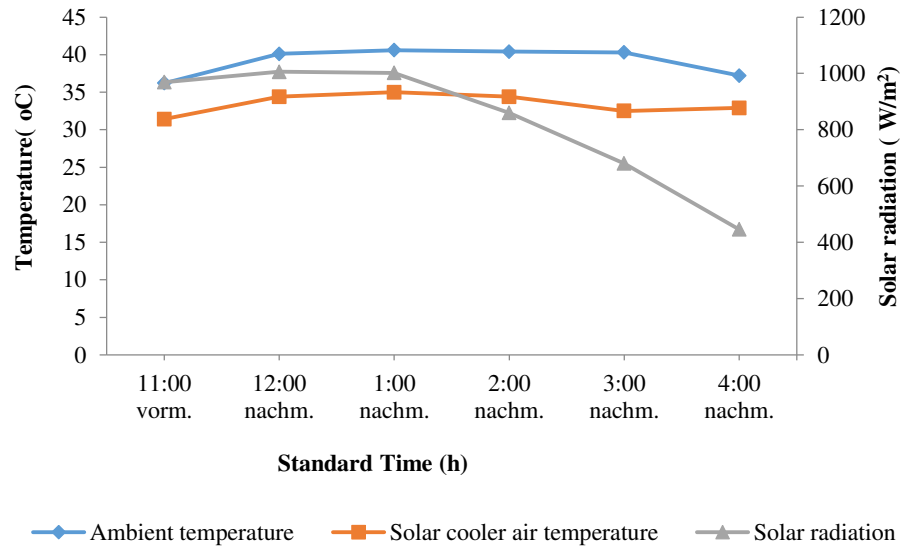

Fig. 4. Solar cooler air temperature, ambient temperature, solar radiation plotted with standard time for13th April

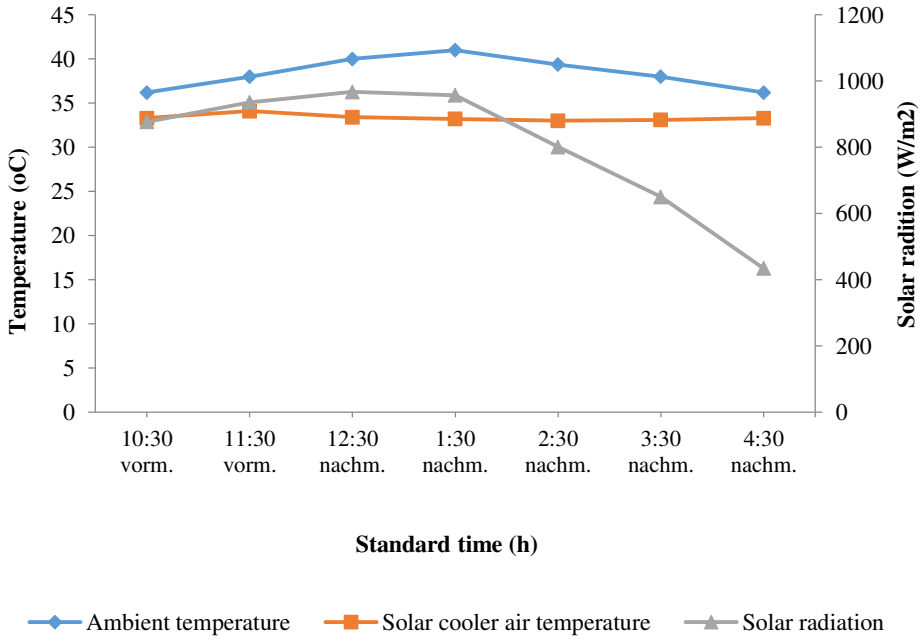

Fig. 5. Solar cooler air temperature, ambient temperature, solar radiation plotted with standard time for 20th April

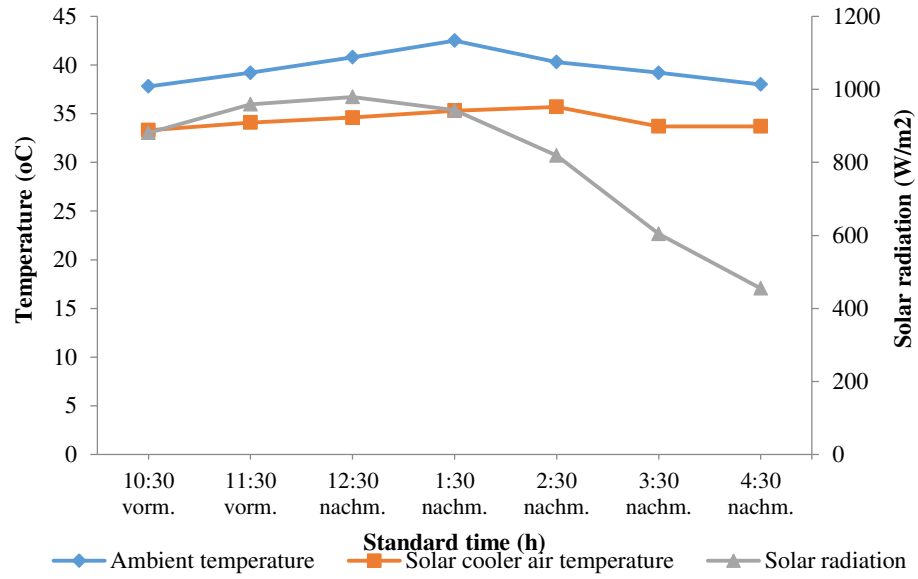

Fig. 6. Solar cooler air temperature, ambient temperature, solar radiation plotted with standard time for 21st April

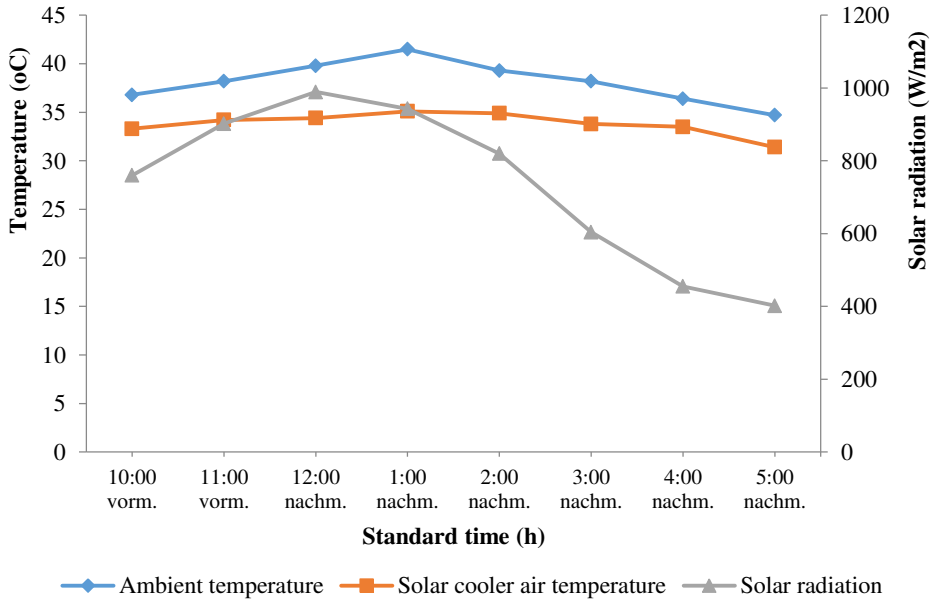

Fig. 7. Solar cooler air temperature, ambient temperature, solar radiation plotted with standard time for 24th April

From the Figure 4 to Figure 7, it can be seen that a reduction of around 5-6 ^{o}C can be achieved with solar air cooler. Solar radiation tends to decrease from 1:00 pm onwards and values reach around 400 W/m^2 around 4:00 pm. The direction of sunrays shifts towards west as solar azimuth angle increases, therefore it becomes important to manually track the solar panel towards south-west and west direction for appropriate use of solar energy. Further, as the angle of incidence also increases in the evening, it is desired that the solar panels are inclined for better reception and absorption of solar radiation.

As mentioned earlier, very few works have been reported about performance of solar air cooler and there is lack of any work, which clearly demonstrates the performance variation of the solar air cooler with standard time and tracking requirement. This work is a step towards filling the research gap. In this work, an understanding has been developed about the performance variation of solar PV cooler with different combinations of solar panels, with and without battery, and with and without tracking. Future work will be conducted to optimize the solar panel size, battery size according to climatic parameters of location and a detailed study with and without tracking will be undertaken.

5. CONCLUSIONS

The study reports the design-development and experimental studies of a solar DC evaporative cooler which may be suitable for rural shops, households in remote areas. As there is lack of studies on detailed performance prediction of solar PV air coolers, present work is a small step to enhance understanding based on the on-field experiments. The cooler uses 36 W DC pump and 36 W DC motor powered by solar PV panels. A combination of 40 W and 75 W panel (115 W) with manual tracking for two to three times in a day without battery backup was found to work well for the developed solar cooler. For the system to work without tracking, the solar panel capacity should be increased. The cooler can run for around 7-8 hours without battery on clear summer days and battery can provide back up for around 3-4 hours. There is scope of further work to optimize the solar panel capacity, battery back up requirement and tracking needs for the developed cooler according to the climatic parameters of the location. Both simulation and experimental studies will be taken up in future to develop an efficient performance model for solar PV based DC air cooler.

ACKNOWLEDGEMENT

Authors gratefully acknowledge the support of Royal Academy of Engineering, UK through Newton-Bhabha Higher Education Partnership Project.

NOMENCLATURE

I_p : Panel current (Amp)
N : Rotational speed (rpm)
S : Solar radiation (W/m^2)
T_a : Ambient temperature (^{o}C)
T_{sc} : Solar cooler air temperature (^{o}C)
u_{sca} : Solar cooler air velocity at 1 meter distance (m/s)
V_p : Panel voltage (Volts)
v_{sca} : Solar cooler air velocity (m/s)

REFERENCES

1. S. Elmetenani, M.L. Yousfi, L. Merabeti, Z. Belgroun, A. Chikouche, Investigation of an evaporative air cooler using solar energy under Algerian climate, *Energy Procedia* 6 (2011) 573–582
2. H. Lotfizadeh and M. Layeghi, Design and performance analysis of a small solar evaporative cooler, *Energy Efficiency*, DOI 10.1007/s12053-013-9199-5, Springer, published online 2014.
3. H. S. Emam, Solar air conditioner, United States patent application publication number US 2014/0096556A1, dated April 10, 2014.
4. Bin-Juine Huang, Tung-Fu Hou, Po-Chien Hsu, Tse-Han Lin, Yan-Tze Chen, Chi-Wen Chen, Kang Li, K.Y. Lee, Design of direct solar PV driven air conditioner, *Renewable Energy* 88 (2016) 95-101
5. Gazinga F. Abdullah, Wasim Saman, David Whaley , Martin Belusko, Life cycle cost of standalone solar photovoltaic system powering evaporative cooler and heat pump water heater for Australian remote homes, *Energy Procedia* 91 (2016) 681 – 691
6. Deepak Bishoyi, K. Sudhakar, Experimental performance of a direct evaporative cooler in composite climate of India, *Energy and Buildings* 153 (2017) 190–200
7. R. Opoku, K. Mensah-Darkwa, A. Samed Muntaka, Techno-economic analysis of a hybrid solar PV-grid powered air-conditioner for daytime office use in hot humid climates – A case study in Kumasi city, Ghana, *Solar Energy* 165 (2018) 65–74.

Cite this article

Saiful Islam and Namrata Sengar, Design, Development and Experimental Study of Solar PV Air Cooler, In: Sandip A. Kale editor, Advanced Research in Solar Energy, Pune, Grinrey Publications, 2021, pp. 61-74

7 Design and Implementation of MPPT Based Boost Converter Topology for Photovoltaic System

Kruthi Jayaram[a,*]

[a]Electrical and Electronics Engineering, BNM Institute of Technology, Bengaluru, India

*Corresponding author: kruthijay@gmail.com

ABSTRACT

The analysis and study of photovoltaic system is gaining utmost popularity since a decade. Unlike Conventional source of energy, solar energy is considered more beneficial because it's renewable in nature, clean source of energy, abundantly available and can easily be generated. There is an increase in demand for generation of electricity even now, due to which researchers are looking for new implementations in the generation of electricity. The output of Solar Photovoltaic is highly dependent on quantity of irradiance dropping on the solar cell. Solar energy holds many applications amongst which Solar Photovoltaic power generation exhibits efficient utilization of solar energy. Since the efficiency of a solar cell is lesser, MPPT is employed in Photovoltaic power generation system to track maximum output power irrespective of irradiance, temperature and electrical load characteristics. In this chapter, MPPT based step-up(boost) converter topology is implemented. The output of the Photovoltaic is fed to boost converter as a connection between Photovoltaic and the load to step up the voltage. The entire operation of step-up converter for Photovoltaic system with MPPT algorithm is analyzed using MATLAB Simulink Software.

Keywords: Photovoltaic Array, Boost (step-up) converter, Maximum power point tracker

Advanced Research in Solar Energy | ISBN: 978-81-948951-7-6
Book Series: Research Transcripts in Energy | Vol: 01

1. INTRODUCTION

Energy is needed for a broad range of applications in domestic, industry and commercial usage. The utilization of energy plays a very crucial role in one's life. It leads to nation development. The utilization of energy has become an integral part of one's life; its supply of such energy should be fixed and reliable, economical, environmentally friendly and socially accepted by all. Evolution and expansion of clean, secure, sustainable and affordable energy sources should be our priority in this century. In this regard, use of solar energy for the production of generation of electricity is a prime importance. Solar energy is the clean and abundant source of energy [1]. Photovoltaic systems are used in variety of applications from battery charging up to satellite communication.

Photovoltaic modules are installed to supply the power to the load via a converter. Solar Photovoltaic modules consist of solar cells which are connected in series according to the module voltage required. Based on the system design the entire PV can be designed. When Photovoltaic module is directly connected to a load, the operating point is hardly at maximum power point. The output of the PV array is connected to DC-DC converter for the sake of Maximum power point tracking in order to extract maximum power from the cell at a given irradiance level. The Solar Photovoltaic module is expressed in terms of the peak power (Wp) output [2].

1.1 Block Diagram

Fig. 1. shows the Block diagram consisting of Photovoltaic panel, DC-DC converter, MPPT controller & a resistive load. PV panel or the solar array can be designed in series and parallel combinations depending on the design requirement. The essential part of photovoltaic system is MPPT controller. The photovoltaic module finds it difficult to attain maximum power always due to which MPPT will be installed. MPPT (Maximum Power Point Tracking) is utilized to match the voltage requirement and the supply efficiently to load by introducing a voltage converter. The input to MPPT controller can be voltage and current.

Basically, MPPT algorithm extracts extreme obtainable power from photovoltaic module under any operating settings. Maximum power point is defined as voltage at which photovoltaic module can harvest extreme power. This maximum power produced differs with solar radiation, ambient temperature and solar cell temperature [4-5].

Module and load interference is provided by DC to DC converters. DC to DC converters are high frequency power conversion circuits which help in converting voltage from one level to the other. Such converters produce output

voltage either greater or lesser than the input voltage. The choice of the appropriate DC to DC converter depends on the kind of application it is being used in. There exist 3 types of DC-DC converter topologies. Namely, Buck (step-down) type, Boost (step-up) type and Buck-Boost type DC-DC converter. This chapter presents a brief account on PV modules, Boost converter, MPPT algorithm where the entire working model is simulated on MATLAB/Simulink. The entire model with the corresponding results is simulated and shown here.

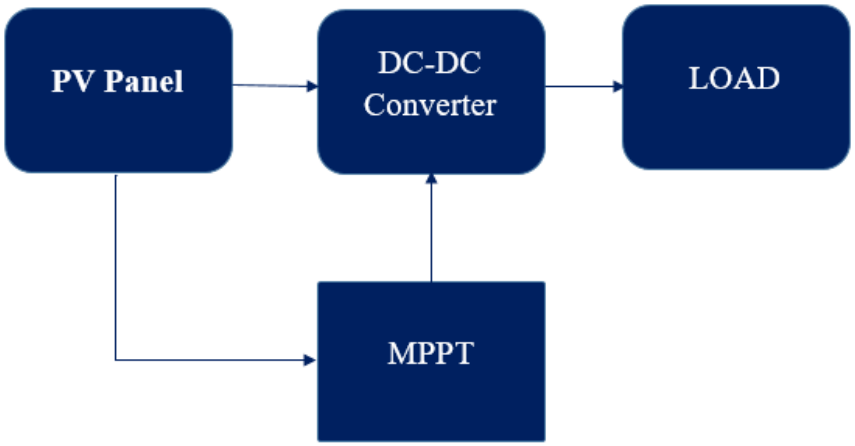

Fig. 1. Block diagram of MPPT based Boost converter topology for PV system

2. PHOTOVOLTAIC MODULE

Solar cell or a Photovoltaic cell works on a principle of photovoltaic effect. Once sunlight falls on the surface of a solar cell, flow of electrons will take place. Therefore, any photovoltaic system comprises of PV modules or array which converts solar irradiation into electricity. Photovoltaic cells are joined in series to form a module. Photovoltaic modules are joined in series and parallel to form an array. Photovoltaic cells are prepared of semiconductor material.

Fig. 2. shows the correspondent circuit diagram of a solar or a Photovoltaic cell. The electric circuit shown contains a current source which is in parallel with the diode, shunt resistance R_{sh}. A series resistance R_s is because of the obstruction in the track of flow of electrons from *n* to *p* junction. In this chapter, a PV module of 1SolTech-1STH-215-P is used. The array has a configuration of two parallel strings and two series-connected modules per string. It has an open circuit voltage V_{oc} of 36.3 Volts and a short circuit current I_{sc} of 7.84A. Irradiance of the module is 1KW/m^2 and cell temperature is 25^{0}C.

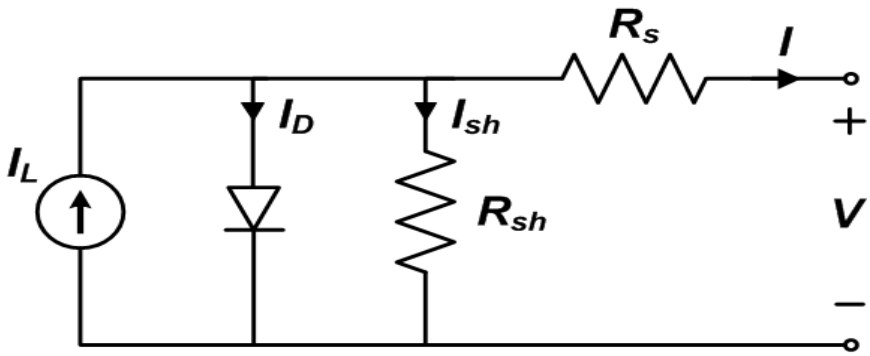

Fig. 2. Correspondent circuit of a PV cell

The above equivalent circuit of a PV cell is depicted with a Current-Voltage and Power-Voltage characteristics as shown in fig3. The first plot is current versus voltage of the cell for different irradiance level. The second plot is power versus voltage of the cell for different irradiance level. Power is calculated by multiplying voltage with current in the cell. The red dot on the curve represents the maximum power point of the cell. The current and voltage at Maximum power point (MPP) is given by Imp and V_{mp}. Since there is a variation in irradiance and temperature, PV characteristics keeps on varying to which an MPP is added to track the maximum output power from the panel.

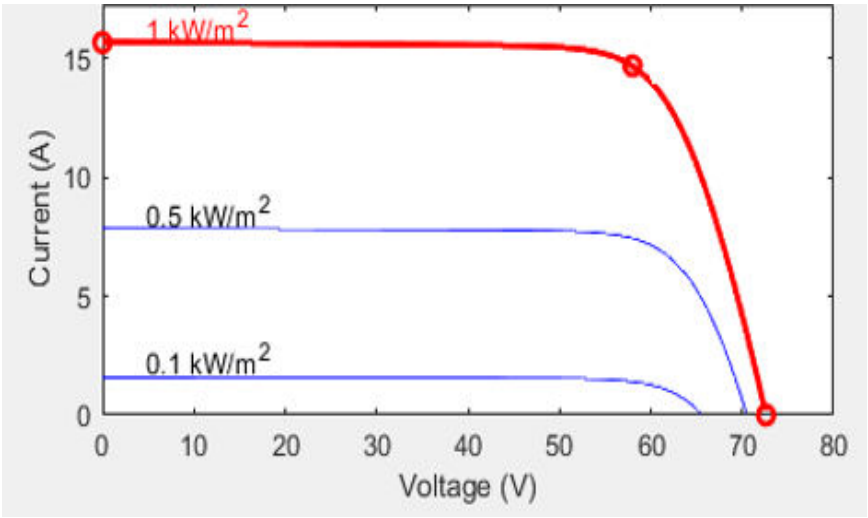

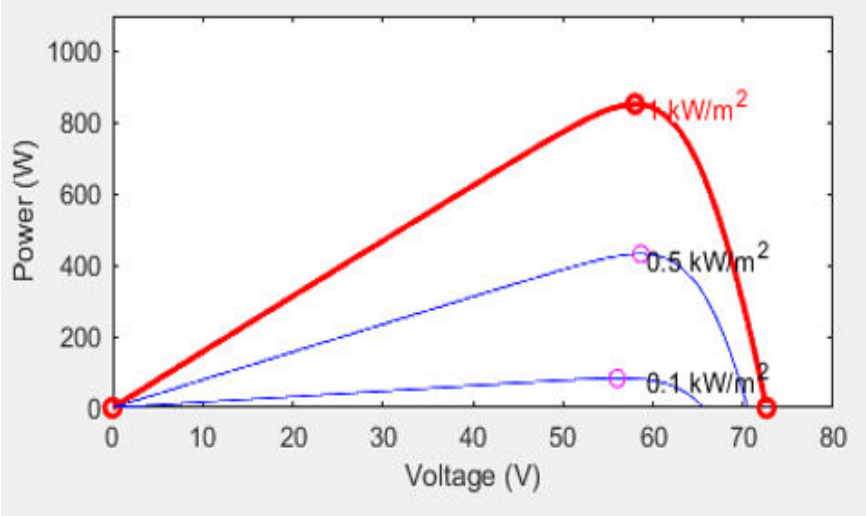

Fig. 3. Current-Voltage and Power-Voltage characteristics of the solar cell used in the model

3. DC-DC CONVERTER

DC-DC converters change one level of DC voltage to one more level of DC voltage. The converter comprises of storing elements like inductor, capacitor, power devices like transistors, diodes etc. One of the applications of using this DC-DC converter is in Charge controllers, Maximum power point tracking etc. The DC to DC circuits are also utilized for noise isolation, power bus regulation and current boosting.

The three types of converter topology used are:

- Buck(step-down) type DC to DC converter (it steps down the input voltage)
- Boost(step-up) type DC to DC converter (it steps up the input voltage)
- Buck boost type DC to DC converter (both step up and step down are possible)

3.1 Boost Converter and its operation

A boost (step-up) converter is a DC to DC converter that provides an output voltage larger than the source voltage. Hence it is called as step-up converter or boost converter. In such type of converter the output current is lesser than source current. Depending on the operating conditions, converter can be functioned in continuous or discontinuous conduction mode.

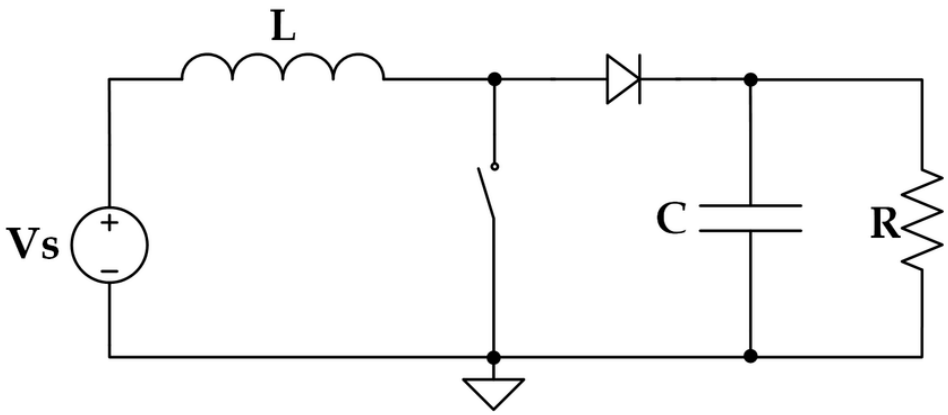

Fig. 4. Ideal Boost (step-up) converter circuit

Fig. 4. shows the circuit of boost (step-up) converter. Boost (step-up) converter comprises of diode, capacitor, input voltage source, switch, inductor and resistor which acts as a load. The task of boost (step-up) converter is to enhance the voltage level. When the switch is in ON state the source delivers energy into the inductor, diode remains reverse biased and voltage across the inductor is equal to input voltage. When the switch is in OFF state, the inductor current must have a path and the diode is forward biased to release the energy stored in the inductor into the load.

4. MPPT (MAXIMUM POWER POINT TRACKER)

Solar photovoltaic when utilized in a photovoltaic system, we decide its operational point based on the type of load it is connected to. The incident of solar radiation on a photovoltaic module differs throughout a day. Since we need to have the operation of the photovoltaic module under maximum power, Maximum power point trackers is being employed. MPPT electronic circuitry is utilized to confirm that maximum quantity of generated power is transported to the load.

Fig. 5. shows the MPPT Algorithm used in the Simulink model. The maximum power point tracking is composed of algorithm and electronic circuitry. It is established on the principle of impedance matching sandwiched between the load and Photovoltaic module, which attains the required maximum power transfer. The impedance equalizing is done by utilizing a DC-DC converter. By using a DC-DC converter, the impedance is matched by varying the duty cycle of the switch. By measuring the voltage and current from the solar module power can be deliberated. The power obtained is an inlet to the algorithm which regulates the duty cycle of the switch, causing in the modification of the

reflected load impedance with respect to the power output of PV module. In this chapter, Perturb and Observe (P&O) technique is used as it is a low cost implementation. P&O algorithm is the meekest method of MPPT to implement.

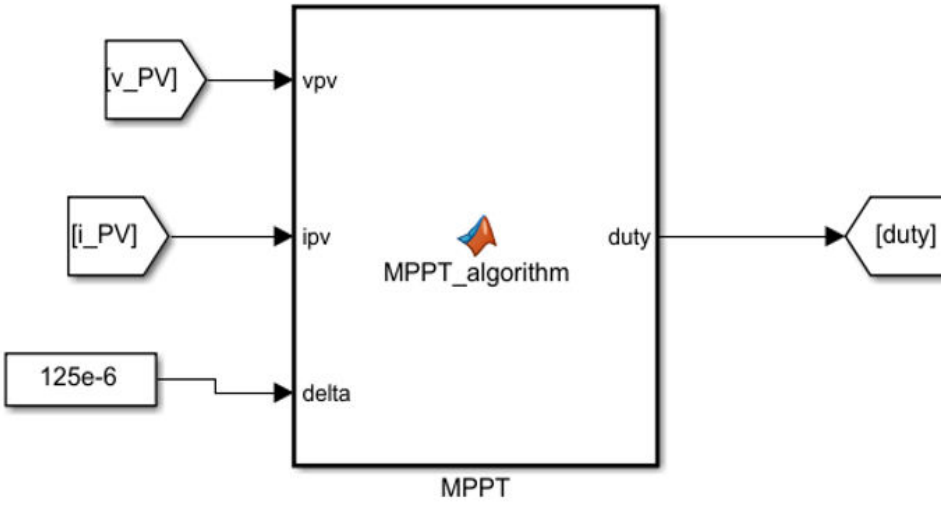

Fig. 5. MPPT Algorithm used in the model

Perturb and Observe (P&O) method:

- Voltage is detected
- Power output is scrutinized by changing the supplied voltage
- As voltage increases, power increases and thereby delta also increases. While reducing voltage if power surges the duty cycle is reduced.
- The voltage at which MPP is gained we call that as reference point.

5. SIMULATION MODEL

The whole Simulation circuit of the complete work is shown in Fig. 6. and Fig. 7. It comprises of Solar panel, MPPT Block, Boost converter with resistive load. Maximum power point tracking block regulates the extreme operating point and permit the gate signal to boost converter where the converter supports to sustain the operating voltage at the maximum power point. The load has a resistance of 20 ohms. The inductance of the boost converter is 2mH. The snubber resistance is 500ohms and the snubber capacitance is 250nF.

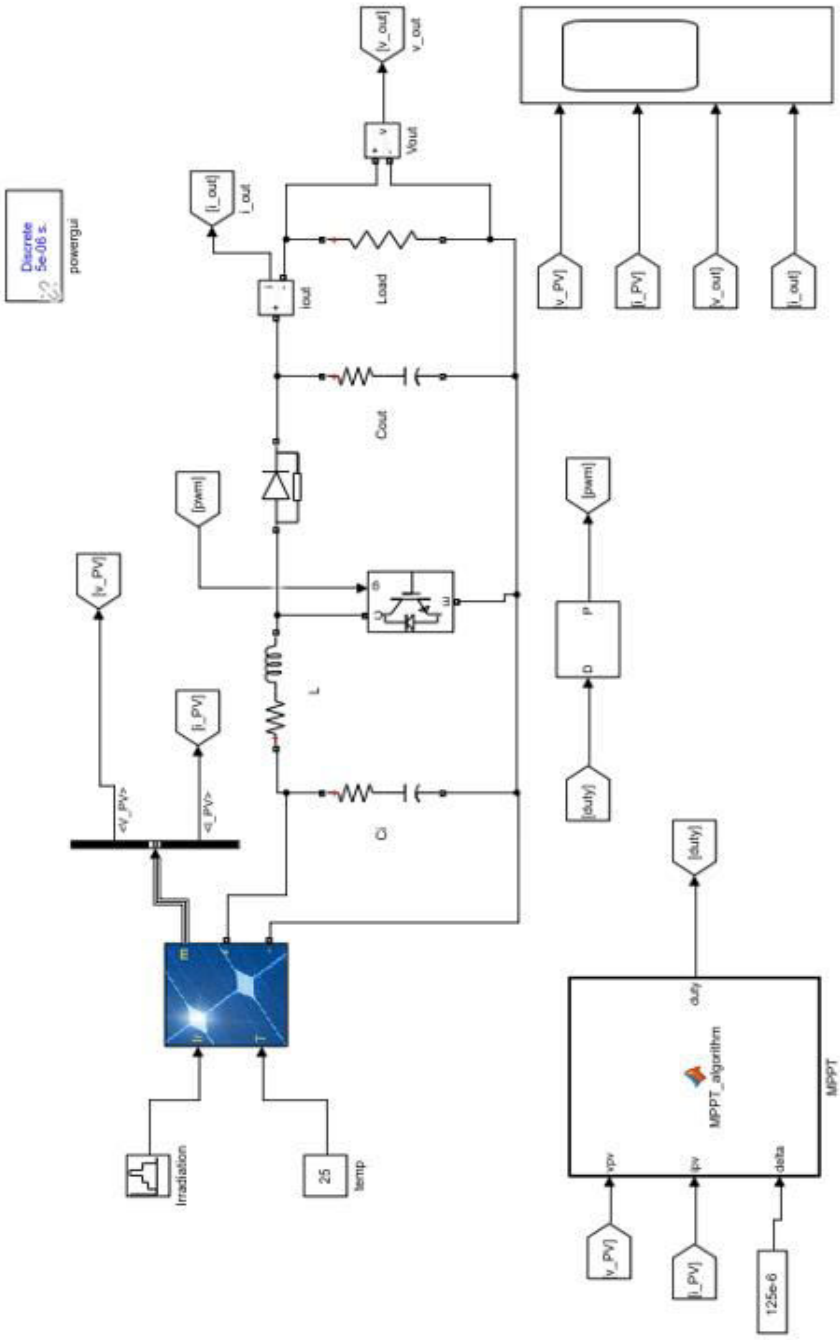

Fig. 6. Simulink model of the proposed work

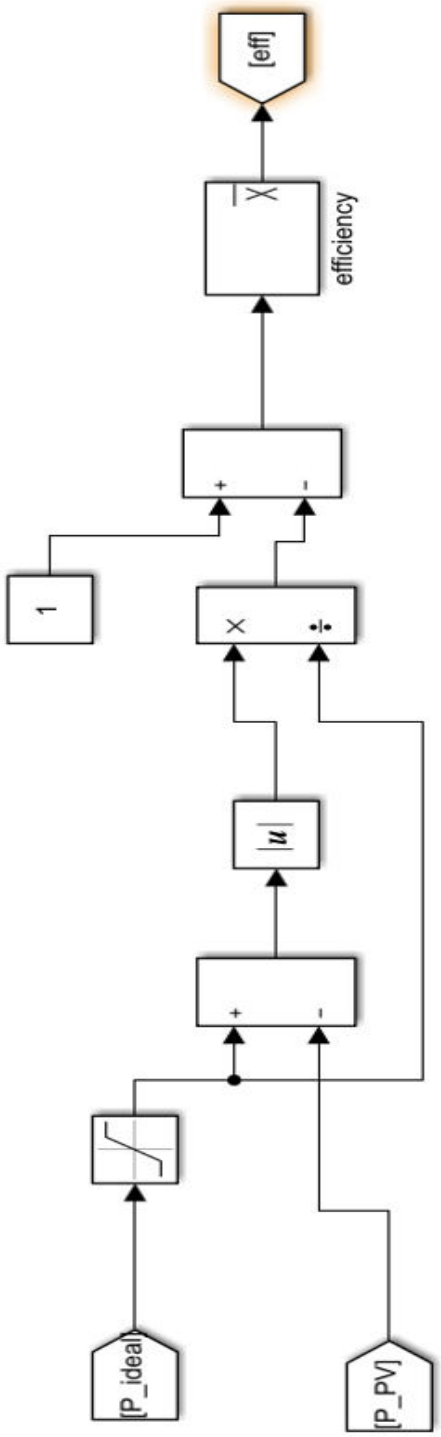

Fig. 7. Simulink model of the proposed work

6. SIMULATION RESULTS

The Voltage that is generated by the PV module is given at the input to the boost converter for a certain duty cycle. The simulation outcomes of the output of PV module and the boost converter for the variation in the solar irradiance are shown below in Fig 8, 9 and 10.

The irradiance of the Photovoltaic module varies with different amount of insolation level at any given period of time. Temperature is fixed at 25^0C. In Fig. 8. and Fig.9. we can observe that for a irradiation of repeating sequence the output voltage and current follows the same sequence. The boost voltage is around 62.5volts. In Fig. 10. we can observe that the irradiation curve is changed to a bell shape curve and the yield of output voltage and current interprets the same according to the input with increase in voltage at the output from the input.

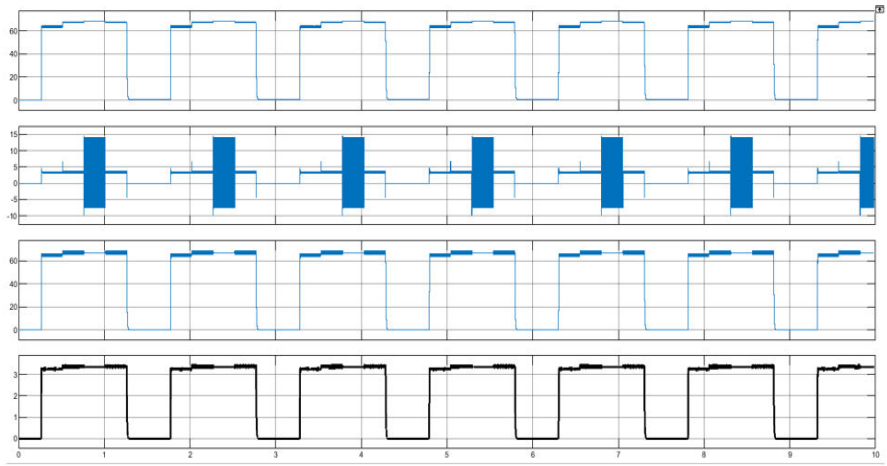

Fig. 8. Simulation results

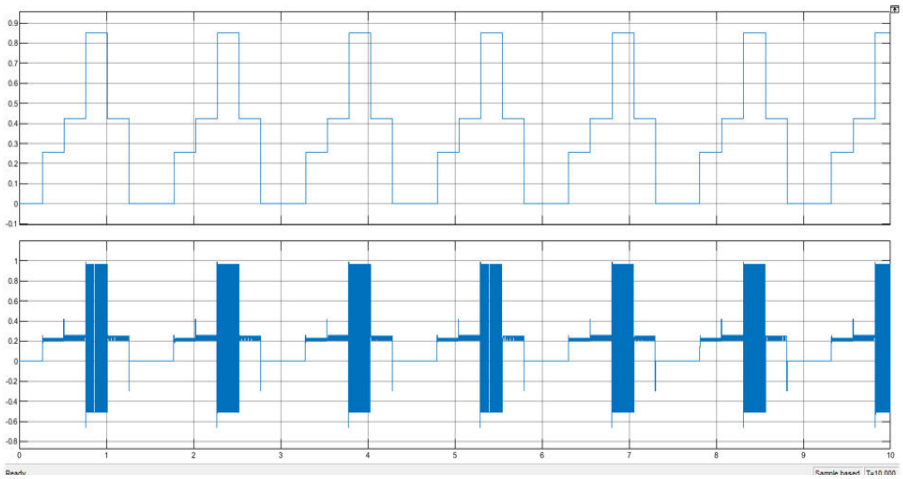

Fig. 9. Simulation results

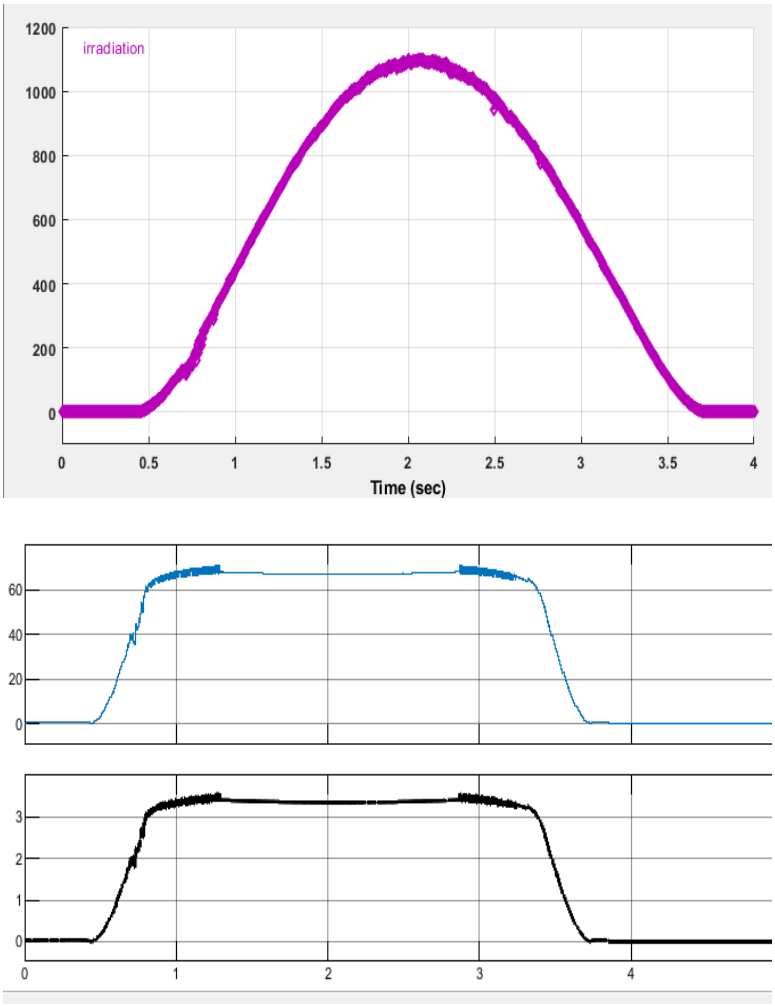

Fig. 10. First figure represents the irradiation curve and the second figure represents the output voltage and current

7. CONCLUSION

In this chapter, the design and implementation of MPPT based Boost converter using P&O algorithm was successfully simulated. The entire architecture of the model is carried out in MATLAB/Simulink software. Since the irradiance level keep varying for a PV module achieveing maximum power is always tedious, hence MPPT is added to the system and analyzed to achieve Maximum power point at any change of solar irradiance with the assistance of boost converter. Boost converter attains the maximum power point that lowers the array voltage to the extreme operating point voltage. Therefore, with the help of MPPT algorithm and boost converter Photovoltaic array topology its is functioned at maximum power point regardless of solar irradiance.

NOMENCLATURE

I_D	:	Diode current (A)
I_L	:	light generated current (A)
I_{mp}	:	Current at maximum power
I_{sh}	:	Current through shunt resistor (A)
$MPPT$	:	Maximum power point tracker
R_s	:	Series resistance (ohm)
R_{sh}	:	Shunt resistance (ohm)
V_{mp}	:	Voltage at maximum power
W_p	:	Peak power

REFERENCES

1. Priyabrata Pattanaik, Boost Converter based on Photovoltaic Energy System, International Journal of Innovative Technology and Exploring Engineering , 2019, Vol.-8 (11S), pp. 897-902
2. C. Laksmanasamy, P. Rathinasamy, Design and Simulation of Boost Converter with MPPT Techniques, International Journal of Advances in Computer and Electronics Engineering, 2017, 02 (05), pp: 01 – 06
3. Mangesh A. Chewale , Viraj B. Savakhande , Vishal R. Sagar, MPPT Based Boost Converter for Photovoltaic Application, 13th International Conference on Recent innovations in science, engineering and management, 23rd February 2018, pp. 322-334
4. Shridhar Sholapur, K. R. Mohan, T. R. Narsimhegowda, Boost Converter Topology for PV System with Perturb And Observe MPPT Algorithm, IOSR Journal of Electrical and Electronics Engineering (IOSR-JEEE), Volume 9, Issue 4 Ver. II (Jul – Aug. 2014), pp. 50-56
5. A K Srivastava, Sanjay Kumar, A S Pandey, D. Mukherjee, Rashmi Behera, Performance Comparison of PV Module Using INC MPPT With Boost & SEPIC Converter, International Journal Of Scientific & Technology Research Volume 8, Issue 11, pp. 2397-2403
6. V. C. Kotak, Preti Tyagi, DC To DC Converter in Maximum Power Point Tracker, International Journal of Advanced Research in Electrical, Electronics and Instrumentation Engineering, 2 (12), pp. 6115-6125

Cite this article

Kruthi Jayaram, Design And Implementation of MPPT Based Boost Converter Topology For Photovoltaic System, In: Sandip A. Kale editor, Advanced Research in Solar Energy, Pune, Grinrey Publications, 2021, pp. 75-86

8 A Novel PID Using A Genetic Algorithm to Track The Maximum Power Point of The PV System

Zahira EL HARIZ[a,*], Hicham Aissaoui[a] and Mohammed Diany[a]

[a]Electrical Engineering Department, Faculty of Science and Technology, Beni Mellal, Morocco

*Corresponding author: zahiraelhariz2015@gmail.com

ABSTRACT

Incremental demand for electrical energy and the resulting increase in environmental problems are the main reasons forcing managers in the energy sector to expand the use of renewable energy sources in the production of electricity. In the future, the use of renewable energy systems will be increased and will play a very important role in the economic indices of power systems. The hybrid energy systems use two or more renewable energy sources, to increase the reliability and profitability of the installation. This article proposes a new application of the proportional-integral-derivative (PID) controller based on genetic algorithms and the P&O method to effectively reach the maximum power point tracking (MPPT) of solar panel. To evaluate the efficiency and profitability of the proposed methodology, a comparison study of this method with the classical P&O method was carried out.

Keywords: Genetic Algorithm, PV panels, MPPT, PID controller, P&O.

Advanced Research in Solar Energy | ISBN: 978-81-948951-7-6
Book Series: Research Transcripts in Energy | Vol: 01

1. INTRODUCTION

The limitation of centralized energy sources opens up a great opportunity for renewable energy sources which are increasingly becoming a promising energy solution. Decentralized production systems offer several advantages by allowing sites or companies to engage in the fight against climate change, to choose the source of their energy or even to reduce their electricity bill and guarantee better autonomy of the network. Different methods of optimization have been detailed in the literature [1-3] [14] [15] as dynamic programming [4], multi-objective [5], linear programming [6] [7], and metaheuristic method [8] [9] [10].

To increase the efficiency of the photovoltaic system, it is necessary to force the DC / DC converter systems to operate the point of maximum power, hence the need to use MPPTs which play a very important role in photovoltaic systems, they maximize the power of the PV system for variable meteorological conditions and minimize energy losses and the global cost. Different MPPT methods have been used and developed to search the maximum power, observation and a perturbation method [11], which is an easy method, based on the iterative algorithms, but it present an oscillation problem. The Incremental Conductance technique (IC) [12], the flow logic control Method (FLC) [13] which is successfully implemented in the solar panel to tracker the maximum power. In this chapter a new MPPT method based on the P&O, PID controller and genetic algorithm is presented, the rentability and the efficiency of this methodology are successfully studied.

2. PHOTOVOLTAIC MODULE

The site selected for this study is named "MGHILA" and located near BENI MELLAL (32 ° 20′22 ″ N 6 ° 21′39 ″ W)) with an average altitude above sea level of 571 meters. The Meteonorm version 7.3.3 database was used to evaluate the weather conditions of the site. Figure 1 to Figure 4 show respectively the maximum & minimum values of daily temperature, global and diffuse irradiation, sunshine duration and the temperature of the site. During the year, the temperature generally ranges from 6 °C to 39 °C and is rarely below 5 °C or above 40 °C. The very hot season lasts 3 months, from 7 June to 7 September, with an average daily maximum temperature above 30 °C. The hottest day of the year is 14 July, with an average maximum temperature of 47 °C and a minimum of 27 °C. The average solar radiation varies between 0 and 240 kW/m^2.

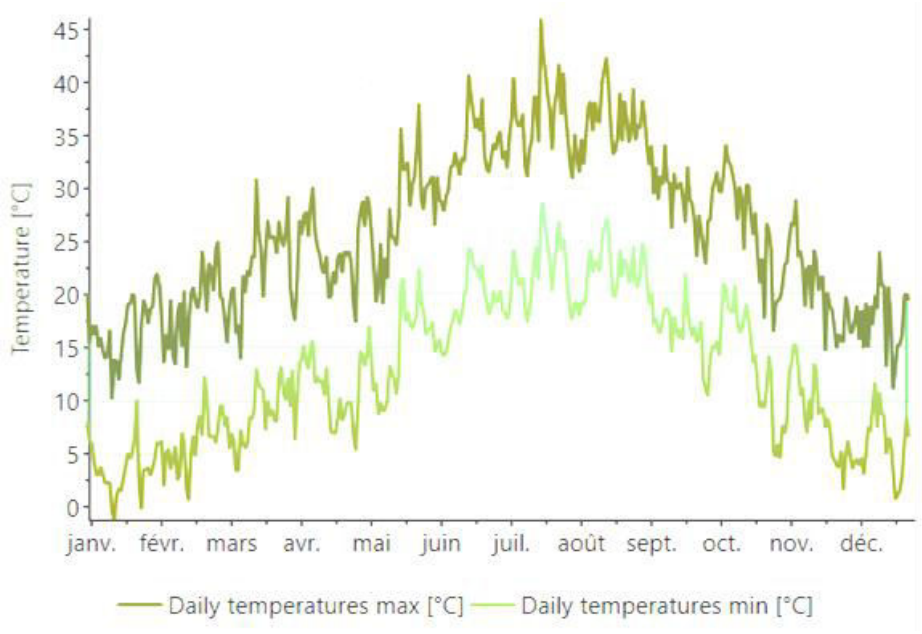

Fig. 1. Maximum and minimum daily temperatures

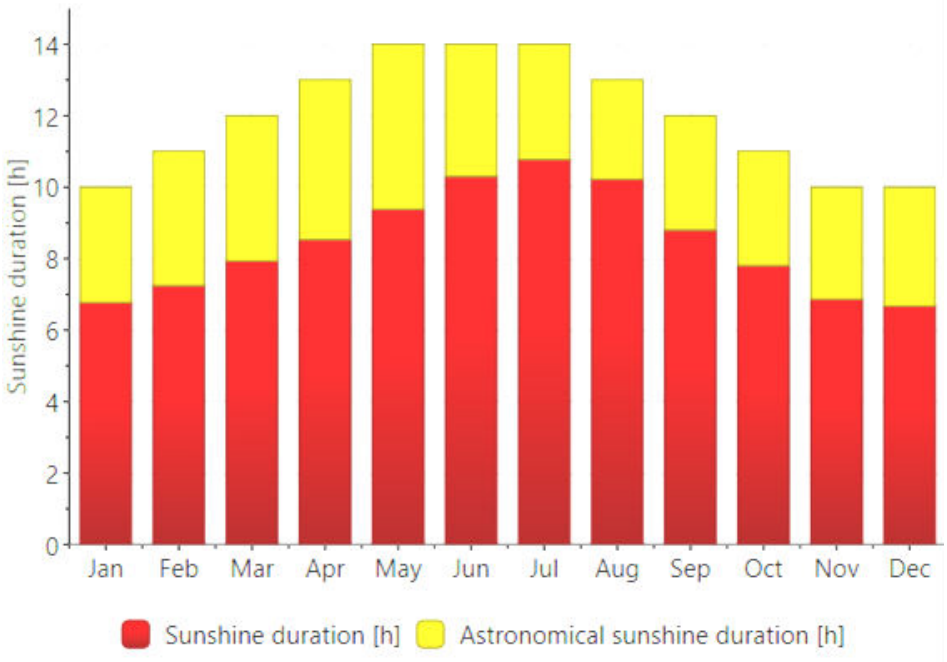

Fig. 2. Sunshine duration

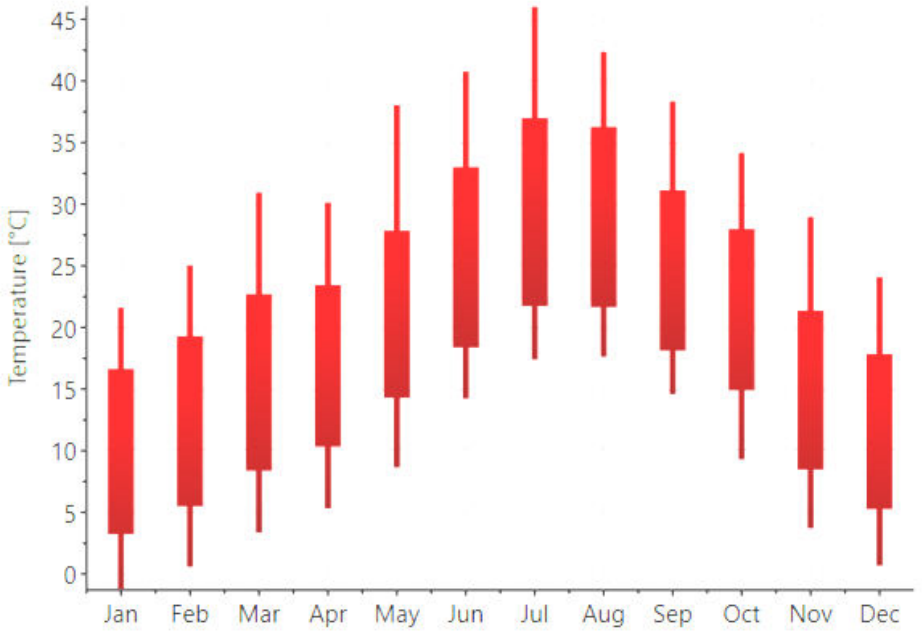

Fig. 3. Site temperatures

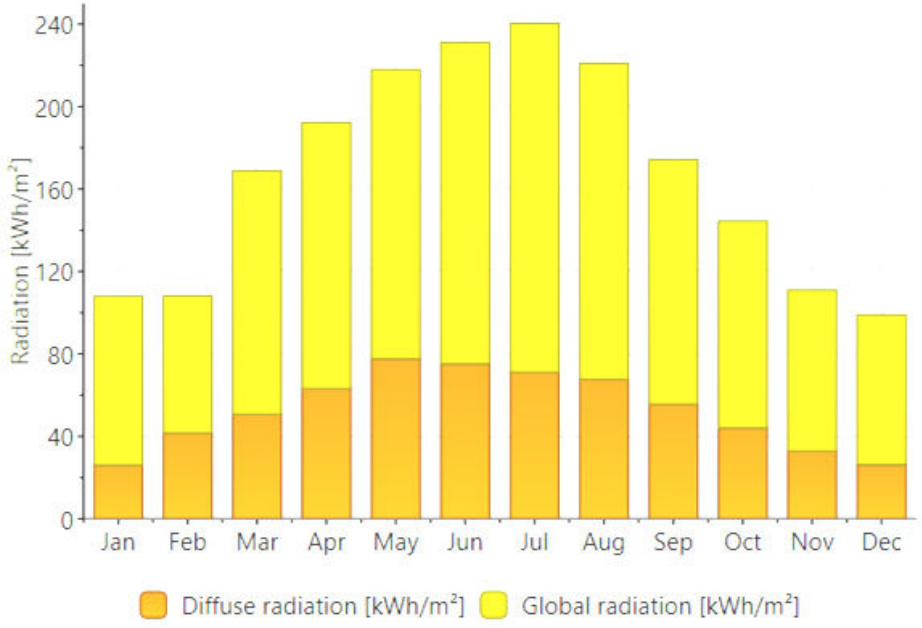

Fig. 4. Diffuse and global radiation

3. MAXIMUM POWER POINT TRACKING

The solar energy is the most important source as an environmentally friendly renewable energy source. The characteristics of the solar model (I-V and P-V), at different values of temperature and irradiation, are presented below. Figures 5 and 6 illustrate the plots of I -V and P -V for a different values of temperature 0, 25, 50, 75 and 100 ◦C at a fixed irradiation equal to 1000 W/m^2. Similarly, figures 7 and 8 show the I − V and P −V characteristics for different values of irradiation 200, 400, 600, 800 and 100 W/m^2 at a fixed temperature equal to 25◦C. The operating point of the photovoltaic system where the maximum power is reached is called the maximum power point (MPP). The MPP controller is an essential element for tracking the maximum power point of the solar panel by varying the duty cycle of the DC / DC converter in order to reach the maximum power point.

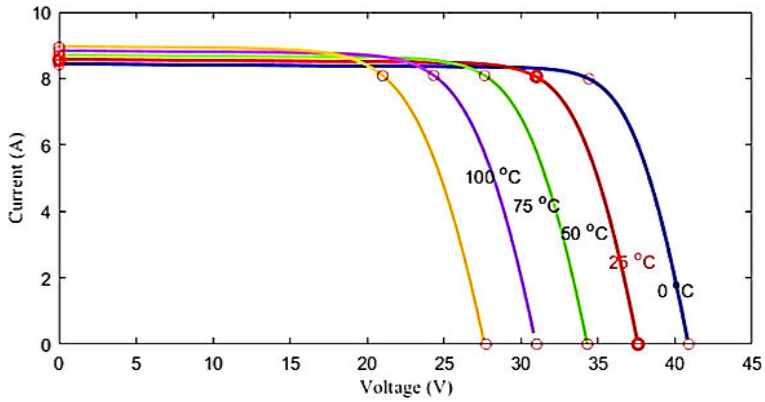

Fig. 5. Characteristic I−V at different temperature values

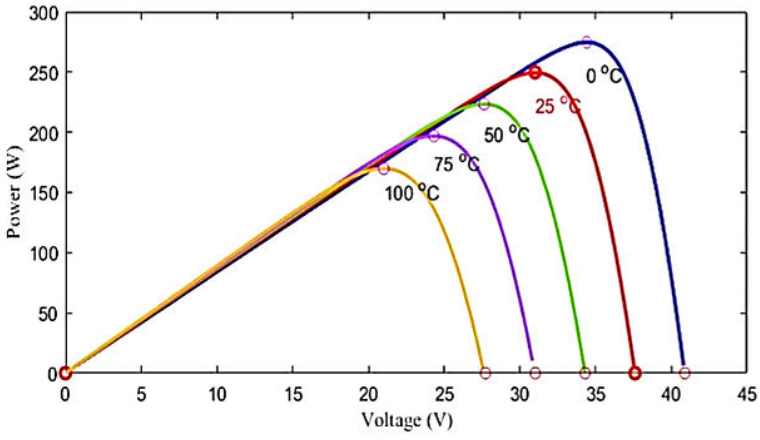

Fig. 6. Characteristic P−V at different temperature values

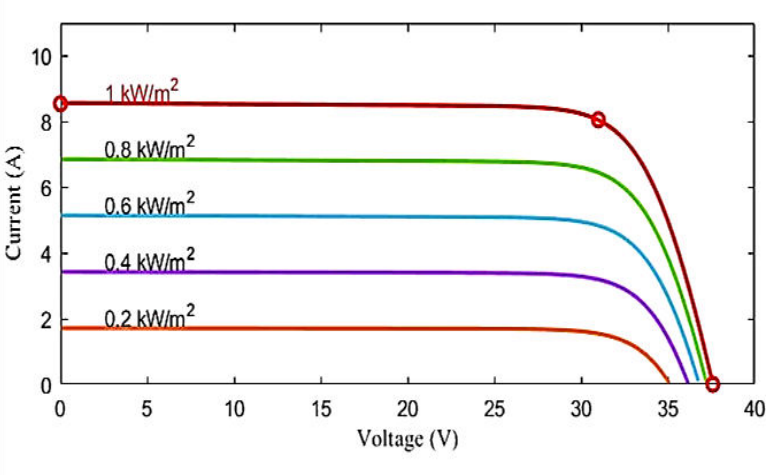

Fig. 7. Characteristic I−V at different irradiation values

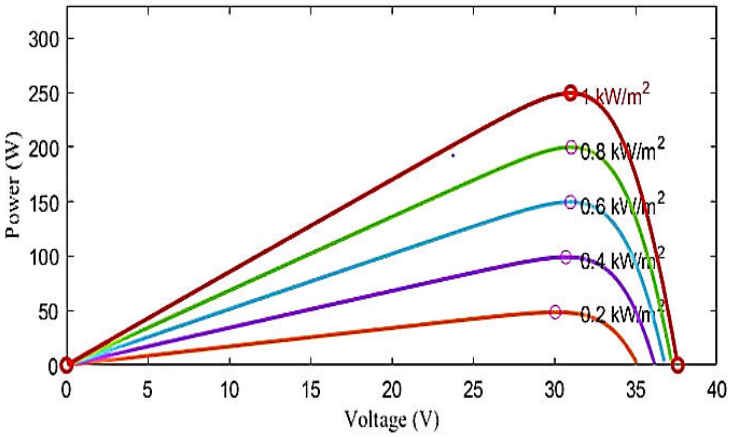

Fig. 8. Characteristic P−V at different irradiation values

In this article, the proposed methodology uses the principle of the perturbation and observation method, the PID regulator and the genetic algorithm to generate the reference set point dP / dt in order to control the DC / DC converter. Figure 9 presents the MPPT

d P / d V diagram in the form of a block diagram. The principle of the MPP relates to the calculation of the slope d P / d V and to compare it with the reference signal. The error signal will be transmitted to control the DC / DC converter. Thereafter, the controller guides the operating point of the photovoltaic generator to the MPP.

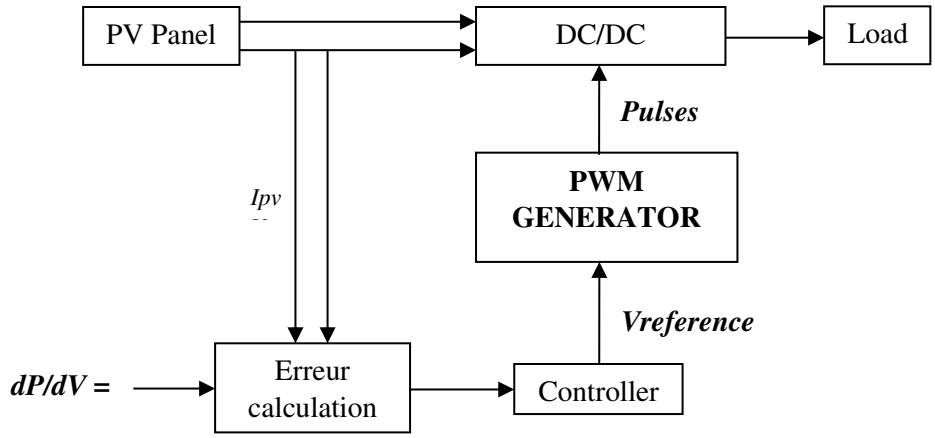

Fig. 9. Maximum Power Point Tracking control scheme

The GA is used to select the best population in any iteration. The first step is to initialize the genetic algorithms. Then the best solution will be memorized, the PID controller is used to eliminate the problem of the conventional P&O method, which oscillates around the set point and causes a point tracking loss of maximum power and energy. The PID controller must adapt according to the current performance of the hybrid system. This performance is used as an error which can be used to provide the Kp, Ki and Kd parameters. Then the program stops and the best solution is announced. the principe of the proposed methodology is summarized as follows:

Step 1 : Iinitialize the population size, the probability of crossing, the probability of mutation, the maximum number of generations and the limits of the decision variables.
Step 2 : Decode the binary value to real number.
Step 3: Calculate the fitness for each chromosome.
Step 4: Select the best chromosome
Step 5: Apply the crossover operators based on the principle of the P&O method.
Step 6; Apply the mutation operators
Step 7: Repeat the steps mentioned before until the shutdown criterion is met
The Adapted GA-P&O selects the different values of the PID regulator parameters Kp, Ki and Kd to reach the maximum power value of the solar panel.

The different parameters used in the proposed method are defined in the Table 1.

Table 1. Parameters of the genetic algorithm

Description	Parameters
Population size	50
Maximum of iteration	100
Crossover probability	0.8
Mutation probability	0. 1
Number of bits per chromosome	16

4. RESULT AND DISCUSSION

In this section, the proposed methodology is compared with the results of the P&O method. To evaluate in a more efficient way, variable irradiation was used to make detailed performance comparisons in terms of speed, passing and accuracy. The P&O MPPT method using a genetic algorithm and based on the PID controller begins with an initial evaluation of data and continues until the stop criterion is met. The proposed method was executed using Matlab Simulink in order to check their performance. Three series chains compose the photovoltaic generator; each string is composed by 16 BPMSX120 solar panels connected in parallels. Table 2 below shows the technical parameters of the solar panels:

Table 2. Technical characteristic of the photovoltaic panel

Parapeters	Symbols	Values
Short-circuit current	Isc	3.87 A
Open circuit voltage	Voc	42.1 V
Voltage at MPP	VMPP	33.7 V
Current at MPP	IMPP	3.56 A
Power at MPP i	PMPP	120 W

Figures 10-12 respectively illustrate the simulation results of the proposed methodology, they show the good agreement between the voltage, the current and the power of the photovoltaic panel with the results of the classic P&O method, which has presented an oscillation problem around the point of maximum power, and subsequently cause energy losses from the solar panel and without oscillations for the proposed methodology. This methodology, compared to the P&O method, gives more optimal results. using this method, it is possible to quickly find the maximum power with less overshoot and stabilization time of each controller as well as the Ripple. The efficiency of the proposed method according to the variation of the meteorological data of the

site (temperature and solar irradiance) is evaluated. Through the results of simulations, it can be concluded that, when the temperature and solar irradiance change, the duty cycle of the DC / DC converter varies to its desired value, which forces the current and voltage of the solar panel at follow their optimum values, and subsequently the power of the PV module has reached its maximum value.

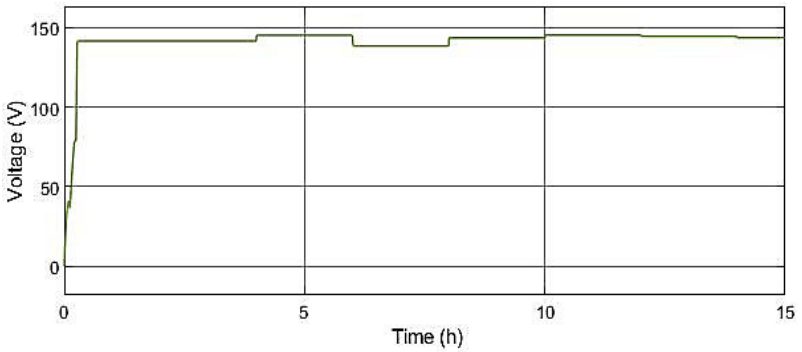

Fig. 10. PV voltage variation of the proposed method

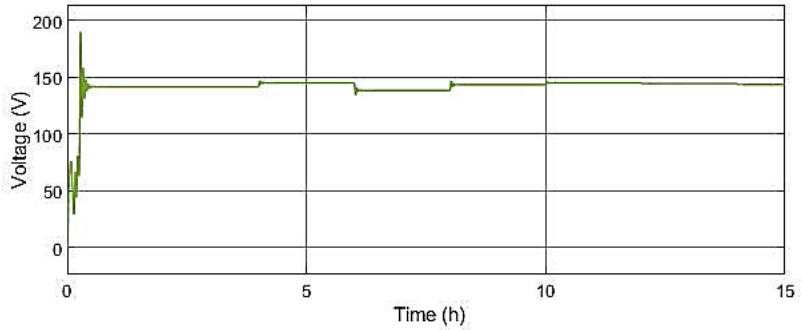

Fig. 11. PV Courant voltage of the P&O method

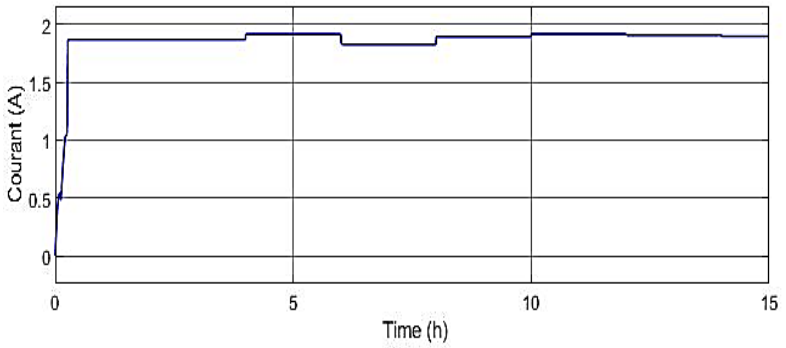

Fig. 12. PV Courant variation of the proposed method

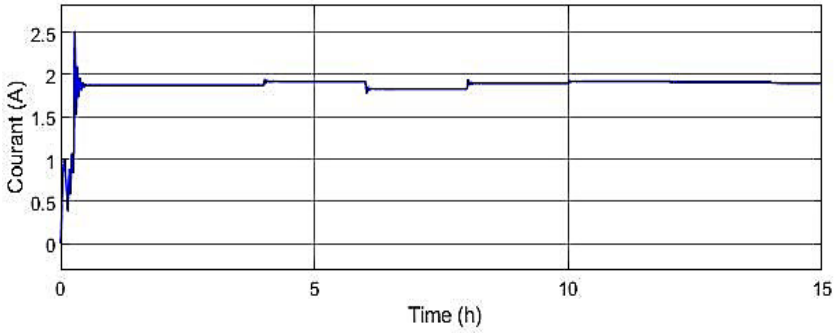

Fig. 13. PV Courant variation of the P&O method

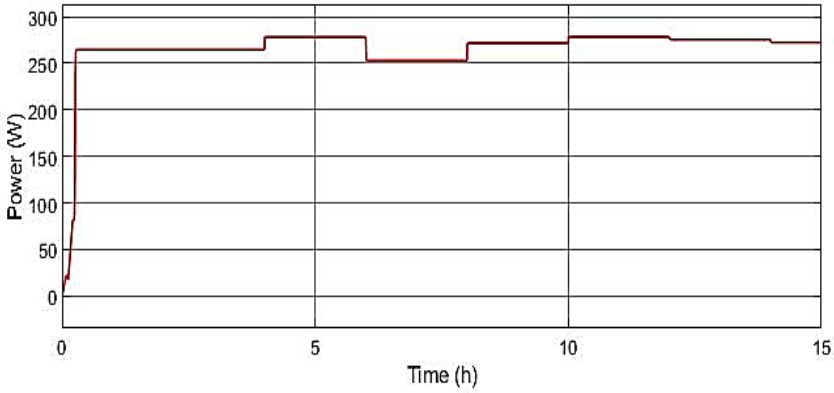

Fig. 14. PV power variation of the proposed method

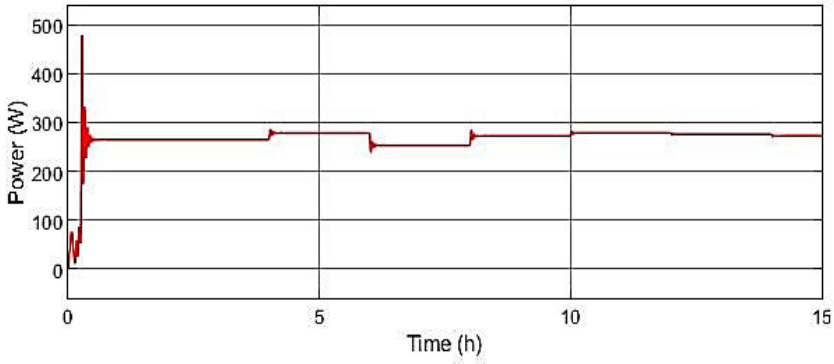

Fig. 15. PV power variation of the P&O method

5. CONCLUSION

In this article, a genetic algorithm adapted to the P&O method and based on PID is test to track the MPP of a solar system. It is shown that the tracking speed of the proposed method is faster compared to the P&O method. The results simulation of the proposed controller gave an exact response with faster tracking speed and near zero oscillations; It could track the MPP for any rapid variations in weather data including large fluctuations in insolation and partial shading condition.

REFERENCES

1. C. Pradip, K. Vinoth Kumas, and M. Lydia, "*A Comprehensive Overview on PV Based Hybrid Energy Systems*", International Journal of Renewable Energy Research, vol. 9, no. 3, pp. 1241–1248, 2019., Mohammedia, pp. 1- 5, 26-27 April 2018.
2. K. D. Mercado, J. Jiménez, and M. C. G. Quintero, "*Hybrid renewable energy system based on intelligent optimization techniques*", Proceedings of International Conference on Renewable Energy Research and Applications (ICRERA 2016), November 2016.
3. Katheryn Donado Mercado , Jamer Jiménez , M. Christian G. Quintero, "*Hybrid renewable energy system based on intelligent optimization techniques*" , IEEE International Conference on Renewable Energy R esearch and Applications(ICRERA), Birmingham, pp. 661-666, March 2017.
4. L. Height and L. Heights, "*The Optimization of Hybrid Energy Conversion Systems Using the Dynamic Programming Model*", Int. J. energy Res., vol. 1, no. November 1986, 1988.
5. R. Chedid and M. Ieee, "*Wind-Solar Power Systems*", vol. 12, no. 1, pp. 79–85, 1997
6. R. Chedid and Y. Saliba, "*Optimization and control of autonomous renewable energy systems*", Int. J. Energy Res., vol. 20, no. 7, pp. 609–624, 1996.
7. Y. Mizuno, N. Matsui, Y. Tanaka, and F. Kurokawa, "*A new approach of optimum energy scheduling of emergency generators using linear programing in a large hospital*", Proceedings of International Conference on Renewable Energy Research and Applications (ICRERA 2016), pp. 832-836, November 2016.

8. K. E L Bouyahyiouy and A. Bellabdaoui, "*A new approach to solving the full truckload vehicle routing problem using genetic algorithm*", The 3rd IEEE International Conference on Logistiqcs Operations Managemnt GOL'2016, 23-25 may 2016, Fes, Morocco.
9. K. El Bouyahyiouy and A. Bellabdaoui, "*An ant colony optimization algorithm for solving the full truckload vehicle routing problem with profit*", 2017 Int. Colloq. Logist. Supply Chain Manag., pp. 142–147, 2017.
10. Tanaka, M., Eto, H., Mizuno, Y., Matsui, N., & Kurokawa, F. (2017, November). "*Genetic algorithm based optimization for configuration and operation of emergency generators in medical facility*". In 2017 IEEE 6th International Conference on Renewable Energy Research and Applications (ICRERA) (pp. 919-924). IEEE.
11. N. Femia, et al, "*Optimization of perturb and observe maximum power point tracking method"*. IEEE Trans Power Electron. 20 (4) (2005) 963–73.
12. A. Zegaoui, M. Aillerie, P. Petit, J.P. Sawicki, A. Jaafar, C. Salame, J.P. Charles, "*Comparison of two common maximum power point trackers by simulating of PV generators*". Energy Proceedia, 6 (2011) 678–687.
13. A. Messai, A. Mellit, A. Guessoum, S.A. Kalogirou, "*Maximum power point tracking using a GA optimized fuzzy logic controller and its FPGA implementation*". Solar Energy. 85 (2011) 265–277.
14. Zahira. El hariz, Hicham. Aissaoui, and Mohammed. Diany, *"Multi-Objective Optimal Control of Hybrid Energy System"* International Journal Of Renewable Energy Research, vol. 9, no. 4, 2019.
15. Zahira. El hariz, Hicham. Aissaoui, and Mohammed. Diany, *"Optimal Unit Sizing of PV / Wind / Battery / Sector Generating System"* IEEE International Conference on Optimization and Applications (ICOA), 2018.

Cite this article

Zahira EL HARIZ, Hicham Aissaoui and Mohammed Diany, A Novel PID Using A Genetic Algorithm to Track The Maximum Power Point of The PV System, In: Sandip A. Kale editor, Advanced Research in Solar Energy, Pune, Grinrey Publications, 2021, pp. 87-98

9 Photovoltaic Generation System and Grid Source Connected to Load Using qZ Source

Henchiri Abdelhamid[a,*], Bahi Tahar[b] and Lakhdara Amira[c]

[a]Laboratory of Mechanical Engineering and Materials, 20 August 1955-Skikda University, Skikda, Algeria
[b]Laboratory of Automatic Systems signal, Badji Mokhtar University, Annaba, Algeria
[c] Laboratory of Electrical energy Guelma , LGEG , 8 may 1945 University, Guelma, Algeria

*Corresponding author: lakhdara.amira1985@gmail.com

ABSTRACT

The consumption of fossil fuels is increasingly necessary because of the need for electric power despite the fact that the emission of gas increases pollution and global warming of our planet. Therefore, renewable energies such as solar, wind, hydraulic, etc. are promising solutions that help to overcome the problems with which our world is confronted. In this work, we will present a power structure to harvest the maximum possible amount of energy from a photovoltaic system as a main source of renewable energy. The topology used for the adaptation between the power source and the load is based on qZ source because of its advantages, mainly this type of adapter is used to interface the low direct voltage to high direct voltage to reduce the stages of converters and semiconductor components. The validity of the proposed technique is proven by the analysis of the results obtained from the MatLab / Simulink simulation.

Keywords: Renewable energies, Photovoltaic generator, Grid Source , Grid, qZ Source

Advanced Research in Solar Energy | ISBN: 978-81-948951-7-6
Book Series: Research Transcripts in Energy | Vol: 01

1. INTRODUCTION

During several previous years, research has proven the negative consequences on the environment due to the use of fossil fuels as well as their limit to meet the needs of the population in the near future. Unlike fossil energies, renewable energies are energies with unlimited resources. The sun represents the most abundant energy source, which encourages researchers to direct their efforts to harnessing this source therefore photovoltaic systems are essential as a means of converting solar energy into electrical energy.

It is well know that fossil fuels are used extensively for the production of electricity [1]. Unfortunately, this technology has proven to have remarkable drawbacks, including pollution and the indisputable depletion of fossil resources. In view of this unfortunate finding, research has been launched intensively for the use of renewable energies (RE) as an alternative to fossil resources. However, despite the fact that REs are inexhaustible (abundant) they have the disadvantage resulting from their intermittent nature [2]. Therefore, these installations require the use of the optimization algorithm to extract the maximum power (MPPT) whatever the climatic conditions: irradiation (E) and temperature (T) [3].

Indeed, power converters play a very important role for the conversion of solar energy in photovoltaic systems. So, several researches have been done in order to improve these power converters in techno-economic view, this research studies the possibility of replacing the structure by associating a power converter with an impedant source topology called Z-source [4, 5]. This topology is of DC / DC type, it allows the function of raising the DC voltage of the power source to a higher DC voltage intended for the load.

The aim of this work is to improve the reliability and the efficiency of the production systems of the electric energies with renewable source precisely the photovoltaic system using the Z-source structure. So, in this context we will study the q Z-source structure which is recently introduced [6].

This work is made up of five sections: we start with an introduction. The second section is reserved for modelisation of the photovoltaic generator and qZ source. In the third and fourth sections, the simulation results and discussion are given, respectively. In the fifth section the conclusion is given.

2. STRUCTURE AND MODELISATION

Power generation facilities inevitably consist of static converters necessary for the desired shaping of the energy produced and delivered to consumers. Therefore, despite the remarkable progress in the fields of structures and controls of such converters, However, I do not believe that renewable energy

production facilities continue to require substantial improvements. This work involves studying a power supply structure for a continuous load via the hybridization of two sources, a main source consisting of a photovoltaic generator and an auxiliary source which is a three-phase electrical network where the network voltage is rectified thanks to a three-phase rectifier controlled.

However, since the voltage and consequently the power developed by the photovoltaic generator mainly depend on the meteorological conditions notably, the irradiation (E) and the temperature (T) [6]. We propose in this work to connect the load to the DC bus common to the two sources (main and auxiliary), previously defined through q-Z-source circuit [8-10]. Fig.1 shows the overall structure of the proposed hybridization.

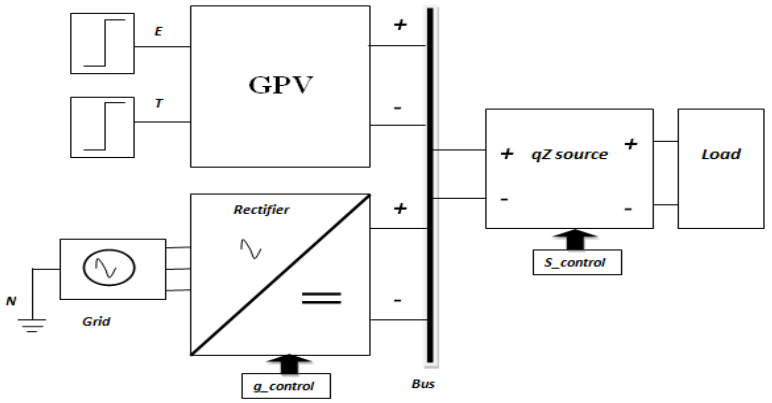

Fig. 1. Global Structure

2.1 Photovoltaic generator

The photovoltaic generator is used to convert solar energy into electrical energy. It is mainly made up of photovoltaic cells connected in series and parallel [11, 12]. The photovoltaic cell equivalent circuit is represented in Fig. 2.

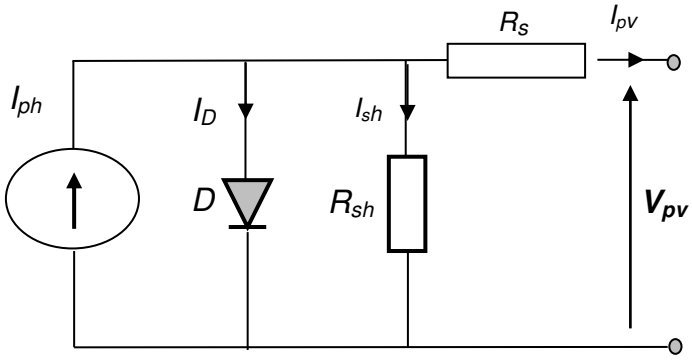

Fig. 2. Electrical equivalent circuit of a photovoltaic cell

Considering Fig. 2, we can write the mathematical model of the photovoltaic module [12, 13]:

$$I_{pv} = I_{ph} - I_d - I_{sh} \tag{1}$$

$$I_{pv} = I_{ph} - I_O(e^{\frac{Vpv+Rs.Ipv}{vtQdns}} - 1) - \frac{V_{pv} + R_s I_{pv}}{R_p} \tag{2}$$

2.2 qZ Source

The Sources dedicated to the production of electrical energy by means of renewable energy sources such as photovoltaic sources generate a variable direct voltage. This section introduces the notion of z-sources which are characterized by the use of LC type impedance network arranged in "X", allowing the simultaneous closing of the up and down switches of the same arm of the converter to accomplish its function of raising the voltage V_{dc} by considering the two operating modes which depend on the short-circuit state or not of the arm of the same arms [14].
A unique feature of "z-source" converters is the "shoot-through" state whereby two solid state switches of the same phase branch can be activated simultaneously. Otherwise, this systems are attractive advantage for photovoltaic systems applications. Fig. 3 shows the quasi-source Z grid.

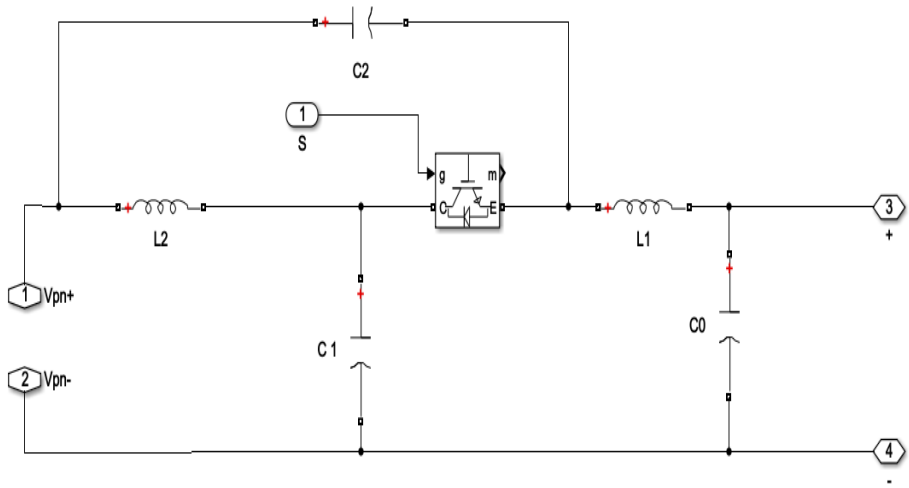

Fig. 3. Quasi-source Z grid circuit

3. RESULTS

Taking into account, on the one hand, the specific operating features that photovoltaic installations are extensively used by climatic conditions, and on the other hand, the place of its installation, in particular an isolated site in this case, scenarios of variations in irradiation and temperature were considered for the analysis of the solar pumping structure proposed in this work.

The performance analysis of the studied structure is carried out under varying levels of irradiation and temperature. The simulation results presented in this section were obtained using the MatLab/ Simulink software. The discussion of these simulations is presented in the next section.

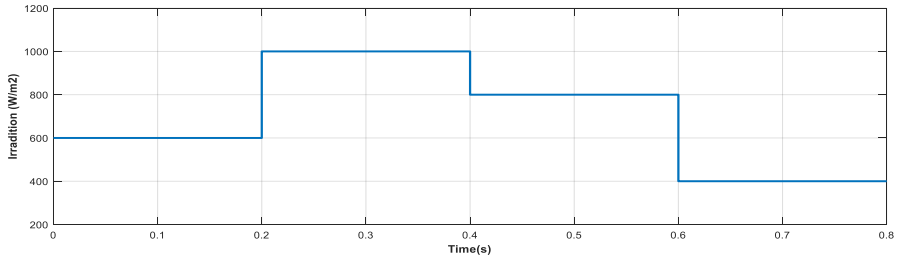

(a)

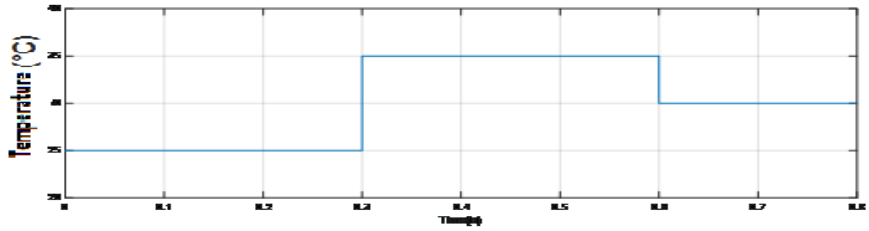

(b)

Fig. 4. Irradiance and Temperature levels

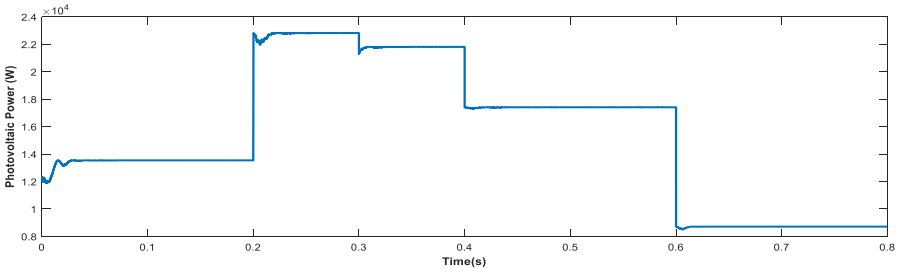

(a)

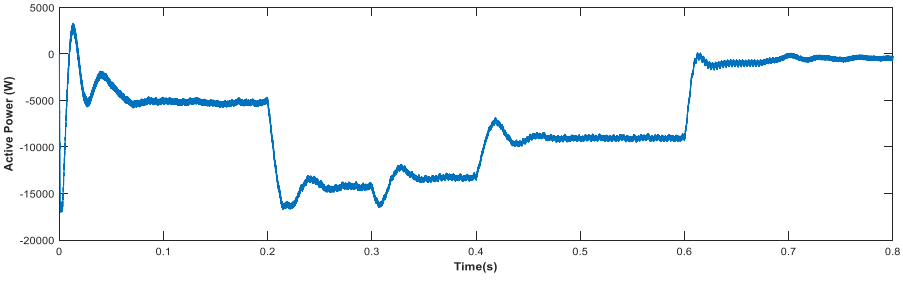

(b)

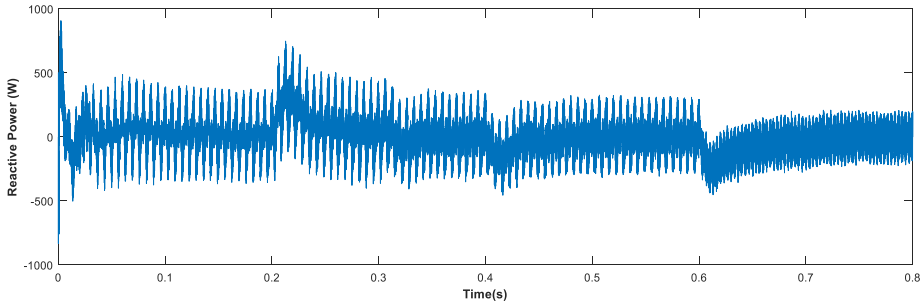

(c)

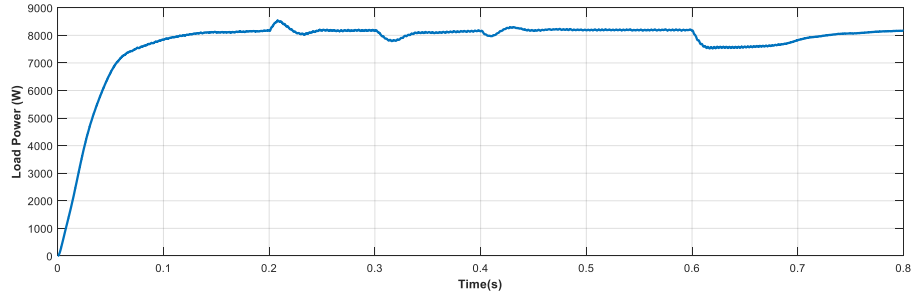

(d)

Fig. 5. Power of the different components of the chain

4. DISCUSSION

The studied structure (see Fig. 1) was carried out using the MatLab software under different levels of irradiation and temperature for operation over the sun. So, the interest was to analyze how the structure worked under varying weather conditions. hus, Fig. 4 shows that the irradiance varies in levels, i.e. four (4) stages (600W / m^2, 1000W / m^2 (standard irradiance), 800W / m^2 and finally 400W / m^2) corresponding to the different time intervals as shown. Fig. 4a. However, for the same simulation time (0.8s) the temperature undergoes the values (25 °C, 35 °C then returns to 25 ° C) where T = 25 °C is the standard value of the temperature. However, under these conditions of irradiation and temperature in Fig. 5 presents the photovoltaic power (Fig.5a), the active (Fig.5b) and reactive (Fig.5c) of the electrical network and finally the power absorbed by the load (Fig.5d). Under these conditions, one distinguishes, mainly, three (3) intervals relating to the combinations between the instantaneous levels of irradiation and the temperature, thus the photovoltaic installation produces for each interval, the instantaneous powers reach 21.5Kw under standard conditions. . However, the load absorbs around 8Kw. This validates the simultaneity or alternation of operation of the two sources (main and auxiliary) to satisfy the instantaneous power required by the load.

5. CONCLUSION

The chapter proposes a structure for supplying a load through operation between a photovoltaic system and the electricity grid, depending on the levels of irradiation and temperature. The use of such a structure has shown great promise for a water pumping application in geometrically remote locations. Indeed, the qZ source used as interface under the photovoltaic source and load is alternative for renewable energy source applications. The adaptation of the power required by the load and ensured by using a Z Source network. The simulation results are provided to verify the efficiency of the proposed structure.

NOMENCLATURE

k	:	Boltzmann's constant
q	:	charge of an electron
T	:	cell temperature
V_{pv}	:	PV module voltage (V)
I_{pv}	:	PV module current (A)
I_o	:	diode reverse saturation current (A)
I_{ph}	:	light current (A)
Qd	:	ideality factor
R_p	:	shunt resistance (Ω)
R_s	:	series resistance (Ω)
ns	:	number of cells in series
vt	:	vt =kT/q is thermal voltage (V)

REFERENCES

1. Kapil Dev, S., Sumit, S., Sunil, K. , Active Power Control of Grid Connected Hybrid Fuel Cell & Solar Power Plant, *International Electrical Engineering Journal*, 2015, Vol. 6 , No.5, pp. 1891-1897.
2. Kapil dev , S., Ayyub, M. Sumit, S., Ahmad, F., Advanced Controllers Using Fuzzy Logic Controller (FLC) for performance Improvement, *International Electrical Engineering Journal,* 2014, Vol. 5, No. 6, pp. 1452- 1458.
3. A. Mellit, A. and Kalogirou, S. A., Artificial intelligence techniques for photovoltaic applications: A review, *Prog. Energy Combustion Sci.,* 2008, vol. 34, pp. 574–632.
4. Anderson, J. and Peng, F. Z. , A class of quasi-Z-source inverters, in *Proc. IEEE Industry Applications Society Annual Meeting*
5. Park, J., Kim, H, Nho, E., Chun, T. and Choi, J. Grid-connected PV system using a quasi-Z-source inverter, *in Proc. 24th Ann. IEEE Applied Power Electronics Conf.*

6. Balamurugan, D., Rajesh, R., ANFIS based MPPT for GRID Connected Photovoltaic Generation System using Quasi-z-source Inverter, *International Electrical Engineering Journal (IEEJ*) , 2014, Vol. 5 , No.4, pp. 1321-1327.
7. SaifIftekhar, Md., et al, Maximum Power Point Tracking U sing Very High Frequency Resonant DC/DC Converter for Photovoltaic Systems, 2nd Int'l Conf. on Electrical Engineering and Information & Communication Technology (ICEEICT), 2015, Jahangirnagar University, Dhaka-I 342, Bangladesh, 21-23 May.
8. Yu, T., Xie, S., Zhang, C., Z-source AC-AC converters solving commutation problem. *IEEE Transactions on Power Electronics* , 2007, 22(6):2146–2154.
9. Anderson, J. and Peng, F. Z., Four quasi-Z-source inverters, *in Proc.IEEE PESC'08*, Jun. 2008, pp. 2743-2749.
10. Huang, Y., Shen, M.,. Peng, F. Z and Wang, J. , Z-source inverter for residential photovoltaic systems, *IEEE Trans. Power Electron*., Nov. 2006, vol. 21, no. 6, pp. 1776–1782.
11. Esram, T., Chapman, P. L., Comparison of Photovoltaic Array Maximum Power Point Tracking Techniques, IEEE Transaction on Energy Conversion, 2007, Vol. 22. No. 2, pp. 439-449.
12. Eid A. Gouda, Mohamed. F. Kotb, and Dina A. Elalfy, Modelling and Performance Analysis for a PV System Based MPPT Using Advanced Techniques, EJECE, European Journal of Electrical and Computer Engineering , January 2019 , Vol. 3, No. 1.
13. Lakhdara, A., Bahi,T., Moussaoui,A., Energy Management and control of a photovoltaic system connected to the electrical network , 17th International *Multi-Conference on Systems, Signals and Devices* (SSD'20), July 20–23, 2020, Sfax, Tunisia.
14. Peng., F.Z., Z-source inverter , *In 37th IAS Annual Meeting. Conference Record of the Industry Applications Conference, oct.* 2002*,* volume 2, pages 775 –781 vol.2, Oct 2002.

Cite this article

Henchiri Abdelhamid, Bahi Tahar and Lakhdara Amira, Photovoltaic Generation System and Grid Source Connected to Load Using q-z-Source, In: Sandip A. Kale editor, Advanced Research in Solar Energy, Pune, Grinrey Publications, 2021, pp. 99-106

10 Control and Management of a Photovoltaic System Equipped with a Storage Battery

Lekhchine Salima[a,*], Bahi Tahar[b] and Layate Zakaria[c]

[a] LGMM Laboratory, Department of Electrical Engineering, 20 August 1955University, Skikda, Algeria

[b] Automatic and Signals Laboratory, Badji Mokhtar University, Annaba, Algeria

[c]Technology Department, Djilali Bounaama University, Khemis Miliana-Ain Defla, Algeria

*Corresponding author: slekhchine@yahoo.fr

ABSTRACT

Solar-powered electricity production systems require the use of storage systems in order to ensure continuity of service when the irradiation and temperature do not allow sufficient power production for the load. However, the functioning of the storage system is coordinated by a specific installation specification. This work deals with the modeling and control of photovoltaic system used a storage battery on an isolated site. The solar conversion chain considered as well as the converter and fuzzy MPPT strategy commands were programmed under the MatLab / Simulink environment and the simulation results agree with the theories regardless of the variations in meteorological conditions.

Keywords: Renewable energies, fuzzy MPPT, storage battery, simulation.

Advanced Research in Solar Energy | ISBN: 978-81-948951-7-6
Book Series: Research Transcripts in Energy | Vol: 01

1. INTRODUCTION

The production of energy is a challenge of great importance for the years to come. Indeed, the energy needs of industrialized societies continue to increase. In addition, developing countries will need more and more energy to achieve their development. Since, currently the world's energy production is derived from fossil sources, because rise to greenhouse gas emissions and consequently increase in pollution. Elsewhere, an excessive consumption of the stock of natural resources thus considerably reducing the reserves of this type of energy in ways those are dangerous for future generations [1].

The renewable energies (RE) are gradually becoming energies in their own right, competing with fossil energies in terms of cost and production performance [2]. In particular, the solar energy is currently experiencing strong development in the world, given its ecological character [3], [4]. However, due to the random nature of the operation of renewable energy conversion systems the photovoltaic generators (GPV) are generally coupled to a storage system (SS) ensuring continuous energy availability. The type of SS are generally used for this conversion system is lead acid battery. The maturity of this technology and its low cost are the main reasons for using these batteries [1].

The aim of this work is to present a detailed study of a photovoltaic system with storage batteries. However, in order to analyze the functioning of the considered system, several simulation cases are presented and discussed.

2. STRUCTURE AND MODELING OF CONVERSION CHAIN

The considered configuration is intended for installation in an isolated site and the structure contains a GPV connected to a DC load via a step-up boost converter who is controlled by a signal (duty cycle) delivered by fuzzy logic Maximum Power Tracking (FL-MPPT) as shown in Fig.1.

Moreover, as the irradiation and the temperature vary continuously according to the meteorological conditions, a storage device is provided in order to store the surplus of the energy produced and also to supply it when the panels no longer manage to satisfy the power demanded by load (Reversible Buck-Boost Converter).

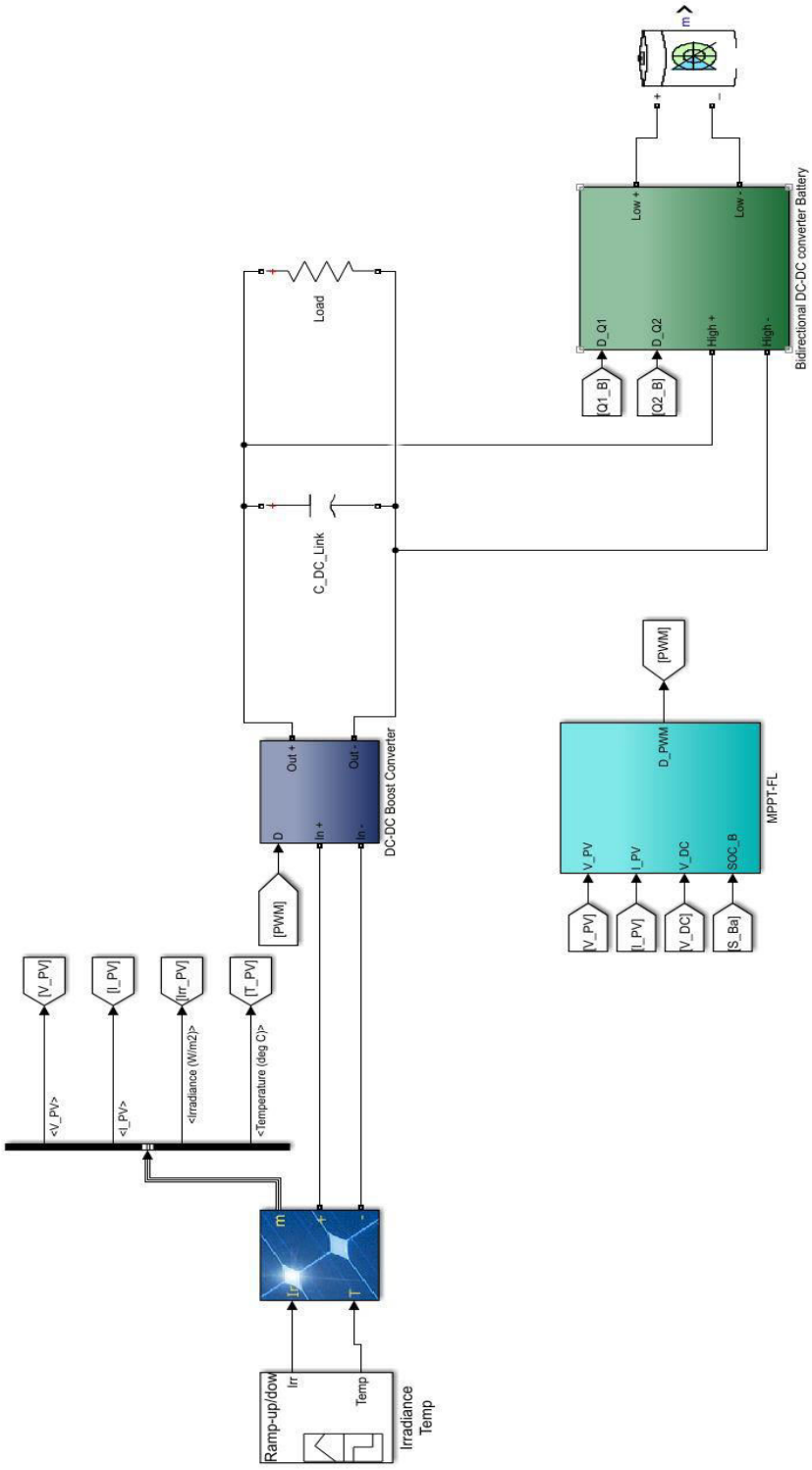

Fig. 1. Structure of the conversion chain

2.1 Photovoltaic Cell

In this work, for the model of the cell it is considered that of a single diode (D) whose equivalent circuit is represented by Figure 2 [5, 6], where, R_p and R_s are the parallel and series resistances, respectively:

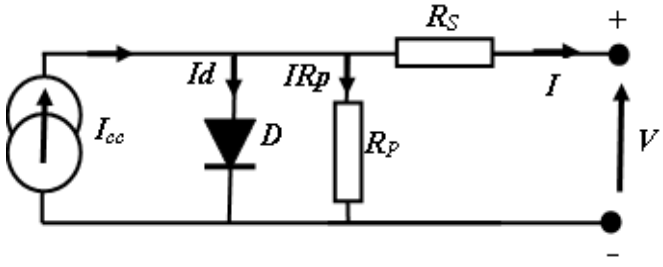

Fig. 2. Equivalent circuit of a photovoltaic cell

From which, we deduce the expressions of the output current are, respectively, given by the following equation [7- 9]:

$$I = I_{cc} - I_d - I_{R_p} \tag{1}$$

$$I = I_{cc} - I_{01}[e^{q(\frac{V+I*R_s}{n_1 kT})} - 1] - I_{02}[e^{q(\frac{V+I*R_s}{n_2 kT})} - 1] - \frac{V + I*R_s}{R_p} \tag{2}$$

I_0 (A): saturation current of the diode;

K: Boltzmann constant;

T_c (K), the charge of the electron;

n: non-ideality factor of the junction of the diode.

Where,

I_{cc}(A): Short circuit current (Photovoltaic);

Id (A): Current through the diode;

IRp (A): Current through the parallel resistor.

So, with different conditions and assumptions, the current-voltage equation of cell is written [10, 11]:

$$I = I_{cc} - I_0 e^{\frac{q}{nkT_c}(V+I*R_s)} \tag{3}$$

2.2 Boost converter

The electrical connection circuit is shown in figure 3.

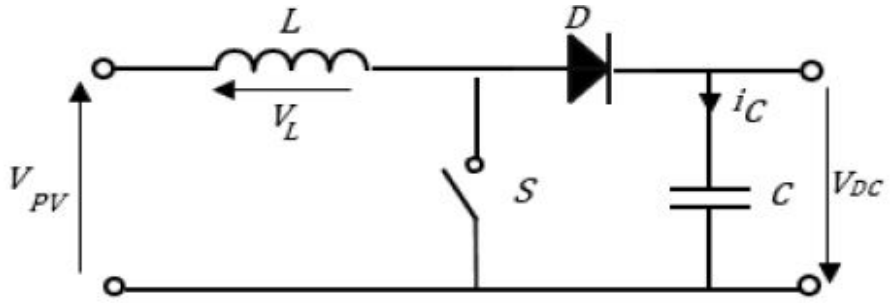

Fig. 3. Electric circuit of the Boost converter

During a duty cycle (T), the operation of the Boost converter is defined by [9]:

For (αT), S is closed, the current in L increases progressively, and as it goes, this inductance stores energy. The switch (S) then opens the inductance (L) opposes the decrease in current (I_L), generates a voltage which will be added to source voltage. It will be applied to the load (R) through the diode (D). The mathematical model of the parallel converter is:

$$L\frac{di_L}{dt} = E - V_{dc}\left(1-\alpha\right) \tag{4}$$

$$C\frac{dV_{dc}}{dt} = i_L\left(1-\alpha\right) - \frac{V_{dc}}{R} \tag{5}$$

The dynamic converter equations are derived for the current in the inductor and the voltage across the capacitor in the continuous conduction regime expressed by (4) and (5), where, I_L: current in the coil;

E: input voltage; V_{dc}: output voltage and α: dury cycle.

Let $x_1 = I_L$ and $x_2 = V_{dc}$ then the equations of state become:

$$\begin{aligned} \frac{di_L}{dt} &= \frac{E}{L} - \frac{\left(1-\alpha\right)}{L}V_{dc} \\ \frac{dV_{dc}}{dt} &= \frac{\left(1-\alpha\right)}{C}i_L - \frac{V_{dc}}{RC} \end{aligned} \tag{6}$$

Then, the classical representation in state space x = AX + Bu is:

$$\begin{bmatrix} \dot{i}_1 \\ \dot{V}_{dc} \end{bmatrix} = \begin{bmatrix} 0 & -\frac{(1-\alpha)}{L} \\ \frac{(1-\alpha)}{C} & -\frac{1}{RC} \end{bmatrix} \begin{bmatrix} i_1 \\ V_{dc} \end{bmatrix} - \begin{bmatrix} \frac{1}{L} \\ 0 \end{bmatrix} E \tag{7}$$

The control signal α is included in the discrete domain of {0; 1} and it indicates the state of the switch S: open for 0 and closed for 1. It can be replaced by its average value over a switching period which represents the duty cycle $\alpha = T_{on} / T_s$ where T_{on} is the conduction time and T_s is the chopping period.

2.3 Buck-Boost converter

A Buck-Boost converter is a switching power supply which converts a DC voltage into another DC

voltage of lower or greater value but of reverse polarity [12, 13]. The corresponding electrical circuit is shown by figure 4.

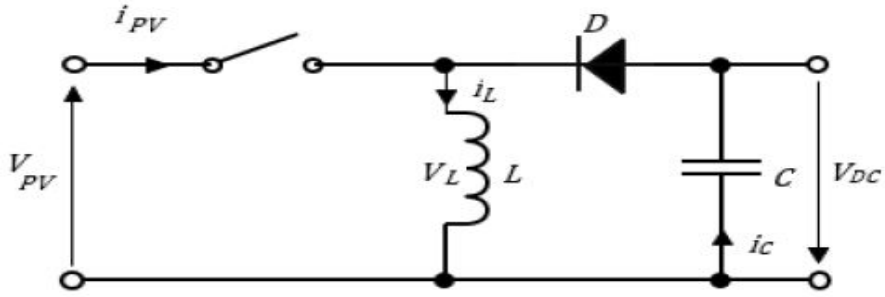

Fig. 4. Electrical circuit of the "Buck-Boost" converter

The presentation of the operation of this type of converter by mathematical equation must be carried out taking into account the state of switch S. When the switch is in the on state, then $T_{on} = \alpha.T_s$. As a result, the energy stored in the inductance increases. When S is blocked, then $T_{off} = (1 - \alpha)$ .Ts and the energy accumulated in the inductance transfers to the capacitance and the load.

$$L\frac{di_L}{dt} = \alpha E - V_{dc}(1-\alpha) \tag{8}$$

$$C\frac{dV_{dc}}{dt} = -i_L(1-\alpha) - \frac{V_{dc}}{R} \tag{9}$$

In switch-on mode, S is equal to 1, the diode is blocked and the equations in this case are:

$$L\frac{di_L}{dt} = \alpha E \tag{10}$$

$$C\frac{dV_{dc}}{dt} = -\frac{V_{dc}}{R} \tag{11}$$

When the switch is blocked, S is equal to 0 and the diode is on. The equations are:

$$C\frac{di_L}{dt} = V_{dc} \tag{12}$$

$$C\frac{dV_{dc}}{dt} = -i_L - \frac{V_{dc}}{R} \tag{13}$$

whether for state representation:

$$\begin{bmatrix} \dot{i}_1 \\ \dot{V}_{dc} \end{bmatrix} = \begin{bmatrix} 0 & -\frac{(1-\alpha)}{L} \\ \frac{(1-\alpha)}{C} & -\frac{1}{RC} \end{bmatrix} \begin{bmatrix} i_1 \\ V_{dc} \end{bmatrix} - \begin{bmatrix} \frac{u}{L} \\ 0 \end{bmatrix} E \tag{14}$$

2.4 Principle of Fuzzy Logic MPPT

By definition, an MPPT control, associated with an intermediate adaptation stage, allows a PV generator to operate in such a way as to continuously produce the maximum of its power [14, 15]. However, within the framework of this chapter the perturbation and observation method P&O (perturbation and observe) based on fuzzy logic is considered.

The structure of such an MPPT control approach is shown in figure 5.

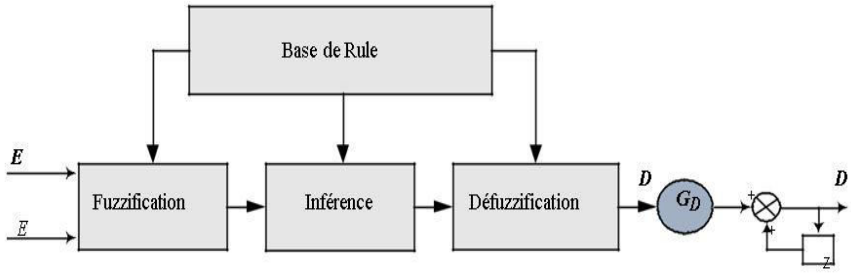

Fig. 5. Fuzzy Logic MPPT

The inputs to the controller are the error e (k) and the variation of the error Δe (k) expressed by [16].

$$E(k)=\frac{P_{pv}(k)-P_{pv}(k-1)}{V_{pv}(k)-V_{pv}(k-1)} \tag{15}$$

$$\Delta E(k)=e(k)-e(k-1) \tag{16}$$

With: Ppv and Vpv are respectively the power and the voltage of the photovoltaic generator.

Input E (k) shows whether the operating point of the load is to the left or right of the maximum power point of the P (V) curve, while input E (k) shows the direction of the point Operating.

The output of the fuzzy controller is ΔD which represents the variation of the duty cycle of the DC-DC converter.

We use a fuzzy controller, the output of the controller ΔD (k) is considered as an incremental duty cycle D (k):

$$D(k)=D(k-1)+GD \tag{17}$$

Table 1. Fuzzy logic MPPT rule base

E/dE	NB	NS	ZO	PS	PB
NB	ZO	ZO	PB	PB	PB
NS	ZO	ZO	PS	PS	PS
ZO	PS	ZO	ZO	ZO	NS
PS	NS	NS	NS	ZO	ZO
PB	NB	NB	NB	ZO	ZO

2.5 Battery modeling

The main properties of a battery are its voltage $V_{\_nom}$ (V) and its capacity C or $Q_{\_cellen}$ (Ah). The product of these two values is a measure of the amount of energy contained in the battery. In an ideal voltage source, the voltage should remain constant at all times, until the battery is completely discharged,

regardless of the current demand. Thus the autonomy of a battery should be able to be calculated directly by equation (18), where $t_{\_dech}$ is the discharge time and I is the required current [17].

$$t_{dech} = \frac{Q_{cell}}{I} \tag{18}$$

However, because lithium batteries do not adopt a behavior, t_{dech} is estimated by the following relation:

$$t_{dech} = \frac{Q_{cell}}{I^{b}} \tag{19}$$

The cellular potential (E) during the discharge of a battery is given by the following equation [18].

$$E = E_0 - K\left(\frac{Q}{Q - it}\right)i - Ri \tag{20}$$

State of charge (SOC) and State of discharge (SOD) Are calculated by the relations (21) and (22), respectively [19]:

$$SOC(t) = \int_{t-1}^{t} I_{bat}(t) - V_{bat}(t)\,dt \tag{21}$$

$$SOD(t) = \frac{\int_0^t i(t)\,dt}{Q_{\max}} \times 100 \tag{22}$$

And, the Depth of Discharge (DOD)

$$D(k) = D(k-1) + GD \tag{23}$$

3. RESULTS

The previous models have been programmed and simulated and the results obtained are presented by the following figures 6 to 13.

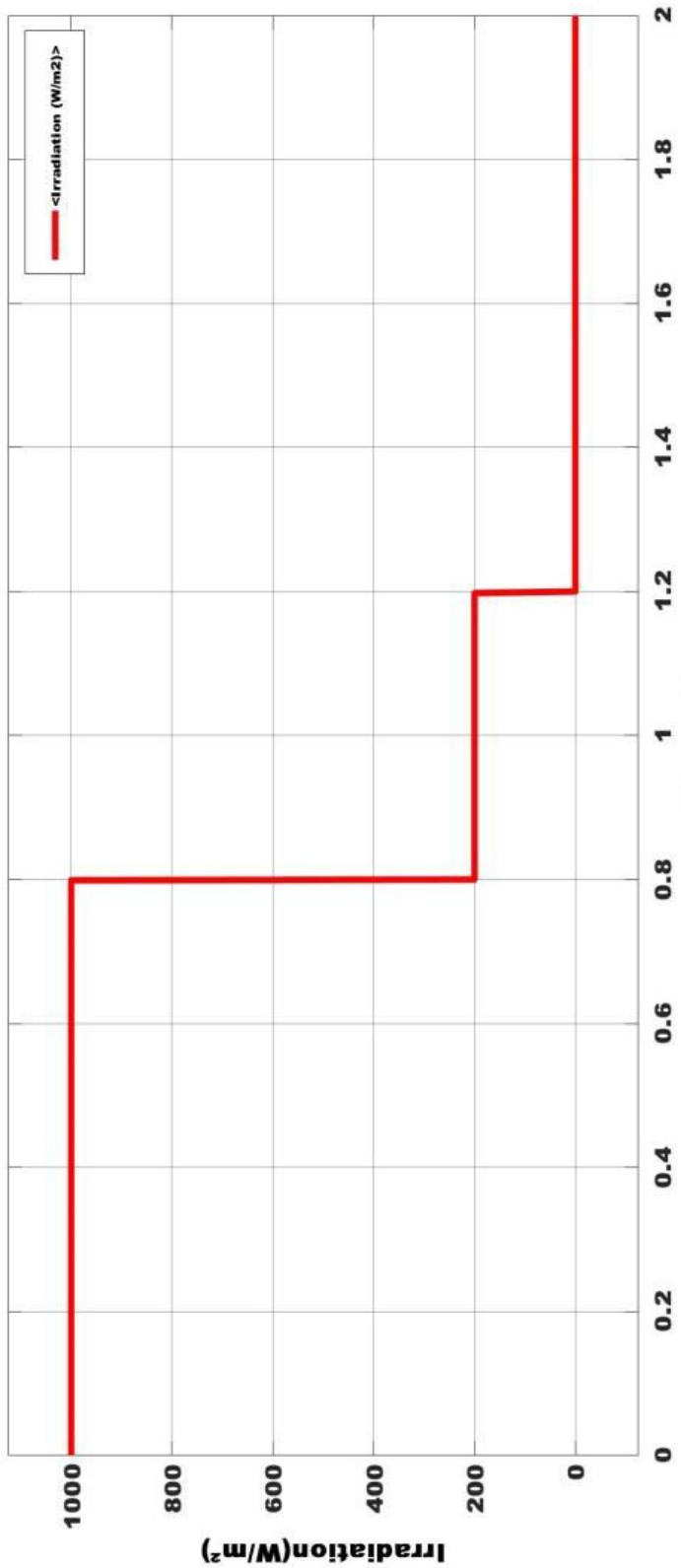

Fig. 6. Irradiation profile

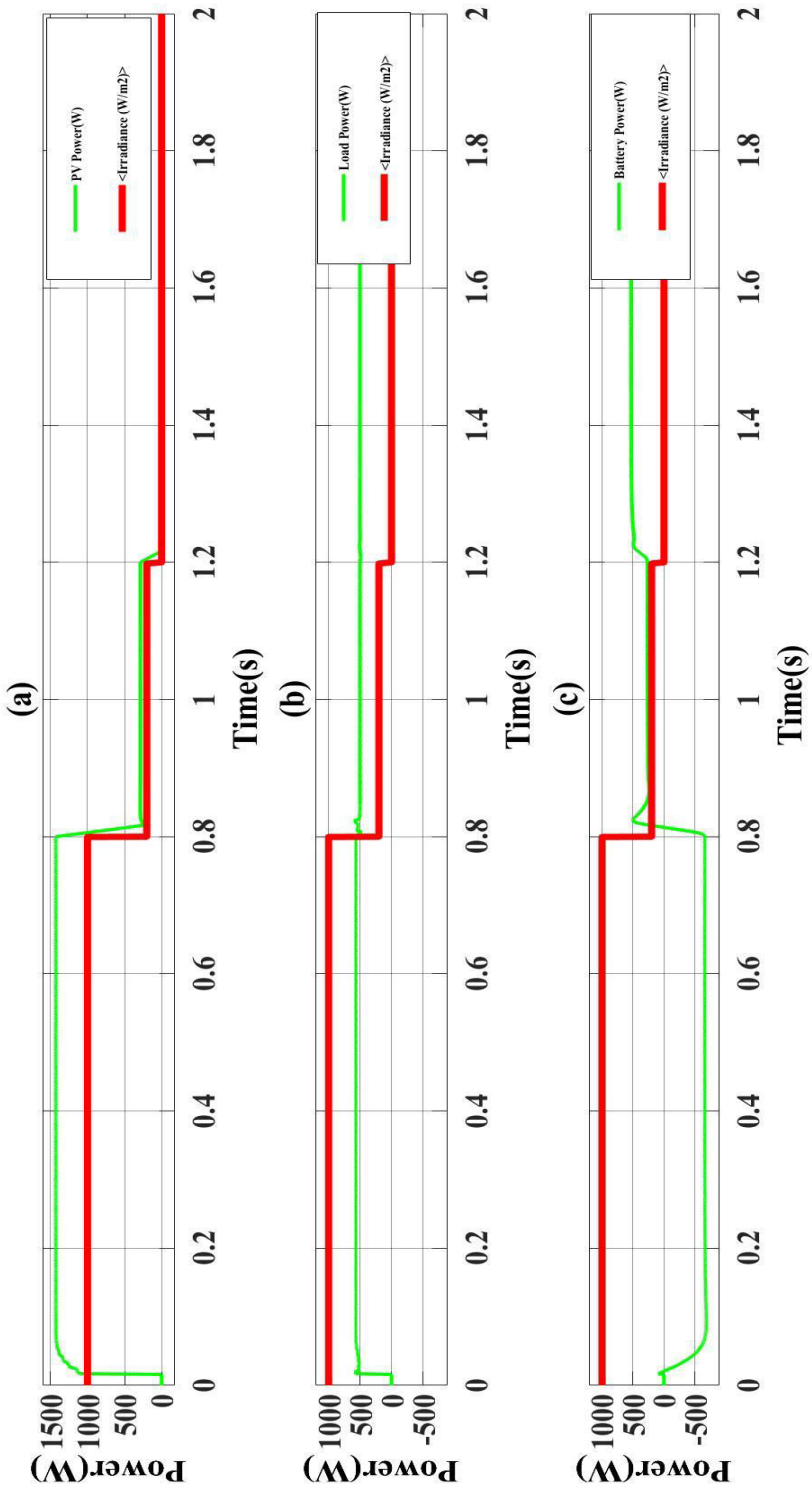

Fig. 7. Shape of the PV power, load, and the battery

Fig. 8. Battery power

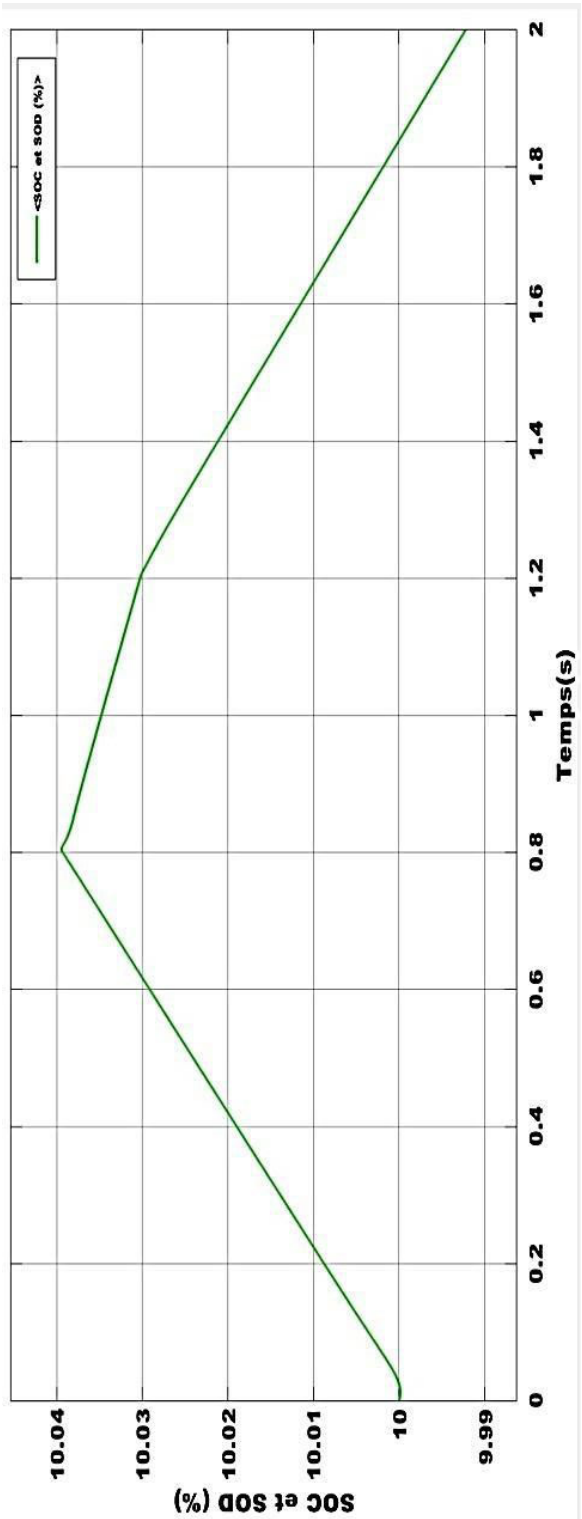

Fig. 9. SOC evolution

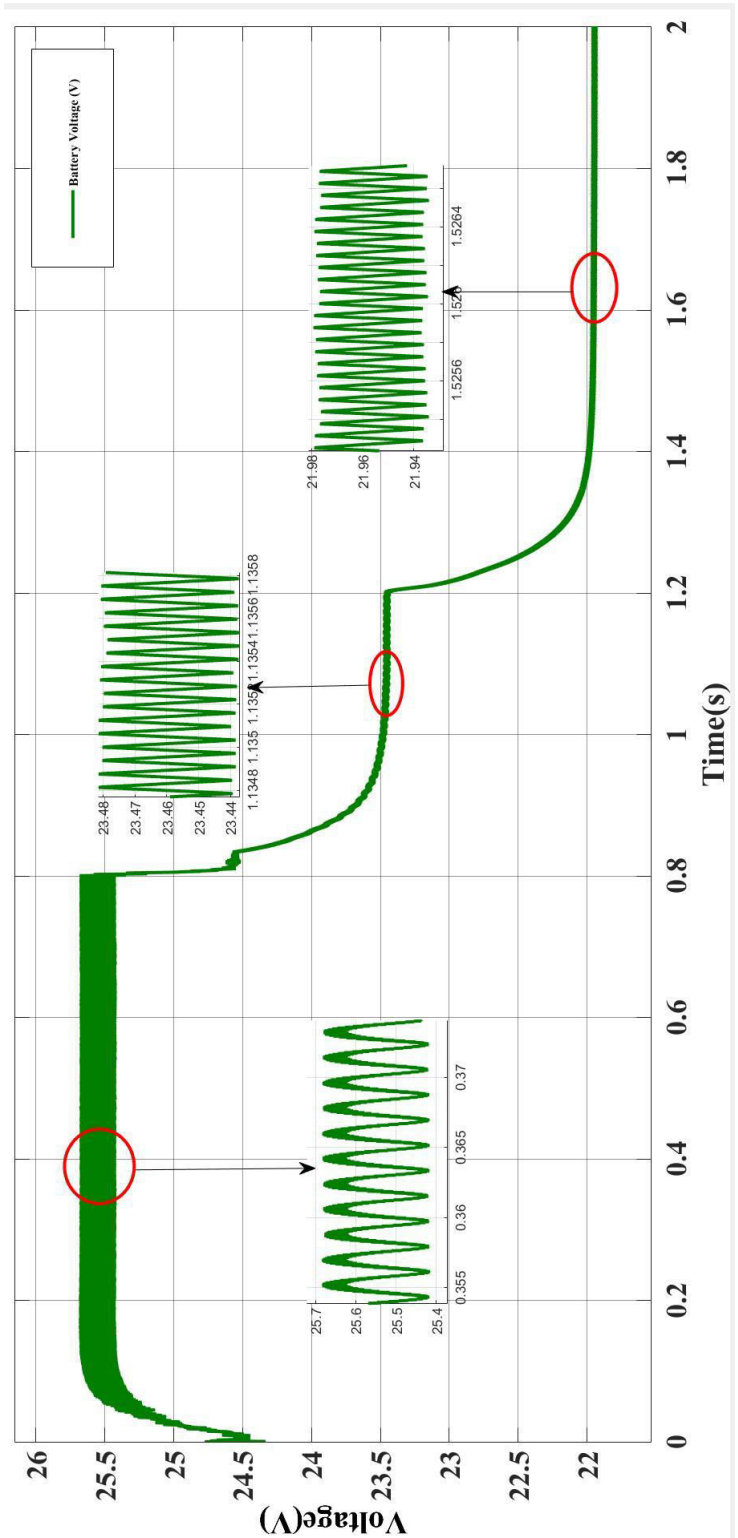

Fig. 10. Battery voltage

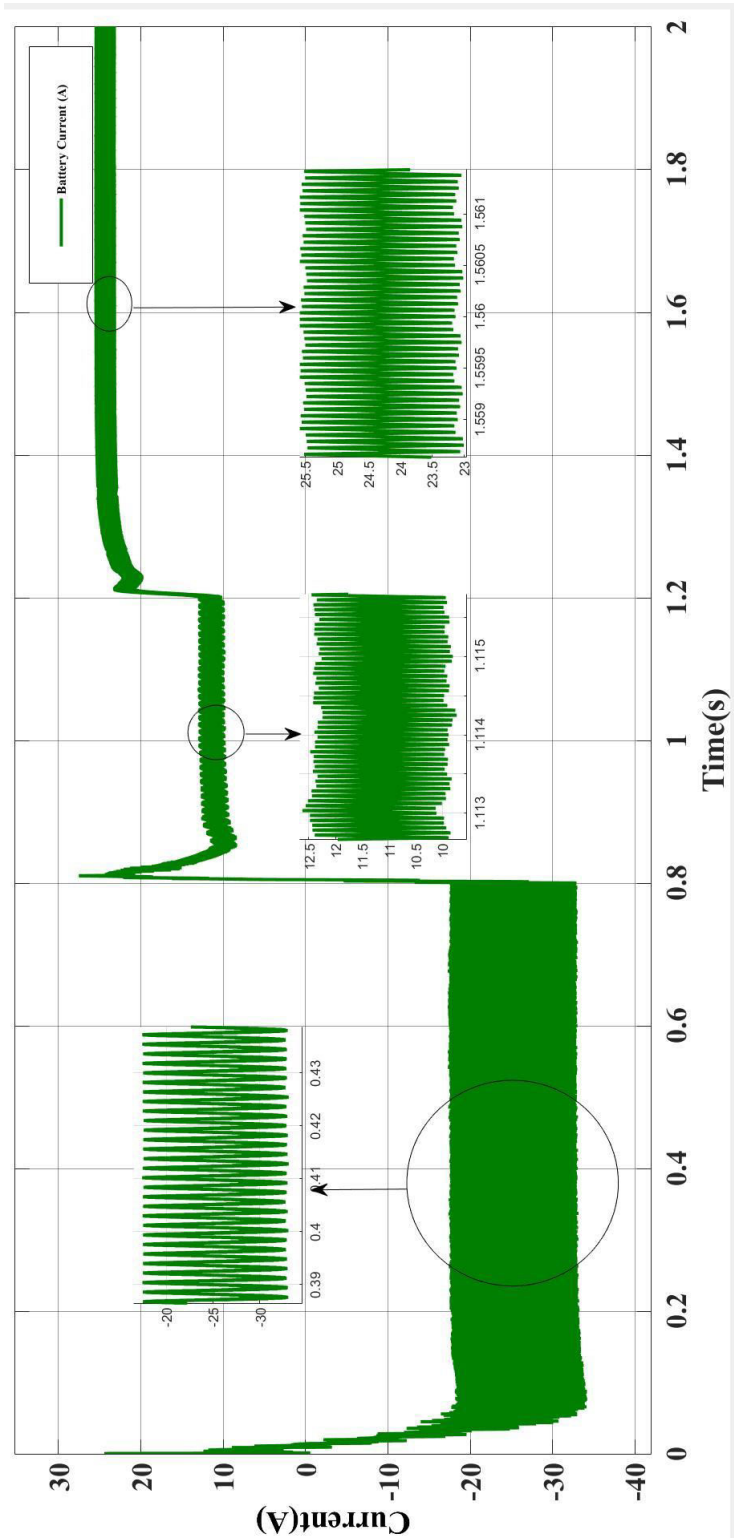

Fig. 11. Battery current

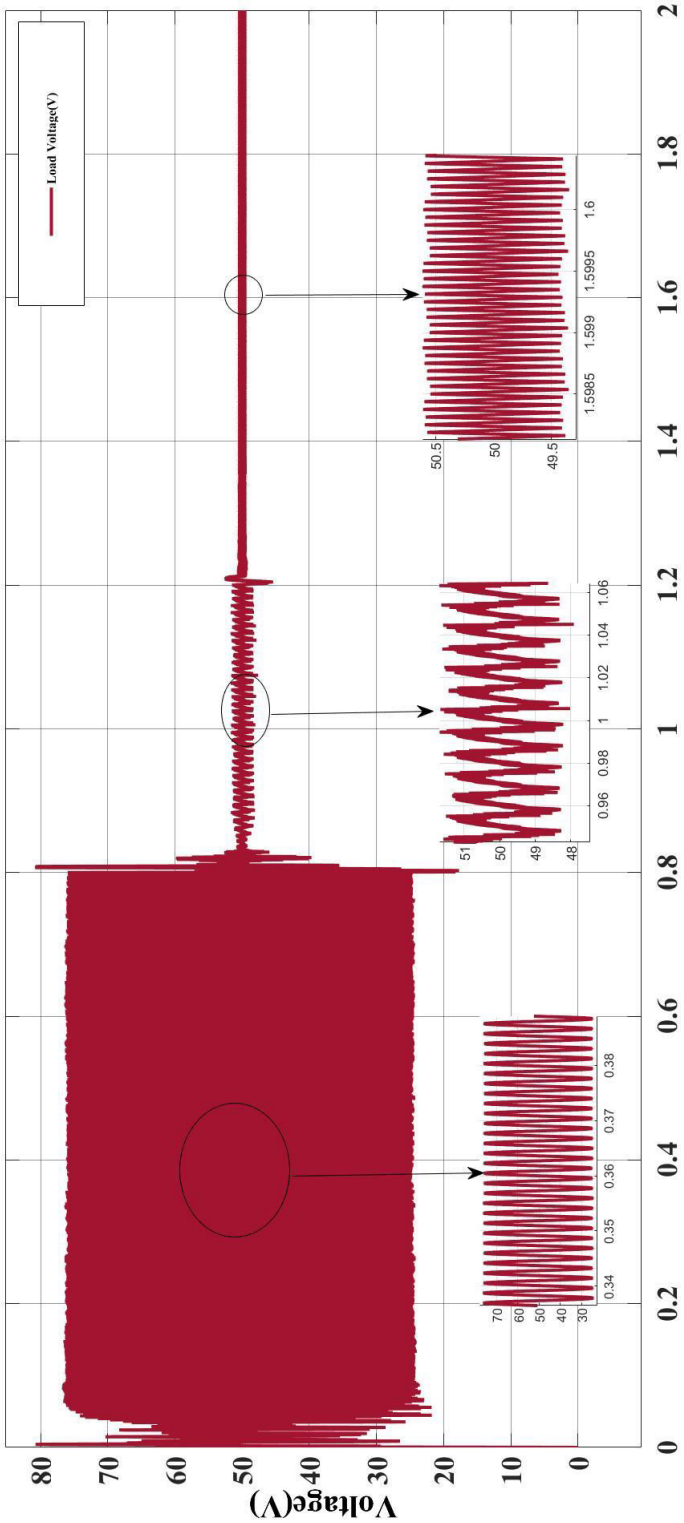

Fig. 12. Voltage across the load

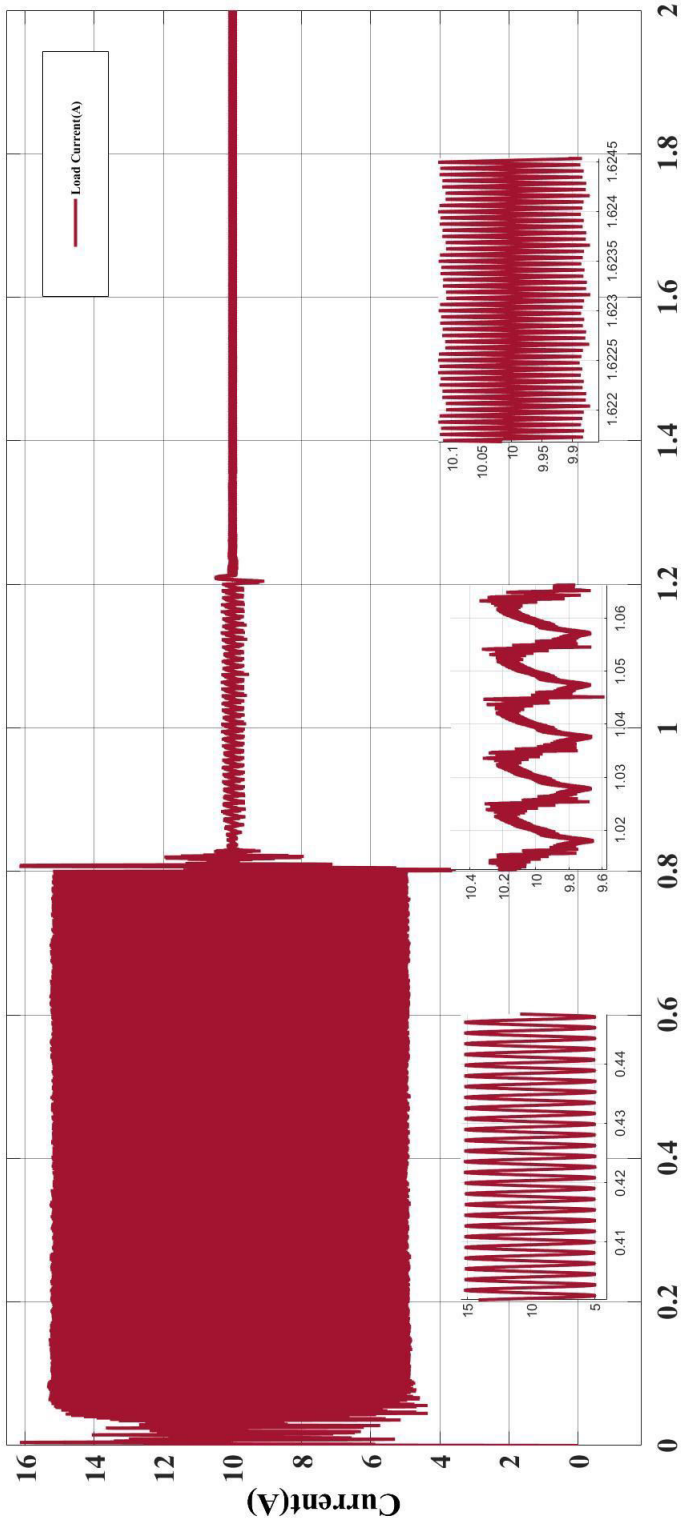

Fig. 13. Charging current

4. DISCUSSION

For conditions T = 25 ° C, and variable irradiation as follows: Ir = 1000w / m² (midday), Ir = 200w / m² (afternoon) and Ir = 0w / m² (at night) as shown in the figure 6. We can then distinguish the following intervals: During the period of time 0s to 0.8s, the irradiation is Ir = 1000w / m² and the temperature is temperature T = 25 ° C. Under these conditions the PV power increases up to the maximum value 1400w (see figure 7_a); Thus, the power absorbed by the load is shown in green in figure 7_b changes to reach approximately 580 w. So, we see that the PV produces a higher power than that required by the load. Consequently, this surplus is stored by the battery (see figure 7_c) and shows it more clearly in figure 8. Then the battery charges, which is found by increasing the SOC from its initial 10% value as shown in Figure 9, gradually going up to almost 10.04%. Consequently, the voltages and currents of the storage system (battery) are illustrated by figures 10 and 11, respectively and furthermore the voltage at the terminals of the load and the current flowing through it are, respectively, shown by figures 12 and 13. So this interval corresponds to the battery charge mode.

In the period [0.8s, 1.2s] of irradiation Ir = 200w / m² (afternoon) and a temperature T = 25 ° C. PV power decreases when irradiation decreases. The PV system produces only maximum power of about 220W which is lower than the one required by the load (figure 7_a and b). Thus the missing power is then provided by the battery (battery charge mode) as proven by the change of the sign and the decrease of the SOC (figure 7_c) from the previous state 10.0.4% to 10% at time 1.2.

Therefore, this interval corresponds to the battery discharge mode. Period from 1.2 to 2s: In this period the irradiation is zero Ir = 0w / m² (night) and the temperature is T = 25 ° C. PV power decreases to 0w. The PV no longer produces power, but the battery plays the role of a generator by continuing to be discharged to ensure all the power required by the load and at the same time ensure continuity of service despite the shutdown of production of power by the PV.

The voltages and currents corresponding to the load and the battery are presented by the figures mentioned previously.

5. CONCLUSION

The conditions on the irradiation variation and the temperature constancy correspond perfectly to the changes in the powers of the PV, battery and load. They clearly show the two modes of battery operation of the three intervals considered, the battery effectively operates in charge mode during the first

interval and in discharge mode for the last two intervals. The scenarios considered for this work attest to the correct functioning of the various components of the chain and this in particular the storage system.

NOMENCLATURE

DOD	:	Depth of Discharge
E	:	Battery potential
E_0	:	Constant battery voltage
E_{bat}	:	Battery voltage
FL-MPPT	:	Fuzzy Logic Maximum Power Point Tracking
GPV	:	Photovoltaic generator
NB	:	Negative Big
NS	:	Negative Small
P&O	:	Perturbation and Observation
PB	:	Positive Big
PS	:	Positive Small
PV	:	Photovoltaic
Q	:	battery capacity
SOC	:	State Of Charge
SOD	:	State Of Discharge
ZO	:	Zero

REFERENCES

[1] Shiau, J.-K., Wei, Y.-C.; Lee, M.-Y. Fuzzy Controller for a Voltage-Regulated Solar-Powered MPPT System for Hybrid Power System Applications: Energies, Vol. 8, pp. 3292–3312, 2015

[2] B. Rajanna, S. Lalitha, G. Joga Rao, S K. Shrivastava, Solar Photovoltaic Generators with MPPT and Battery Storage in Microgrids: *International Journal of Power Electronics and Drive Systems* Vol. 7, pp. 701-712, Sep. 2016.

[3] R. Nagarajan, R. Yuvaraj, V. Hemalatha, S. Logapriya, A. Mekala, S. Priyanga, Implementation of PV - Based Boost Converter Using PI Controller with PSO Algorithm: *International Journal Of Engineering And Computer Science*, Volume 6 Issue 3 March 2017, Page No. 20479-20484

[4] A. Raj, A. Gopinath, Proportional plus Integral (PI) Control for Maximum Power Point Tracking in photovoltaic Systems: *International Research Journal of Engineering and Technology*, Volume: 02 Issue: 06, pp.408-412, 2015.

[5] Mostefa Koulali, Mohamed Mankour, Karim Negadi, bdelkader Mezouar, Energy Management of Hybrid Power System PV Wind and Battery Based Three Level Converter: *Tecnica -italian Journal of Engineering Science* Vol. 63, No. 2-4, June, 2019, pp. 297-304

[6] Vinay Kumar, U. Salma, Mathematical Modelling of a Solar Cell and its Performance Analysis under Uniform and Non-Uniform Insolation: *IJERT*, Vol. 6 Issue 12, 2017

[7] Henchiri ,A, Bahi , T, Khochemane, L, Lekhchine, S. Control of the DC Voltage Output Photovoltaic System: *5th International Conference on Green Energy and Environmental Engineering* , 28-30 April 2018 , Tunisia.

[8] O. Gergaud, G. Robin, B. Multon, H. Ben Ahmed U. Salma , M. Vinay Kumar, Double integral sliding mode control approach for a three-phase grid -tied photovoltaic systems : *International Journal of Mechanical Engineering and Technology ,* Volume 10, Issue 01, January 2019.

[9] S. Radhika , S. Swathi and Sarfaraz Nawaz Syed, Design and Analysis of Current Mode Control of Boost Converter: *International Journal of Science and Research ,* Volume 5 Issue 1, January 2016.

[10] L Navinkumar Rao , Sanjay Gairola , Sandhya Lavety, Noorul Islam, Design of DC-DC Boost Converter with Negative Feedback Control for Constant Current Operation: *(IJPEDS)* Vol. 8, No. 4, December 2017, pp. 1575~1584, December 2017.

[11] M. A. Ghasemi, H. M. Foroushani, M. Parniani, Partial shading detection and smooth maximum power point tracking of PV arrays under PSC: *IEEE Trans. Power Electron*., vol. 31, no. 9, pp. 6281-6292, Sep. 2016.

[12] S. Soheli, G. Sarowar ; Md. Ashraful Hoque, Md. Saidul Hasan, Design and Analysis of a DC -DC Buck Boost Converter to Achieve High Efficiency and Low Voltage Gain by using Buck Boost Topology into Buck Topology: *IEEE Xplore*: 18 February 2019.

[13] F. Dinniyaha, W. Wahaba, M. Alif, Simulation of Buck-Boost Converter for Solar Panels using PID Controller: *Energy Procedia*, 115, pp. 102–113, 2017.

[14] C. Algarín, J. Taborda Giraldo and O. Rodríguez Álvarez, Fuzzy Logic Based MPPT Controller for a PV System: *Energies*, 10, 2036; doi:10.3390/en10122036, 2017.

[15] S. Narendiran, S. Sahoo ; R. Das, A. Kumar Sahoo, Fuzzy logic controller based maximum power point tracking for PV system: IEEE Xplore: DOI: 10.1109/ICEES.2016.7510590,14 July 2016.

[16] E N. Yaqin, A G. Abdullah, D L. Hakim and A B D. Nandiyanto, MPPT based on Fuzzy Logic Controller for Photovoltaic System using PSIM and Simulink: *IOP Conference Series: Materials Science and Engineering, Volume 288, The 2nd Annual Applied Science and Engineering Conference (AASEC 2017),*24 August 2017, Bandung, Indonesia.

[17] O. Gomozov, J. P. Trovao, X. Kestelyn, and M. Dubois, Adaptive energy management sys-tem based on a real-time model predictive control with non-uniform sampling time for mul-tiple energy storage electric vehicle: *IEEE Transactions on Vehicular Technology*, No. 99, 2016.

[18] Aneke, M. and M. Wang Energy storage technologies and real/life applications-A state of the art review: *Applied Energy*,179: pp. 350-377, 2016.

[19] A. Cordoba-Arenas, S. Onori, Y. Guezennec, and G. Rizzoni, Capacity and power fade cycle-life model for plug-in hybrid electric vehicle lithium-ion battery cells containing blended spinel and layered - oxide positive electrodes: *Journal of Power Sources*, vol. 278, pp. 473–483, 2015.

Cite this article

Lekhchine Salima, Bahi Tahar and Layate Zakaria, Control and Management of a Photovoltaic System Equipped with a Storage Battery, In: Sandip A. Kale editor, Advanced Research in Solar Energy, Pune, Grinrey Publications, 2021, pp. 107-127

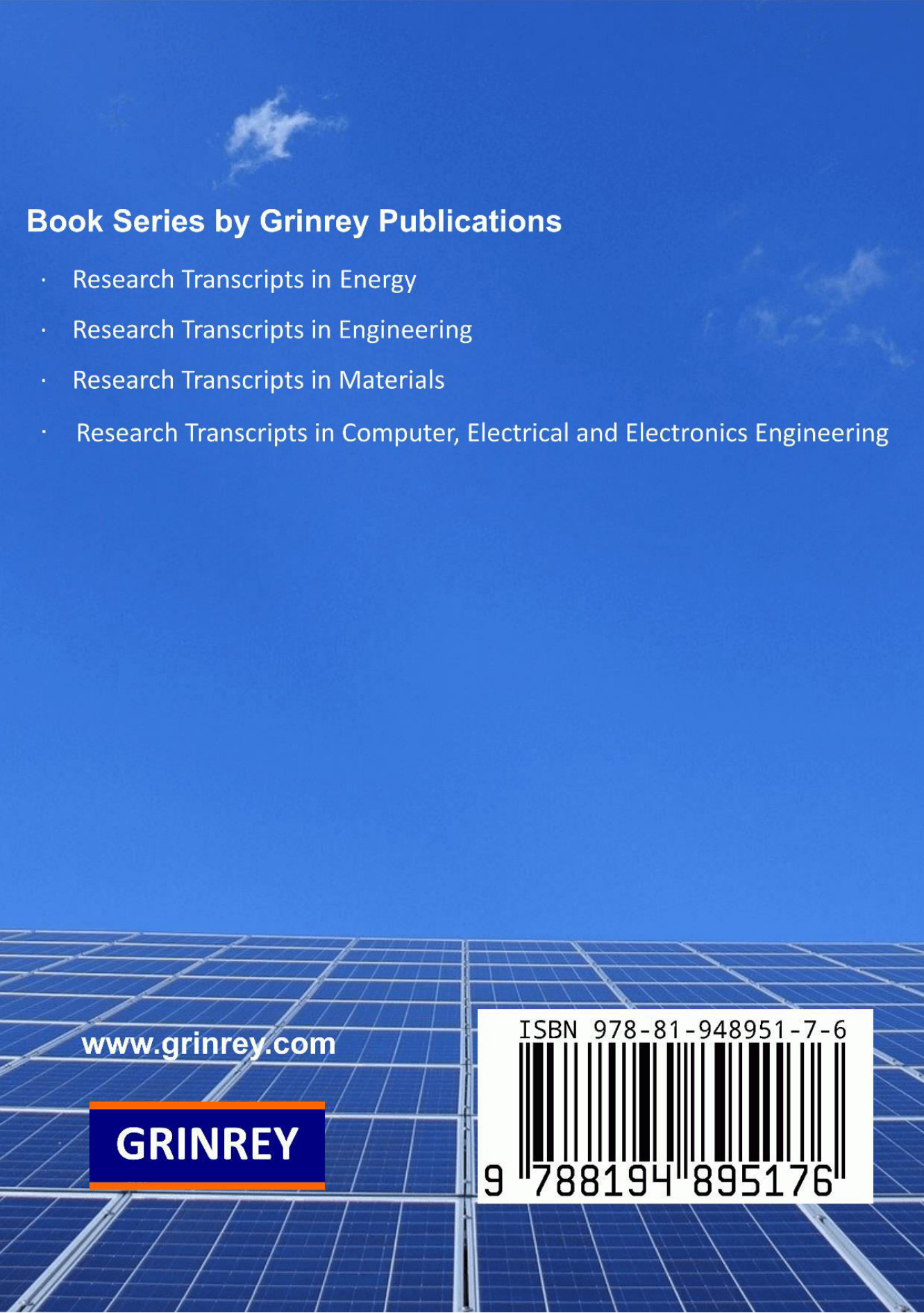

Book Series by Grinrey Publications

- Research Transcripts in Energy
- Research Transcripts in Engineering
- Research Transcripts in Materials
- Research Transcripts in Computer, Electrical and Electronics Engineering

www.grinrey.com

GRINREY

ISBN 978-81-948951-7-6